FATIGUE LIFE ESTIMATION OF TURBINE BLADES DUE TO TRANSIENT THERMAL, VIBRATORY, AND CENTRIFUGAL STRESSES

CENTRE FOR NEWFOUNDLAND STUDIES

TOTAL OF 10 PAGES ONLY
MAY BE XEROXED

(Without Author's Permission)

DEEPAK DHAR

FATIGUE LIFE ESTIMATION OF TURBINE BLADES DUE TO TRANSIENT THERMAL, VIBRATORY, AND CENTRIFUGAL STRESSES

By

Deepak Dhar (B.Eng)

A Thesis submitted to the School of Graduate Studies

in partial fulfilment of the

requirements for the degree of

Master of Engineering

Faculty of Engineering and Applied Science

Memorial University of Newfoundland

Oct. 1994

St. John's Newfoundland Canada

National Library of Canada
Bibliothèque nationale du Canada

Acquisitions and Bibliographic Services Branch
Direction des acquisitions et des services bibliographiques

395 Wellington Street
Ottawa, Ontario
K1A 0N4

395, rue Wellington
Ottawa (Ontario)
K1A 0N4

Your file Votre référence

Our file Notre référence

THE AUTHOR HAS GRANTED AN IRREVOCABLE NON-EXCLUSIVE LICENCE ALLOWING THE NATIONAL LIBRARY OF CANADA TO REPRODUCE, LOAN, DISTRIBUTE OR SELL COPIES OF HIS/HER THESIS BY ANY MEANS AND IN ANY FORM OR FORMAT, MAKING THIS THESIS AVAILABLE TO INTERESTED PERSONS.

L'AUTEUR A ACCORDE UNE LICENCE IRREVOCABLE ET NON EXCLUSIVE PERMETTANT A LA BIBLIOTHEQUE NATIONALE DU CANADA DE REPRODUIRE, PRETER, DISTRIBUER OU VENDRE DES COPIES DE SA THESE DE QUELQUE MANIERE ET SOUS QUELQUE FORME QUE CE SOIT POUR METTRE DES EXEMPLAIRES DE CETTE THESE A LA DISPOSITION DES PERSONNE INTERESSEES.

THE AUTHOR RETAINS OWNERSHIP OF THE COPYRIGHT IN HIS/HER THESIS. NEITHER THE THESIS NOR SUBSTANTIAL EXTRACTS FROM IT MAY BE PRINTED OR OTHERWISE REPRODUCED WITHOUT HIS/HER PERMISSION.

L'AUTEUR CONSERVE LA PROPRIETE DU DROIT D'AUTEUR QUI PROTEGE SA THESE. NI LA THESE NI DES EXTRAITS SUBSTANTIELS DE CELLE-CI NE DOIVENT ETRE IMPRIMES OU AUTREMENT REPRODUITS SANS SON AUTORISATION.

ISBN 0-612-01849-0

Canada

ABSTRACT

The present work involves the study of the three dimensional transient heat transfer and vibratory analysis of turbine blades with mixed and non-linear boundary conditions. The equations derived for the heat transfer analysis are general (three dimensional) in nature and are new contributions in this field. The mathematical model for both the heat transfer and the vibration analysis is formulated using curved, solid, C^0 continuity, quadratic, serendipity, twenty noded isoparametric finite elements.

The equations which are non-linear in nature for the transient temperature distribution within the turbine blade are derived using the finite element analysis. The non-linearities arise due to the radiative heat transfer and also due to the change in the material properties of the turbine blade with temperature. Using a finite difference scheme, the non-linear differential equations are transformed to non-linear algebraic equations in the time domain. The transient temperatures obtained from the heat transfer analysis are used in the calculation of the temperature gradients and transient thermal stresses. The vibratory analysis is done at first for finding the undamped natural frequencies of the turbine blade. These free vibration studies include the effect of the non-linearity in the stiffness matrix caused by the rotation of the turbine blade. The frequencies arising from the free vibration analysis also change because of the change in the material properties of the turbine blade as the temperature of the turbine blade changes with time. Thereafter, the stresses due to (a) the nozzle excitation and (b) the centrifugal stresses at different rotor speeds are calculated. The nozzle excitation

forces are modelled as a sinusoidal pulse. Finally, the total effect of all the three different types of stresses (transient thermal, centrifugal, and vibratory due to the nozzle excitation) on the fatigue life of the turbine blade is studied.

ACKNOWLEDGEMENTS

I am thankful to Dr. Anand M. Sharan for his contribution of time, invaluable expert advice, and providing the necessary funds and facilities which has helped me immensely during the course of this investigation. Working with him has been both a valuable personal and professional experience.

I would also like to express my sincere gratitude to Dr. C. A. Sharp, Dean of School of Graduate Studies and NSERC Canada for providing the financial support during the course of my graduate studies. I am also thankful to Dr. R. Seshadri, Dean of Engineering, Dr. J. J. Sharp, Associate Dean of Engineering, and Institute for Marine Dynamics for extending their cooperation and necessary help during this program.

Finally, special thanks to my friends for their constant encouragement and unfailing support.

This work is dedicated to my parents.

TABLE OF CONTENTS

	PAGE
ABSTRACT	i
ACKNOWLEDGEMENTS	iii
TABLE OF CONTENTS	v
LIST OF FIGURES	ix
NOMENCLATURE	xiv

CHAPTER 1

INTRODUCTION AND LITERATURE SURVEY

1.1 INTRODUCTION	1
1.2 THE LITERATURE SURVEY	5
1.2.1 HEAT TRANSFER ANALYSIS	5
1.2.2 VIBRATORY ANALYSIS	6
1.2.3 FATIGUE LIFE ANALYSIS	7
1.3 OBJECTIVES	8

CHAPTER 2

TRANSIENT HEAT TRANSFER ANALYSIS

2.1 INTRODUCTION	11
2.2 TRANSIENT TEMPERATURE DETERMINATION - THE MATHEMATICAL MODEL	13

2.3 DERIVATION OF THE ELEMENTAL EQUATIONS FOR $[CP^e]$, $[KC^e]$, $\{F_c^e\}$, $\{F_r^e\}$ 27

2.4 ILLUSTRATION OF THEORY 31

2.5 TEMPERATURE GRADIENT DISTRIBUTION ACROSS THE AIRFOIL CROSS - SECTION AT DIFFERENT HEIGHTS OF THE BLADE 32

2.6 TRANSIENT THERMAL STRESS DETERMINATION - THE MATHEMATICAL MODEL 33

2.7 CONCLUSION 63

CHAPTER 3

FREE VIBRATION ANALYSIS

3.1 INTRODUCTION 64

3.2 MATHEMATICAL FORMULATION 65

3.2.1 $[K_s^e]$ ELEMENTAL CONVENTIONAL STIFFNESS MATRIX - THE MATHEMATICAL FORMULATION 70

3.2.2 $[K_\sigma^e]$ ELEMENTAL STRESS STIFFNESS MATRIX - THE MATHEMATICAL FORMULATION 71

3.2.3 $[M^e]$ ELEMENTAL MASS MATRIX - THE MATHEMATICAL FORMULATION 75

3.3 FREE VIBRATION ANALYSIS 75

3.4 EFFECT OF TEMPERATURE VARIATION ON THE NATURAL FREQUENCIES OF THE BLADE 76

3.5 CONCLUSION 92

CHAPTER 4

TRANSIENT STRESS ANALYSIS & FATIGUE LIFE ESTIMATION

4.1 INTRODUCTION 93

4.2 TRANSIENT RESPONSE OF A ROTOR BLADE DUE TO NOZZLE EXCITATION FORCES - THE MATHEMATICAL FORMULATION 94

4.3 TRANSIENT RESPONSE DUE TO CENTRIFUGAL FORCE - THE MATHEMATICAL FORMULATION 101

4.4 VIBRATORY STRESSES 103

4.5 CENTRIFUGAL STRESSES 103

4.6 THERMAL STRESSES 104

4.7 STRESS ANALYSIS OF BLADE DUE TO COMBINED EFFECTS 109

4.8 FATIGUE LIFE ESTIMATION 110

4.9 CUMULATIVE FATIGUE DAMAGE 115

4.10 CONCLUSION 119

CHAPTER 5

CONCLUSIONS AND RECOMMENDATIONS

5.1 A BRIEF DISCUSSION ABOUT THE INVESTIGATION

AND THE CONCLUSIONS 120

5.2 LIMITATIONS OF THE PRESENT INVESTIGATION AND RECOMMENDATIONS FOR FUTURE WORK 122

REFERENCES 124

APPENDIX A EXPRESSIONS FOR SHAPE FUNCTIONS OF CORNER NODES FOR THE TWENTY-NODED ELEMENT 133

APPENDIX B EXPRESSIONS FOR SHAPE FUNCTIONS OF MID-SIDE NODES FOR THE TWENTY-NODED ELEMENT 134

APPENDIX C EXPRESSIONS FOR ELEMENTAL MATRICES AND VECTORS FOR THE TWENTY-NODED ELEMENT 135

APPENDIX D VARIATION OF MATERIAL PROPERTIES OF THE TURBINE BLADE WITH TEMPERATURE 245

APPENDIX E PHYSICAL INTERPRETATION OF STRESS STIFFNESS MATRIX 246

LIST OF FIGURES

NO.	DESCRIPTION	PAGE
1.1	CUTAWAY DIAGRAM OF LYCOMING T53 - L - 13	2
1.2	BURNT FIRST STAGE TURBINE BLADES	3
1.3	CROSS SECTION OF FATIGUED TURBINE BLADE	4
2.1	THREE DIMENSIONAL FINITE ELEMENT MODEL FOR TURBINE BLADE	12
2.2	SOLID ISOPARAMETRIC, SERENDIPITY, C^0 CONTINUITY, 20-NODED ELEMENT (LOCAL COORDINATE SYSTEM)	17
2.3	SOLID ISOPARAMETRIC, SERENDIPITY, C^0 CONTINUITY, 20-NODED ELEMENT (GLOBAL COORDINATE SYSTEM)	18
2.4	NODAL TEMPERATURE VARIATION ALONG THE Z - AXIS AT LEADING EDGE	34
2.5	NODAL TEMPERATURE VARIATION ALONG THE Z - AXIS AT 15 % CHORD LENGTH	35
2.6	NODAL TEMPERATURE VARIATION ALONG THE Z - AXIS AT 30 % CHORD LENGTH	36
2.7	NODAL TEMPERATURE VARIATION ALONG THE Z - AXIS AT 45 % CHORD LENGTH	37
2.8	NODAL TEMPERATURE VARIATION ALONG THE Z - AXIS AT 60 % CHORD LENGTH	38

2.9 NODAL TEMPERATURE VARIATION ALONG THE Z - AXIS AT 75 % CHORD LENGTH 39

2.10 NODAL TEMPERATURE VARIATION ALONG THE Z - AXIS AT TRAILING EDGE 40

2.11 TEMPERATURE CONTOURS ACROSS THE AIRFOIL SECTION AT t = 150 SEC (HEIGHT OF THE BLADE = 2.5 cm.) 41

2.12 TEMPERATURE CONTOURS ACROSS THE AIRFOIL SECTION AT t = 150 SEC (HEIGHT OF THE BLADE = 5.0 cm.) 42

2.13 TEMPERATURE CONTOURS ACROSS THE AIRFOIL SECTION AT t = 150 SEC (HEIGHT OF THE BLADE = 7.5 cm.) 43

2.14 TEMPERATURE CONTOURS ACROSS THE AIRFOIL SECTION AT t = 150 SEC (HEIGHT OF THE BLADE = 10.0 cm.) 44

2.15 TEMPERATURE CONTOURS ACROSS THE AIRFOIL SECTION AT t = 150 SEC (HEIGHT OF THE BLADE = 12.0 cm.) 45

2.16 TEMPERATURE GRADIENTS ACROSS THE BLADE CROSS-SECTION AT t = 150 SEC. (HEIGHT OF THE BLADE = 2.5 cm.) 46

2.17 TEMPERATURE GRADIENTS ACROSS THE BLADE CROSS-SECTION AT t = 150 SEC. (HEIGHT OF THE BLADE = 5.0 cm.) 47

2.18 TEMPERATURE GRADIENTS ACROSS THE BLADE CROSS-SECTION AT t = 150 SEC.

	(HEIGHT OF THE BLADE = 7.5 cm.)	48
2.19	TEMPERATURE GRADIENTS ACROSS THE BLADE CROSS-SECTION AT t = 150 SEC. (HEIGHT OF THE BLADE = 10.0 cm.)	49
2.20	TEMPERATURE GRADIENTS ACROSS THE BLADE CROSS-SECTION AT t = 150 SEC. (HEIGHT OF THE BLADE = 12.0 cm.)	50
2.21	TRANSIENT THERMAL STRESS (σ_{xx}) DISTRIBUTION IN THE BLADE	59
2.22	TRANSIENT THERMAL STRESS (σ_{yy}) DISTRIBUTION IN THE BLADE	60
2.23	TRANSIENT THERMAL STRESS (σ_{zz}) DISTRIBUTION IN THE BLADE	61
2.24	TRANSIENT THERMAL STRESS (σ_{zz}) DISTRIBUTION IN THE BLADE FOR THE FEASIBLE HEATING RATE OF 24° C/SEC AT DIFFERENT INSTANTS OF TIME	62
3.1	TURBINE BLADE AIRFOIL CROSS - SECTION AT THE ROOT AND THE TIP	66
3.2	VARIATION OF FIRST FIVE NATURAL FREQUENCIES OF TURBINE BLADE AT ROTOR SPEED OF 300 RPM	78
3.3	VARIATION OF FIRST FIVE NATURAL FREQUENCIES OF TURBINE BLADE AT ROTOR SPEED OF 900 RPM	79

3.4	VARIATION OF FIRST FIVE NATURAL FREQUENCIES OF TURBINE BLADE AT ROTOR SPEED OF 1500 RPM	80
3.5	VARIATION OF FIRST FIVE NATURAL FREQUENCIES OF TURBINE BLADE AT ROTOR SPEED OF 2100 RPM	81
3.6	VARIATION OF FIRST FIVE NATURAL FREQUENCIES OF TURBINE BLADE AT ROTOR SPEED OF 2700 RPM	82
3.7	VARIATION OF FIRST FIVE NATURAL FREQUENCIES OF TURBINE BLADE AT ROTOR SPEED OF 3300 RPM	83
3.8	VARIATION OF FIRST FIVE NATURAL FREQUENCIES OF TURBINE BLADE AT ROTOR SPEED OF 3900 RPM	84
3.9	COMPARISON OF FIRST ACTUAL CRITICAL SPEED WITH FIRST PROJECTED CRITICAL SPEED USING STRESS STIFFNESS MATRIX	85
3.10	COMPARISON OF SECOND ACTUAL CRITICAL SPEED WITH SECOND PROJECTED CRITICAL SPEED USING STRESS STIFFNESS MATRIX	86
3.11	COMPARISON OF FIRST CRITICAL SPEED OBTAINED FROM VARIOUS METHODS	87
3.12	COMPARISON OF SECOND CRITICAL SPEED OBTAINED FROM VARIOUS METHODS	88
3.13	COMPARISON OF THIRD CRITICAL SPEED OBTAINED FROM VARIOUS METHODS	89

3.14	COMPARISON OF FOURTH CRITICAL SPEED OBTAINED FROM VARIOUS METHODS	90
3.15	COMPARISON OF FIFTH CRITICAL SPEED OBTAINED FROM VARIOUS METHODS	91
4.1	REPRESENTATION OF THE NOZZLE EXCITATION FORCES AS A SINUSOIDAL PULSE	97
4.2	VIBRATORY STRESSES AT VARIOUS ROTOR SPEEDS	105
4.3	CENTRIFUGAL STRESSES AT VARIOUS ROTOR SPEEDS	106
4.4	THERMAL STRESSES AT VARIOUS TIMES	107
4.5	TRANSIENT THERMAL STRESS (σ_{zz}) DISTRIBUTION IN THE BLADE FOR THE FEASIBLE HEATING RATE OF 24° C/SEC AT DIFFERENT INSTANTS OF TIME	108
4.6	FATIGUE FAILURE SURFACE DEFINED BY BAGCI LINE	113
4.7	BLADE LOADING PATTERN	114
4.8	MAGNIFIED STRESS LEVELS BETWEEN 3100-3200 RPM DURING START-UP AT ROTOR ACCELERATION OF 800 RPM/MIN	116
4.9	MAGNIFIED STRESS LEVELS BETWEEN 3100-3200 RPM DURING START-UP AT ROTOR ACCELERATION OF 1500 RPM/MIN	117

NOMENCLATURE

k_{xx}	thermal conductivity in the x-direction
k_{yy}	thermal conductivity in the y-direction
k_{zz}	thermal conductivity in the z-direction
Q	heat generated within the body
ρ	mass density of the material
c	specific heat
l_x, l_y, l_z	direction cosines normal to the surface
h	convective heat transfer coefficient
T_∞	gas temperature
σ	Stefan-Boltzmann constant
ε	emissivity of the body
χ	a functional
V	volume of the blade
q	specified heat flux
δT	first variation of T
S_1	surface experiencing heat flux
S_2	surface experiencing convection and radiation boundary conditions
[D]	thermal conductivity matrix
[B]	temperature gradient interpolation matrix

$[N]$	shape function matrix
$\{T\}$	nodal temperature vector
$[CP]$	capacitance matrix
$[KC]$	conduction matrix
$\{F_c\}$	force vector due to convection
$\{F_r\}$	force vector due to radiation
ξ, η, ζ	local coordinate directions
$[J]$	jacobian matrix
$\lvert J \rvert$	determinant of jacobian matrix
W_i, W_j, W_k	weights used in Gauss-quadrature
G	Global
e	element
t	time
Δt	time increment
$\{g\}$	temperature gradient vector
$\{\sigma\}$	stress vector
$[D_1]$	material property matrix
$\{\varepsilon\}$	strain vector
$\{\varepsilon_o\}$	initial strain vector
$\sigma_{xx}, \sigma_{yy}, \sigma_{zz}$	normal stresses
$\sigma_{xy}, \sigma_{yz}, \sigma_{zx}$	shear stresses
$\varepsilon_{xx}, \varepsilon_{yy}, \varepsilon_{zz}$	normal strains

ε_{xy}, ε_{xz}, ε_{zy}	shear strains
$[B_1]$	strain displacement matrix
E	modulus of elasticity
ν	Poisson's ratio of the material
α	coefficient of thermal expansion
$\{f\}$	force vector due to thermal expansion
$\{d\}$	displacement vector
$[K_s]$	conventional stiffness matrix
$[K_\sigma]$	stress stiffness matrix
$\{c\}$	nodal local coordinate vector
U	strain energy
$[M]$	mass matrix
λ	eigenvalue of the system
$[C]$	damping matrix
ω	angular speed of the rotor
ω_{nk}	natural frequency of kth mode
ω_{dk}	damped natural frequency of kth mode
ξ_k	damping ratio of kth mode
$[\Phi]$	matrix of modal vectors
$\{F\}$	dynamic force vector
$\{Q\}$	force vector transformed in modal coordinates by normalized modal matrix

{QF}	force vector transformed in modal coordinates by m-orthonormalized modal matrix
n	number of elements
G	global
e	elemental

CHAPTER 1

INTRODUCTION AND LITERATURE REVIEW

1.1 INTRODUCTION

In the fast few decades, the turbines have found an ever increasing service in the field of power generation and in the propulsion of jet engines. The major gas turbine components are shown in the Fig. 1.1. The air, as we see in this figure, is let in through an air-inlet or a diffuser, it is then compressed and led to combustor where the temperature of high-pressure air is increased. The air-fuel mixture is directed through the nozzles onto the turbine blade and thus converting energy of the gas, evidenced by a high pressure and temperature, into kinetic energy and then to the shaft work.

As is evident, the major brunt of the energy conversion is thus taken up by the turbine blade which is exposed to a variety of hostile environment and forces such as thermal, centrifugal and vibratory. All these causes (separately and collectively) can lead to turbine blade failure which is a major cause of breakdown in the turbomachinery. Figs. 1.2 and 1.3 show some of the examples of turbine blades which have undergone failure. Thus, it is essential to have an accurate estimate of the damage done by these forces on the turbine blade in the early stages of design which, in turn, can avoid the causes of the early blade failure, which is the objective of this investigation. This objective is achieved in two stages: at first, the heat transfer analysis of turbine blade is done and transient temperatures of the blade at different time steps are found. These temperatures help in finding the thermal gradients and transient thermal stresses.

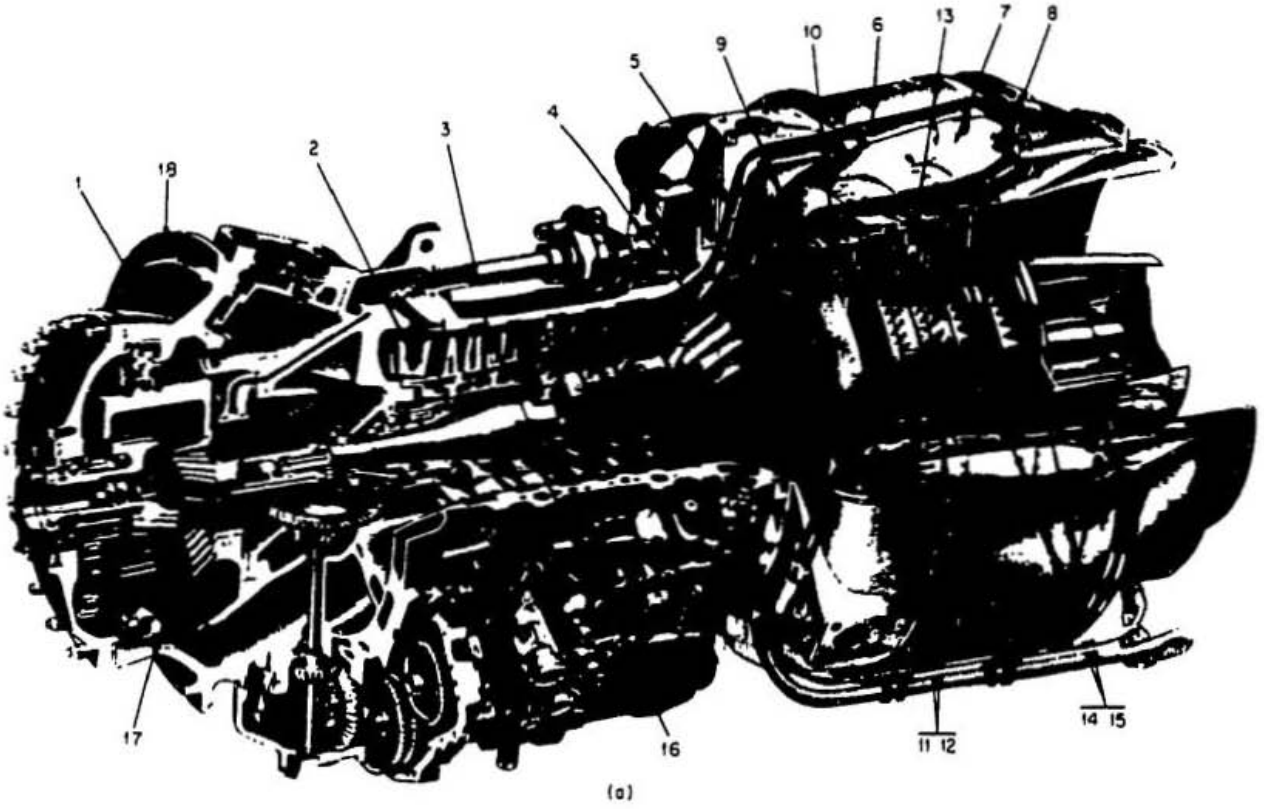

1 ANNULAR INLET
2 VARIABLE INLET GUIDE VANE
3 FIVE-STAGE AXIAL COMPRESSOR
4 SINGLE CENTRIFUGAL COMPRESSOR STAGE
5 RADIAL DIFFUSER
6 AREA SURROUNDING COMBUSTION CHAMBER
7 COMBUSTION CHAMBER
8 VAPORIZER TUBES (IN EARLIER VERSIONS) OR ATOMIZERS
9 COMBUSTION TURNING ZONE
10 AIR-COOLED FIRST TURBINE NOZZLE
11-12 TWO-STAGE COMPRESSOR TURBINE
13 FREE-POWER TURBINE NOZZLE
14-15 TWO-STAGE FREE-POWER TURBINE
16 THROUGH-SHAFT
17 PLANETARY REDUCTION GEAR
18 INLET HOUSING

Fig. 1.1 CUTAWAY DIAGRAM OF LYCOMING T53 - L - 13 [Traager, 1970]

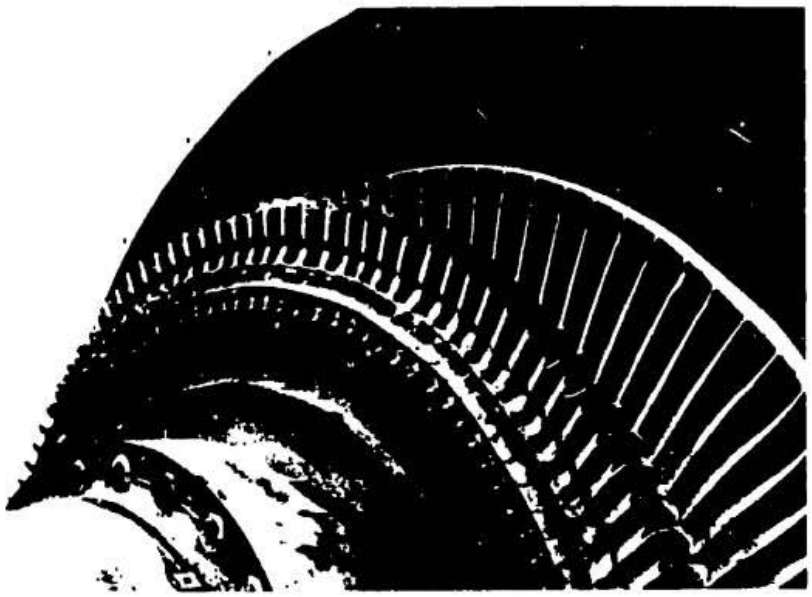

Fig. 1.2 BURNT FIRST STAGE TURBINE BLADES[Boyce, 1982]

Fig. 1.3 CROSS SECTION OF FATIGUED TURBINE BLADE.

MARKINGS NEAR THE TRAILING EDGE INDICATE CYCLIC FATIGUE[Boyce, 1982]

The second part consists in the determination of natural frequencies of the turbine blade in the transient phase. This is used in finding the critical speeds, the vibratory stresses and the centrifugal stresses. When combined together, this gives the overall picture of the stresses in the turbine blade and finally, the fatigue life estimation of the turbine blade is done.

1.2 THE LITERATURE SURVEY

1.2.1 HEAT TRANSFER ANALYSIS

Since the advent of gas turbines and their subsequent application in various sectors of industry, there has been a rising demand for more and more power output. The blade loadings have continually risen typically in increased hostile environment due to temperature, wetness, speed and corrosion. These developments demand (a) greater output per blade, (b) smaller frame size or greater output per unit volume (c) higher operating speeds, and (d) higher processing temperatures and pressures. Above all, the reliability is the most demanding requirement. In general, simultaneous satisfaction of these demands has called for an increased attention to the accurate heat transfer and vibratory analysis of turbine blades.

Daniels *et al* (1981) and Mohanty *et al* (1977) reported some of the latest developments in heat transfer analysis of turbine blades. Maya *et al* (1978) and Mukherjee (1978) calculated the transient thermal stresses of the gas turbine blades. However, their studies included the heat exchange process by convection only and thus their temperature and thermal stress distribution studies of the turbine blade were

inadequate. One of the major deficiencies of these studies was the non-inclusion of the radiative heat exchange terms which are quite significant at the higher operating temperatures. Moreover, their investigation was based on the assumption that the maximum stress would take place only at one of the points at leading edge, trailing edge or mid-section of the turbine blade. Allen (1982) studied the effect of temperature dependent mechanical properties on thermal stresses in turbine blades. The influence of turbine blade geometry on its thermal stress state was studied by Bogov (1978). The experimental verification of finite element calculation of the thermal stress state of gas turbine blades was done by Gryaznov *et al* (1979). Bahree (1987) carried out the two-dimensional heat transfer analysis of the turbine blade using finite element analysis. His investigation was based on the assumption that the thermal gradients along the height of the turbine blade are negligible during the transient state as compared to the thermal gradients along the airfoil cross-section of the blade.

1.2.2 VIBRATORY ANALYSIS

The dynamic analysis of the turbine blade has been a challenging field for the engineers for a long time. Numerous mathematical approaches have been used to derive the dynamic equations. Most of the mathematical techniques were based on the Newtonian approach and, as a first approximation, the geometry of the turbine blade was modelled as a tapered beam having a rectangular cross-section. Rao and Carnegie (1970) used the Ritz-Galerkin method to obtain the bending frequencies for the first three modes of vibration of tapered cantilever blades having rectangular cross-section. Mabie

and Rogers (1974) analyzed the effect of various boundary conditions on the natural frequency of the turbine blade. Their method of solution was based on the use of the Bessel's functions. Sato (1980) used Ritz method to carry out the effect of axial force on the frequencies of blades with ends restrained elastically against rotation. Sisto and Chang (1984) formulated a finite element model to calculate the natural frequencies of the blade. Their model, however, was appropriate for thin and high aspect ratio blades only. Nagarajan and Alwar (1984) used the twenty-noded finite element to analyze the free vibration behaviour of the blade without temperature variation. Bahree (1987) did the transient free vibration analysis of the turbine blade using twenty-noded finite element for the turbine blade which included the effect of the change in temperature. The effect of the stress stiffness matrix, caused by the rotation of the turbine blade, was not carried out in his study. Warikoo (1989) analyzed the propeller-shaft transverse vibrations. His work included the non-linear stiffness variation but, it did not include the effect of change of the temperature on the transient natural frequencies of the turbine blade.

1.2.3 FATIGUE LIFE ANALYSIS

In spite of the fact that various design procedures for preventing failure of turbine blades due to fatigue are being used, there is yet no indication that a satisfactory situation exists with reference to basic data that will lead to establishing sound procedures in this regard. This is because of the fact that blade fatigue is a multi-dimensional problem and as such has been undergoing continuous investigations for a long time. The various reasons which lead the blade to failure are: high gas temperature, blade excitation,

material behaviour under high temperature and loading conditions, crack initiation and propagation, creep due to high temperature conditions, and other various thermo-elastic and aero-elastic effects. Rieger (1983) discussed various aspects involved in the life estimation of a turbine blade. Rao (1991) and Vyas (1986) reported some of the latest findings on life estimation of turbine blading. Heywood (1962) studied the designing against fatigue failure. Rust and Swaminathan (1982) did corrosion fatigue testing of steam turbine blading alloys. Collins (1981) reported failure of materials in mechanical design.

1.3 OBJECTIVES

Based on the survey of the previous research works, and more specifically, Bahree's (1987) work where (a) two - dimensional heat transfer analysis was done, (b) the non-linear terms in the stiffness matrix were neglected, and (c) the gas force excitations were modelled as impulses of an arbitrary height, in this work a three dimensional heat transfer model is analyzed; the non-linear stiffness terms have been included, and the gas force excitations are based on fluid flow over an airfoil cross section.

1. To derive the **transient temperature distribution** equations in a turbine blade using **twenty-noded isoparametric** finite elements.
2. To determine the **temperatures and thermal gradients** at various points on the

airfoil cross-section and along the height of the turbine blade by solving a non-linear system of equations. The non-linearity arises due to the radiative boundary conditions along the surface of the turbine blade and also due to the variation of the material properties.

3. To find the **transient thermal stresses** due to the transient temperature obtained.
4. To study the **free vibration** characteristics of the turbine blade using **twenty-noded isoparametric** finite elements.
5. To study the effect of the **stress stiffness matrix** and the **change in the material properties of the blade(as temperature changes)** on the natural frequencies of the turbine blade.
6. To study the **dynamic stresses** in the turbine blade due to nozzle excitation forces modelled as a **sinusoidal pulse**.
7. To study the effect of rotor speed on **centrifugal forces**.
8. To study the **combined stress analysis** in the turbine blade due to the effects of all of the stresses mentioned above.
9. To study the **fatigue life estimation** of the turbine blade due to the combination of thermal, vibratory and centrifugal stresses.

In Chapter 2, a mathematical model for the three-dimensional heat transfer analysis of the turbine blade is established. The non-linear equations for the transient temperature determination in the turbine blade are obtained by using a twenty-noded isoparametric finite element formulation. These non-linear system of differential equations are

expressed as a system of algebraic equations in the time domain by using the Crank-Nicolson finite difference scheme. The temperatures, thermal gradients, and stresses at various points on the airfoil cross-section and along the height of the blade are then determined by solving these non-linear system of equations. A feasible heating path for the gas turbine is established to carry out the thermal stress analysis.

In Chapter 3, the three-dimensional mathematical model for the turbine blade is used to study the free vibration characteristics of the turbine blade. The effect of stress stiffness matrix caused by the rotation of the turbine blade, on the natural frequency of the turbine blade is studied. The effect of the change in the material properties of the blade(as temperature changes) on the natural frequencies of the turbine blade is also studied.

In Chapter 4, the nozzle excitation forces have been modelled as a sinusoidal pulse. The responses due to nozzle excitation and centrifugal forces are used to calculate the dynamic stresses in the turbine blade. The fatigue life of the turbine blade is estimated based on the thermal and dynamic stresses obtained.

Finally, the conclusions and recommendations for future work are presented in Chapter 5.

CHAPTER 2

TRANSIENT HEAT TRANSFER ANALYSIS

2.1 INTRODUCTION

In order to increase the efficiency of a turbine, it is very essential that higher inlet pressures and temperatures be used. However, higher inlet temperatures, though important from thermodynamic point of view, severely increase the thermal loading on the turbine blade, and as a result, high thermal stresses are induced in the turbine blade. The impact of these thermal stresses is known to peak both, during the acceleration, and the deceleration stages of the gas turbine engine. The reason is that there is a significant temperature difference which is sufficiently large to cause plastic deformation (Bahree, 1987) at various points of the blade. Hence, it becomes very important to calculate the temperature distribution within the turbine blade with great accuracy. The present investigation is based on the three-dimensional analysis of the turbine blade. The mathematical model for the non-linear transient heat transfer analysis is formulated using curved, solid, C^0 continuity, serendipity, twenty-noded isoparametric finite elements. This type of element is chosen because of its versatility in accurately mapping the complex geometry of the turbine blade.The results obtained from three-dimensional model show that in addition to the thermal gradients along the airfoil cross-section of the turbine blade, there are significant thermal gradients along the height of the turbine blade, as well. These elements of the turbine blade (shown in Fig. 2.1) exchange heat with the surrounding high temperature gas by convection and radiation

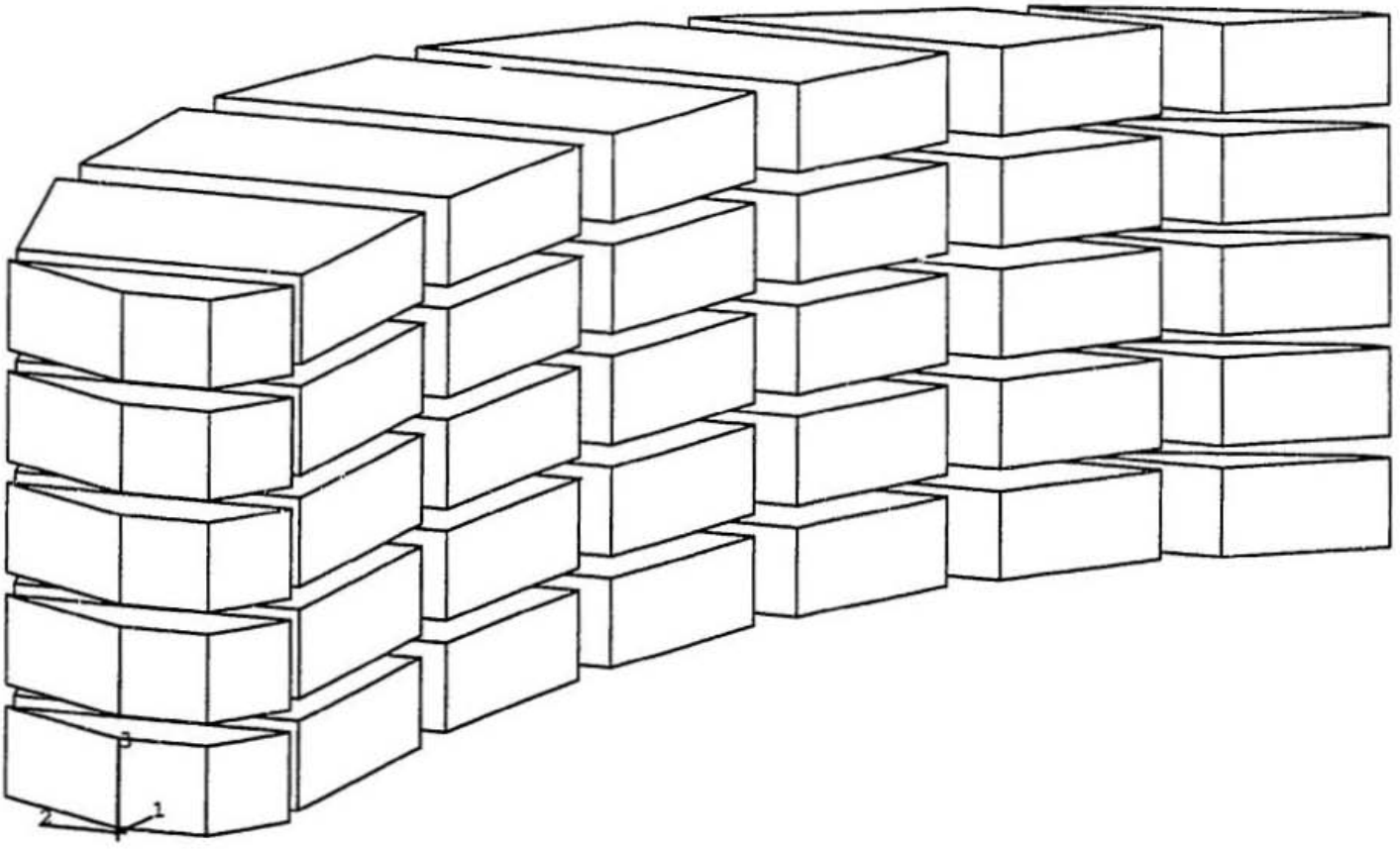

Fig. 2.1 THREE DIMENSIONAL FINITE ELEMENT MODEL FOR TURBINE BLADE

processes. Because of the radiation term, we get a non-linear system of differential equations. The Crank-Nicolson finite difference scheme is then used to transform these non-linear differential equations into non-linear algebraic equations in the time domain. Then, using an iteration technique, the non-linear algebraic equations are solved to obtain the nodal and elemental temperatures. Once these transient nodal temperatures are known, the thermal gradients (a) across the airfoil cross-section and (b) along the height of the turbine blade, are calculated. Using theses transient temperatures, one can calculate the thermal stresses. In order to keep these thermal stresses well within the yield stress limit, a feasible heating path is also obtained in the present investigation.

2.2 TRANSIENT TEMPERATURE DETERMINATION - THE MATHEMATICAL MODEL

In the following derivation, the general form of the three-dimensional equations are obtained first and then the appropriate conditions relevant to our problem are applied. The governing three-dimensional partial differential equation for heat flow in any solid can be written as

$$k_x \frac{\partial^2 T}{\partial x^2} + k_y \frac{\partial^2 T}{\partial x^2} + k_z \frac{\partial^2 T}{\partial z^2} + Q = \rho c \frac{\partial T}{\partial t} \tag{2.1}$$

and its boundary condition as

$$k_x \frac{\partial T}{\partial x} l_x + k_y \frac{\partial T}{\partial y} l_y + k_z \frac{\partial T}{\partial z} l_z + h(T - T_\infty) + q + \sigma\varepsilon(T^4 - T_\infty^4) = 0 \tag{2.2}$$

We make use of the calculus of variations to solve the partial differential equation, Eq.

(2.1) and the boundary condition, Eq. (2.2) associated with it. This solution is obtained by minimizing the corresponding variational functional and solving the resulting system of algebraic equations. We can rearrange the Eq. (2.1) and write it as

$$-k_x\frac{\partial^2 T}{\partial x^2} - k_y\frac{\partial^2 T}{\partial y^2} - k_z\frac{\partial^2 T}{\partial z^2} - \left\{ Q - \rho c\frac{\partial T}{\partial t} \right\} = 0 \tag{2.3}$$

Now the variational functional can be set up by multiplying Eq. (2.2) and Eq. (2.3) by the first variation of T i.e., δT and integrating over the whole domain. This results in the equation

$$\delta_\chi = \int_V \left[-k_x\frac{\partial^2 T}{\partial x^2} - k_y\frac{\partial^2 T}{\partial x^2} - k_z\frac{\partial^2 T}{\partial z^2} - \left(Q - \rho c\frac{\partial T}{\partial t} \right) \right] \delta T \, dV \tag{2.4}$$

$$+ \int_S \left[k_x\frac{\partial T}{\partial x} l_x + k_y\frac{\partial T}{\partial y} l_y + k_z\frac{\partial T}{\partial z} l_z + q + h(T - T_\infty) + \sigma\varepsilon(T^4 - T_\infty^4) \right] \delta T \, dS$$

Rearranging Eq.(2.4) one gets

$$\delta_\chi = \int_S k_x\frac{\partial T}{\partial x} l_x \, \delta T \, dS - \int_V k_x\frac{\partial^2 T}{\partial x^2} \delta T \, dV + \int_S k_y\frac{\partial T}{\partial y} l_y \, \delta T \, dS - \int_V k_y\frac{\partial^2 T}{\partial y^2} \delta T \, dV$$

$$+ \int_S k_z\frac{\partial T}{\partial z} l_z \, \delta T \, dS - \int_V k_z\frac{\partial^2 T}{\partial z^2} \delta T \, dV + \int_S q \, \delta T \, dS - \int_V \left(Q - \rho c\frac{\partial T}{\partial t} \right) \delta T \, dV$$

$$+ \int_S h(T - T_\infty) \, \delta T \, dS + \int_S \sigma\varepsilon(T^4 - T_\infty^4) \, \delta T \, dS$$

(2.5)

Using Green's Divergence Theorem, we can transform surface integral into volume integral. Thus the integral in Eq. (2.5) can be written as:

$$\int_S k_x \frac{\partial T}{\partial x} l_x \, \delta T \, dS = \int_V k_x \frac{\partial^2 T}{\partial x^2} \delta T \, dV + \int_V \frac{k_x}{2} \delta \left(\frac{\partial T}{\partial x} \right)^2 dV \tag{2.6}$$

$$\int_S k_y \frac{\partial T}{\partial y} l_y \, \delta T \, dS = \int_V k_y \frac{\partial^2 T}{\partial y^2} \delta T \, dV + \int_V \frac{k_y}{2} \delta \left(\frac{\partial T}{\partial y} \right)^2 dV \tag{2.7}$$

and

$$\int_S k_z \frac{\partial T}{\partial z} l_z \, \delta T \, dS = \int_V k_z \frac{\partial^2 T}{\partial z^2} \delta T \, dV + \int_V \frac{k_z}{2} \delta \left(\frac{\delta T}{\delta z} \right)^2 dV \tag{2.8}$$

Substituting the integral from the Eqs. (2.6) to (2.8) into Eq. (2.5), the new equation will be

$$\delta_\chi = \int_V \frac{k_x}{2} \delta \left(\frac{\delta T}{\delta x} \right)^2 dv + \int_V \frac{k_y}{2} \delta \left(\frac{\delta T}{\delta y} \right)^2 dV$$

$$+ \int_V \frac{k_z}{2} \delta \left(\frac{\delta T}{\delta z} \right)^2 dV - \int_V Q \, \delta T \, dV + \int_V \rho c \frac{\delta T}{\delta t} \delta T \, dV$$

$$+ \int_S q \, \delta T \, dS + \int_S \frac{h}{2} \delta \, (T - T_\infty)^2 \, ds + \int_S \sigma \, \varepsilon \, \delta \left(\frac{T^5}{5} - T_\infty^4 \, T \right) dS \tag{2.9}$$

Removing the variational operator δ from both sides of the equation above, we get

$$\chi = \int_V \frac{1}{2}\left[k_x \left(\frac{\delta T}{\delta x} \right)^2 + k_y \left(\frac{\delta t}{\delta y} \right)^2 + k_z \left(\frac{\delta T}{\delta z} \right)^2 - 2\, Q\, T + 2\, \rho\, c\, T\, \frac{\delta T}{\delta t} \right]$$

$$+ \int_{S_1} q\, T\, dS + \int_{S_2} \left[\frac{h}{2} (T - T_\infty)^2 + \sigma\, \varepsilon \left(\frac{T^5}{5} - T_\infty^4\, T \right) \right] dS \qquad (2.10)$$

where S_1 is the surface experiencing heat flux and S_2 is the surface experiencing convection and radiation boundary conditions.

Referring to Fig. 2.2 where there are 20-nodes per element, one can use the finite element equalities mentioned below to formulate the finite element equations corresponding to Eq. (2.10). Also, the temperature T is assumed continuous not over the whole domain but it is defined over an individual element. The equations are:

$$[\, D^e \,] = \begin{bmatrix} k_x^e & 0 & 0 \\ 0 & k_y^e & 0 \\ 0 & 0 & k_z^e \end{bmatrix} \quad ;$$

$$\text{if } k_x = k_y = k_z = k \text{ then} \qquad (2.11)$$

$$[\, D^e \,] = k \begin{bmatrix} 1 & 0 & 0 \\ 0 & 1 & 0 \\ 0 & 0 & 1 \end{bmatrix} \quad ;$$

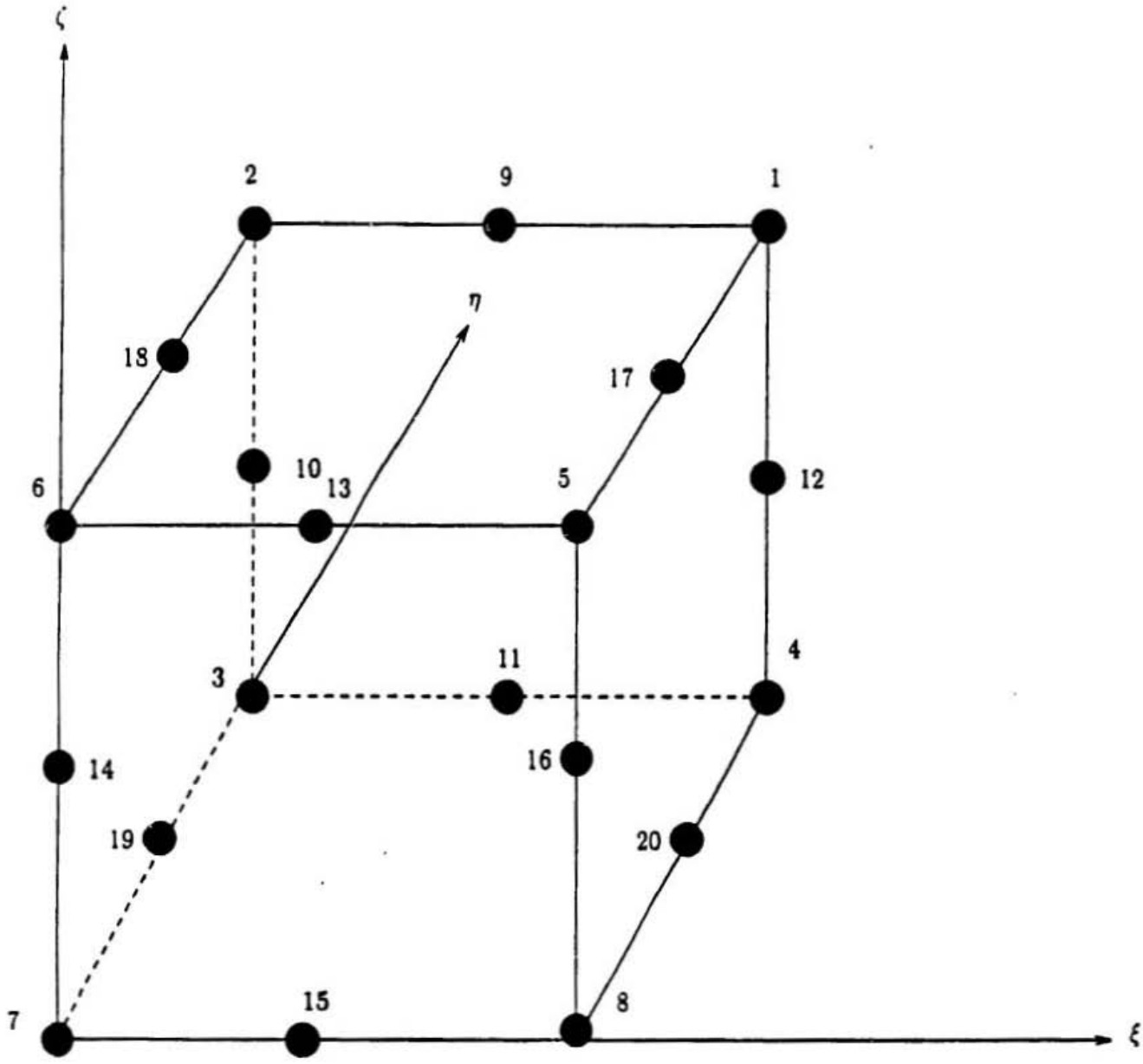

Fig. 2.2 SOLID ISOPARAMETRIC, SERENDIPITY, C° CONTINUITY, 20-NODED ELEMENT (LOCAL COORDINATE SYSTEM)

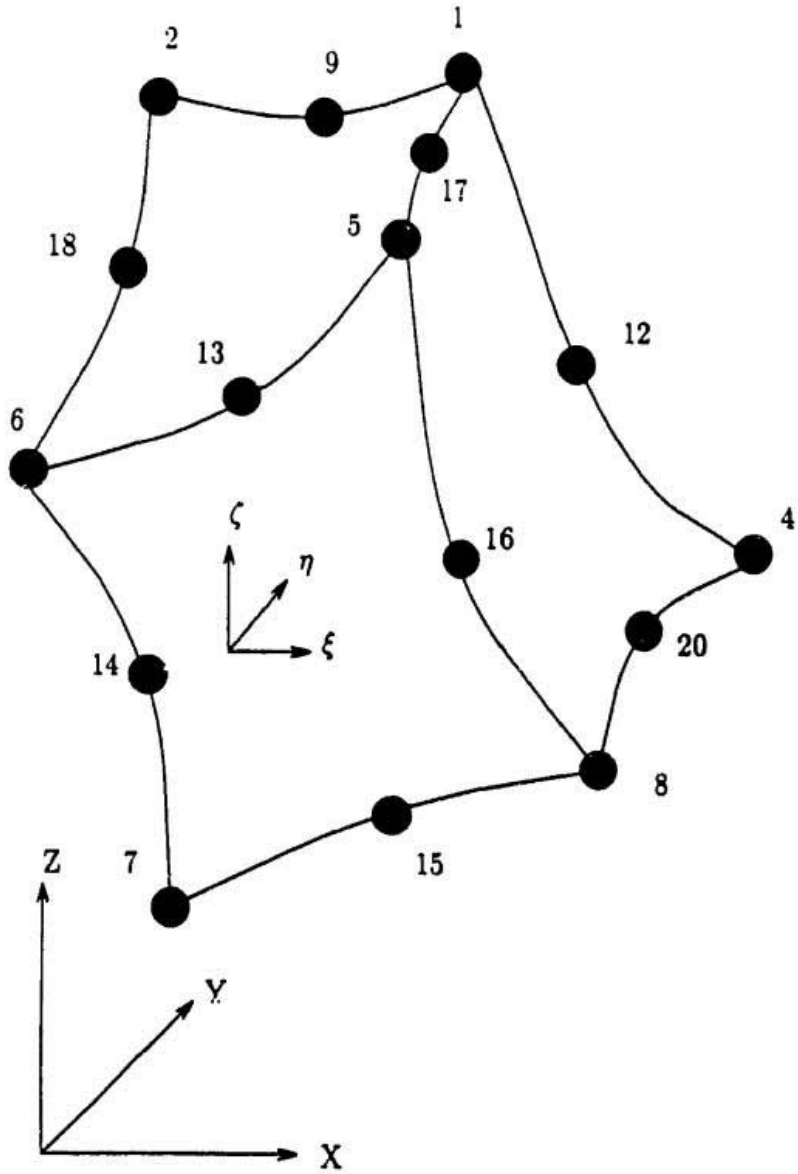

Fig. 2.3 SOLID ISOPARAMETRIC, SERENDIPITY, C° CONTINUITY, 20-NODED ELEMENT (GLOBAL COORDINATE SYSTEM)

$$[\ B^e\ ] = \begin{bmatrix} \frac{\partial N_1^e}{\partial x} & \frac{\partial N_2^e}{\partial x} & \frac{\partial N_3^e}{\partial x} & \cdots & \frac{\partial N_{20}^e}{\partial x} \\ \frac{\partial N_1^e}{\partial y} & \frac{\partial N_2^e}{\partial y} & \frac{\partial N_3^e}{\partial y} & \cdots & \frac{\partial N_{20}^e}{\partial y} \\ \frac{\partial N_1^e}{\partial z} & \frac{\partial N_2^e}{\partial z} & \frac{\partial N_3^e}{\partial z} & \cdots & \frac{\partial N_{20}^e}{\partial z} \end{bmatrix}, \text{ and} \tag{2.12}$$

$$T^e = \left[\ N_1^e\ \ N_2^e\ \ N_3^e\ \ .\ .\ .\ \ N_{20}^e\ \right] \begin{Bmatrix} T_1 \\ T_2 \\ T_3 \\ . \\ . \\ . \\ T_{20} \end{Bmatrix} \tag{2.13}$$

where T_1, T_2, ...T_{20} are the nodal temperatures of a twenty-noded finite element. Also, both the terms Q and q in the Eq (2.10) are zero as there is no heat generation and no specified heat fluxes in the present investigation. Therefore, substituting Eqs. (2.11-2.13) into Eq. (2.10), we obtain

$$\chi^e = \int_{V_e} \frac{1}{2} \{\ T^e\ \}^T [\ B^e\ ]^T [\ D^e\ ] [\ B^e\ ] \{\ T^e\ \}\ dV$$

$$+ \int_{S_i} \frac{h^e}{2} \left([\ N^e\ ] \{\ T^e\ \} \right)^2 dS$$

$$+ \int_{V_e} \rho \, c^e \left[N^e \right] \frac{\partial \{ T^e \}}{\partial t} \left[N^e \right] \{ T^e \} \, dV$$

$$- \int_{S_2^e} h^e \, T_\infty \left[N^e \right] \{ T^e \} \, dS + \int_{S_2^e} \frac{h_2^e}{2} \, T_\infty^2 \, dS$$

$$+ \int_{S_2^e} \frac{\sigma \, \varepsilon}{5} \left(\left[N^e \right] \{ T^e \} \right)^5 dS - \int_{S_2^e} \sigma \, \varepsilon \, T_\infty^4 \left[N^e \right] \{T^e\} \, dS \qquad (2.14)$$

The functional χ^e is defined for individual 20-noded element. If we minimize χ^e with respect to the nodal temperature vector, $\{T^e\}$, we will get a stationary value of χ which will satisfy Eqs. (2.1) and (2.2). The minimization of χ can be written as

$$\frac{\partial \chi}{\partial \{T^e\}} = \frac{\partial \chi^1}{\partial \{T^e\}} + \frac{\partial \chi^2}{\partial \{T^e\}} + \ldots + \frac{\partial \chi^n}{\partial \{T^e\}} = 0 \qquad (2.15)$$

where n stands for the number of elements.

The following relationships as given by Segerlind (1976) are used to differentiate Eq. (2.14) with respect to $\{T^e\}$:

$$\frac{\partial}{\partial \{T^e\}} \int_{V_e} \frac{1}{2} \{ T^e \}^T \left[B^e \right]^T \left[D^e \right] \left[B^e \right] \{ T^e \} \, dV$$

$$= \int_{V_e} [\, B^e \,]^T [\, D^e \,] [\, B \,] \{\, T^e \,\} \, dV \quad ; \tag{2.16}$$

$$\frac{\partial}{\partial \{T^e\}} \int_{V^e} \rho \, c^e \, [\, N^e \,] \frac{\partial \{T^e\}}{\partial t} [\, N^e \,] \{T^e\} \, dV$$

$$= \int_{V^e} \rho \, c^e \, [\, N^e \,] \frac{\partial \{T^e\}}{\partial t} [\, N^e \,]^T \, dV \quad ; \tag{2.17}$$

$$\frac{\partial}{\partial \{T^e\}} \int_{S_i^e} \frac{h^e}{2} \left([\, N^e \,] \{T^e\} \right)^2 dS = \int_{S_i^e} h^e \, [\, N^e \,]^T [\, N^e \,] \{T^e\} \, ds \quad ; \tag{2.18}$$

$$\frac{\partial}{\partial \{T^e\}} \int_{S_i^e} h^e \, T_\infty \, [\, N^e \,] \{T^e\} \, ds = \int_{S_i^e} h^e \, T_\infty \, [\, N^e \,]^T \, dS \quad ; \tag{2.19}$$

$$\frac{\partial}{\partial \{T^e\}} \int_{S_i^e} \frac{\sigma \, \varepsilon}{5} \left([\, N^e \,] \{T^e\} \right)^5 dS = \int_{S_i^e} \sigma \, \varepsilon \, [\, N^e \,]^T \left([\, N^e \,] \{T^e\} \right)^4 dS \quad ;$$

(2.20)

$$\frac{\partial}{\partial\{T^e\}}\int_{S_i^e} \frac{h^e}{2}\, T_\infty^2\, dS = 0 \qquad \text{and} \tag{2.21}$$

$$\frac{\partial}{\partial\{T^e\}} \int_{S_i^e} \sigma\, \varepsilon\, T_\infty^4 \left[N^e \right] \{T^e\}\, ds = \int_{S_i^e} \sigma\, \varepsilon\, T_\infty^4 \left[N^e \right]^T dS \tag{2.22}$$

Substituting these relationships into the Eq. (2.14) and summing up the contributions of each element as per Eq. (2.15), we get

$$\begin{aligned}
\frac{\partial \chi}{\partial\{T^e\}} = \sum_{e=1}^{n} & \int_{V^e} \left[B^e \right]^T \left[D^e \right] \left[B^e \right] \{T^e\}\, dV \\
& + \int_{V^e} \rho\, c^e \left[N^e \right] \frac{\partial\{T^e\}}{\partial t} \left[N^e \right]^T dS \\
+ \int_{S_i^e} h^e \left[N^e \right]^T & \left[N^e \right] \{T^e\}\, dS - \int_{S_i^e} h^e\, T_\infty \left[N^e \right]^T dS \\
& + \int_{S_i^e} \sigma\, \varepsilon \left[N^e \right]^T \left(\left[N^e \right] \{T^e\} \right)^4 dS \\
& - \int_{S_i^e} \sigma\, \varepsilon\, T_\infty^4 \left[N^e \right]^T dS = 0
\end{aligned} \tag{2.23}$$

The expressions for various elemental matrices are:

ELEMENTAL CAPACITANCE MATRIX $[CP^e]$ can be expressed as

$$\left[CP^e \right] = \int_{V^e} \rho\, c^e \left[N^e \right]^T \left[N^e \right] dV\,, \tag{2.24}$$

ELEMENTAL CONDUCTION MATRIX $[KC^e]$ can be expressed as

$$[KC^e] = \int_{V^e} [B^e]^T [D^e] [B^e] \, dV + \int_{S_i^e} h^e [N^e]^T [N^e] \, dS \, , \tag{2.25}$$

The FORCE VECTOR $\{F_c^e\}$ for the convection process can be written as

$$\{F_c^e\} = \int_{S_i^e} h^e T_\infty [N^e]^T \, dS \, , \text{ and} \tag{2.26}$$

the FORCE VECTOR $\{F_r^e\}$ for the radiation process will be

$$\{F_r^e\} = \int_{S_i^e} \sigma \, \varepsilon \, T_\infty^4 [N^e]^T \, dS - \int_{S_i^e} \sigma \, \varepsilon \, [N^e] \left([N^e] \{T^e\} \right)^4 dS \tag{2.27}$$

In case of isoparametric finite elements(shown in Fig. 2.3), the most striking feature is that their sides may be curved and that they make use of a special coordinate system (ξ, η, ζ), (the shape functions, $[N_i]$, are defined for the variation of the local coordinate system from +1 to -1). Therefore we can have: $\xi = \pm 1$; $\eta = \pm 1$; and $\zeta = \pm 1$. The shape functions $[N_i]$, for the 20-noded isoparametric element can be expressed as [Zienkiewicz, 1971]:

<u>Corner Nodes</u>

$$N_i = \frac{1}{8} (1 + \xi \, \xi_i) (1 + \eta \, \eta_i) (1 + \zeta \, \zeta_i) (\xi \, \xi_i + \eta \, \eta_i + \zeta \, \zeta_i - 2) \tag{2.28}$$

The details of Eq. (2.28) are given in APPENDIX A.

Typical Mid-side nodes

$$N_i = \frac{1}{4}\left(1 - \xi^2\right)\left(1 + \eta\,\eta_i\right)\left(1 + \zeta\,\zeta_i\right) \tag{2.29}$$

for the case when $\xi_i = 0$, $\eta_i = \pm 1$, and $\zeta_i = \pm 1$. The subscript i stands for the ith node of the twenty-noded element in Eqs. (2.28) and (2.29).

Similarly one can write the equations corresponding to Eq. (2.29) as shown in APPENDIX B.

The expression for elemental matrix $[CP^e]$ in terms of ξ, η, ζ can be written as

$$\left[CP^e\right] = \int_{-1}^{+1}\int_{-1}^{+1}\int_{-1}^{+1} \rho\, c^e \left[\, N^e(\xi, \eta, \zeta)\,\right]^T \left[\, N^e(\xi, \eta, \zeta)\,\right] \left|J(\xi, \eta, \zeta)\right| d\xi d\eta d\zeta \tag{2.30}$$

The term $\left|J(\xi,\eta,\zeta)\right|$ is the determinant of Jacobian matrix which relates the derivatives of the temperature {T} with respect to the local coordinate system $\{\xi, \eta, \zeta\}$ to the derivatives of {T} with respect to the global coordinate system {x, y, z}. The following chain rule evaluates the Jacobian matrix:

$$\frac{\partial T}{\partial \xi} = \frac{\partial T}{\partial x}\frac{\partial x}{\partial \xi} + \frac{\partial T}{\partial y}\frac{\partial y}{\partial \xi} + \frac{\partial T}{\partial z}\frac{\partial z}{\partial \xi} \tag{2.31}$$

where T is a function of x, y, and z.

Hence, the Jacobian matrix [J] can be expressed as

$$[J] = \begin{bmatrix} \frac{\partial x}{\partial \xi} & \frac{\partial y}{\partial \xi} & \frac{\partial z}{\partial \xi} \\ \frac{\partial x}{\partial \eta} & \frac{\partial y}{\partial \eta} & \frac{\partial z}{\partial \eta} \\ \frac{\partial x}{\partial \zeta} & \frac{\partial y}{\partial \zeta} & \frac{\partial z}{\partial \zeta} \end{bmatrix} \tag{2.32}$$

The element J_{11} of [J] can be written as

$$J_{11} = \frac{\partial x}{\partial \xi} = \frac{\partial}{\partial \xi}\Big(\underset{1 \times 20}{[Ni]^e} \Big) \underset{20 \times 1}{\{x\}^e} \tag{2.33}$$

where $\{x\}^e$ contains all the Cartesian coordinates along the x-direction of the 20-noded element with i = 1, 2, 3,..., 20 and $[N_i]^e = \{N_1, N_2, N_3,...N_{20}\}$. The similar procedure is followed for the other elements of matrix [J].

Therefore for the twenty-noded isoparametric element

$$[J(\xi,\eta)] = \begin{bmatrix} \sum_{i=1}^{i=20} \frac{\partial N_i}{\partial \xi}(\xi,\eta,\zeta)x_i & \sum_{i=1}^{i=20} \frac{\partial N_i}{\partial \xi}(\xi,\eta,\zeta)y_i & \sum_{i=1}^{i=20} \frac{\partial N_i}{\partial \xi}(\xi,\eta,\zeta)z_i \\ \sum_{i=1}^{i=20} \frac{\partial N_i}{\partial \eta}(\xi,\eta,\zeta)x_i & \sum_{i=1}^{i=20} \frac{\partial N_i}{\partial \eta}(\xi,\eta,\zeta)y_i & \sum_{i=1}^{i=20} \frac{\partial N_i}{\partial \eta}(\xi,\eta,\zeta)z_i \\ \sum_{i=1}^{i=20} \frac{\partial N_i}{\partial \zeta}(\xi,\eta,\zeta)x_i & \sum_{i=1}^{i=20} \frac{\partial N_i}{\partial \zeta}(\xi,\eta,\zeta)y_i & \sum_{i=1}^{i=20} \frac{\partial N_i}{\partial \zeta}(\xi,\eta,\zeta)z_i \end{bmatrix} \tag{2.34}$$

The inverse of the Jacobian matrix will be indicated as

$$\begin{Bmatrix} \dfrac{\partial N_i}{\partial x} \\ \dfrac{\partial N_i}{\partial y} \\ \dfrac{\partial N_i}{\partial z} \end{Bmatrix} = [J]^{-1} \begin{Bmatrix} \dfrac{\partial N_i}{\partial \xi} \\ \dfrac{\partial N_i}{\partial \eta} \\ \dfrac{\partial N_i}{\partial \zeta} \end{Bmatrix} \tag{2.35}$$

The expression for elemental conduction matrix $[KC^e]$ can be expressed as

$$\begin{aligned} [KC^e] = & \int_{-1}^{+1}\int_{-1}^{+1}\int_{-1}^{+1} [B^e(\xi, \eta, \zeta)]^T [D^e] [B^e(\xi, \eta, \zeta)] \; |J(\xi, \eta, \zeta)| \, d\xi \, d\eta \, d\zeta \\ & + \int_{-1}^{+1}\int_{-1}^{+1} h^e [N^e(\xi, \eta)]^T [N^e(\xi, \eta)] \; |J(\xi, \eta)| \, d\xi \, d\eta \end{aligned} \tag{2.36}$$

The matrix $[B^e]$ in the equation above is expressed as

$$[B(\xi,\eta,\zeta)] = [J(\xi,\eta,\zeta)]^{-1} \begin{bmatrix} \dfrac{\partial N_1}{\partial \xi} & \dfrac{\partial N_2}{\partial \xi} & \cdots & \dfrac{\partial N_r}{\partial \xi} \\ \dfrac{\partial N_1}{\partial \eta} & \dfrac{\partial N_2}{\partial \eta} & \cdots & \dfrac{\partial N_r}{\partial \eta} \\ \dfrac{\partial N_1}{\partial \zeta} & \dfrac{\partial N_2}{\partial \zeta} & \cdots & \dfrac{\partial N_r}{\partial \eta} \end{bmatrix} \tag{2.37}$$

The expressions for elemental vectors $\{F_c^e\}$ and $\{F_{re}\}$ can be expressed as

$$\{F_c^e\} = \int_{-1}^{+1}\int_{-1}^{+1} h^e \, T_\infty [N^e(\xi, \eta)]^T \; |J(\xi, \eta)| \, d\xi \, d\eta \tag{2.38}$$

$$\left\{F_r^e\right\} = \int_{-1}^{+1}\int_{-1}^{+1} \sigma\ \varepsilon\ T_\infty^4 \left[N^e(\ \xi,\ \eta\ )\right]^T\ |J(\xi,\eta)|\ d\xi\ d\eta$$
$$- \int_{-1}^{+1}\int_{-1}^{+1} \sigma\ \varepsilon\ \left[N^e\ (\ \xi,\ \eta)\right]^T \left(\left[N^e(\ \xi,\ \eta\ )\right] \left\{T^e\ (\ \xi,\ \eta\ )\right\} \right)^4\ |J(\xi,\eta)|\ d\xi\ d\eta \tag{2.39}$$

2.3 DERIVATION OF THE ELEMENTAL EQUATIONS FOR $[CP^e]$, $[K^e]$, $\{F_c^e\}$, $\{F_r^e\}$

Using the symbolic software package 'Maple', the evaluations of the elemental capacitance matrix $[CP^e]$, conduction matrix $[KC^e]$, the force vector for the convection $\{F_c^e\}$, and the force vector for the radiation $\{F_r^e\}$ in terms of ξ, η, ζ were done numerically by evaluating the volume integral in these equations. For isoparametric formulation, the elemental matrices and vectors mentioned above were integrated using Gauss quadrature technique. A quadratic polynomial for each side of the 20-noded element was used. Thus 2 Gauss points on each side of the element and 8 Gauss points in total were sufficient to integrate each of the elemental matrices. The expressions for the elemental matrices $[CP^e]$, $[KC^e]$, $\{F_c^e\}$, $\{F_r^e\}$ for the case of a twenty-noded are given in APPENDIX C.

Using Gauss quadrature, final expressions for various matrices would be:

$$\left[CP^e\right] = \sum_{i=1}^{2}\ \sum_{j=1}^{2}\ \sum_{k=1}^{2}\ W_i\ W_j\ W_k\ \rho\ c^e\ \left[N^e\ (\xi,\ \eta,\ \zeta\ )\right]^T \left[N^e(\xi,\ \eta,\ \zeta)\right]\ |J(\xi,\ \eta,\ \zeta)| \tag{2.40}$$

$$[KC^e] = \sum_{i=1}^{2} \sum_{j=1}^{2} \sum_{k=1}^{2} W_i\, W_j\, W_k\, [B^e(\xi, \eta, \zeta)]^T\, [D^e]\, [B^e(\xi, \eta, \zeta)]\, |J(\xi\ \eta\ \zeta)|$$

$$+ \sum_{i=1}^{2} \sum_{j=1}^{2} W_i\, W_j\, h^e\, [N^e(\xi, \eta)]^T\, [N^e(\xi, \eta)]\, |J(\xi, \eta)|$$

(2.41)

$$\{F_c^e\} = \sum_{i=1}^{2} \sum_{j=1}^{2} W_i\, W_j\, h^e\, T_\infty\, [N^e(\xi, \eta)]^T\, |J(\xi, \eta)| \tag{2.42}$$

$$\{F_r^e\} = \sum_{i=1}^{2} \sum_{j=1}^{2} W_i\, W_j\, \sigma\, \varepsilon\, T_\infty^4\, [N^e(\xi, \eta)]^T\, |J(\xi, \eta)|$$

$$- \sum_{i=1}^{2} \sum_{j=1}^{2} W_i\, W_j\, \sigma\, \varepsilon\, [N^e(\xi, \eta)]^T \left([N^e(\xi, \eta)]\, \{T^e(\xi, \eta)\} \right)^4\, |J(\xi, \eta)|$$

(2.43)

where W_i, W_j, and W_k are corresponding weighting functions in the ξ, η, and ζ directions respectively.

After getting the expressions for the elemental matrices and substituting them into the Eq. (2.23), we get the following global equations:

$$[CP^G]\frac{\partial\{T^G\}}{\partial t} + [KC^G]\, \{T^G\} = \{F_c^G\} + \{F_r^G\} \tag{2.44}$$

In the Eq. (2.44), because of the non-linearity introduced by the radiation term, we get a non-linear set of partial differential equation. In the present work, we use the Crank-Nicolson finite difference method to transform the equations above into a system of non-

linear algebraic equations. Therefore in the time domain, for the time step Δt, the first derivative of the nodal temperature vector will be

$$\frac{d\{T^G\}_t}{dt} = \frac{\{T^G\}_{t+\frac{\Delta t}{2}} - \{T^G\}_{t-\frac{\Delta t}{2}}}{\Delta t} \tag{2.45}$$

Similar expressions can be written for $\{T^G\}_t$ and $\{F^G\}_t$ in the following way:

$$\{T^G\}_t = \frac{\{T^G\}_{t+\frac{\Delta t}{2}} + \{T^G\}_{t-\frac{\Delta t}{2}}}{2} \quad \text{and} \tag{2.46}$$

$$\{F^G\}_t = \frac{\{F^G\}_{t+\frac{\Delta T}{2}} + \{F^G\}_{t-\frac{\Delta t}{2}}}{2} \tag{2.47}$$

Substituting Eqs. (2.45), (2.46), and (2.47) into the Eq. (2.44), we get

$$\frac{1}{\Delta t}[CP^G]\{T^G\}_{t+\frac{\Delta T}{2}} - \frac{1}{\Delta t}[CP^G]\{T^G\}_{t-\frac{\Delta t}{2}}$$

$$+ \frac{1}{2}[KC^G]\{T^G\}_{t+\frac{\Delta t}{2}} + \frac{1}{2}[K^G]\{T^G\}_{t-\frac{\Delta t}{2}}$$

$$= \frac{1}{2}\{F_C^G\}_{t+\frac{\Delta T}{2}} + \frac{1}{2}\{F_C^G\}_{t-\frac{\Delta t}{2}} + \frac{1}{2}\{F_R^G\}_{t+\frac{\Delta t}{2}} + \frac{1}{2}\{F_R^G\}_{t-\frac{\Delta t}{2}} \tag{2.48}$$

The unknown terms in the equation above are the nodal temperature vector $\{T^G\}$ and the vectors $\{F_C{}^G\}$, $\{F_R{}^G\}$ at time $t+\Delta t/2$. All the vectors and the matrices at the previous instant of time $(t-\Delta t/2)$ are known. Therefore the Eq. (2.48) can be written as

$$\left(\left[KC^G\right] + \frac{2}{\Delta t}\left[CP^G\right]\right)\left\{T^G\right\}_{t+\frac{\Delta t}{2}} = \left(\frac{2}{\Delta t}\left[CP^G\right] - \left[KC^G\right]\right)$$
$$\left\{T^G\right\}_{t-\frac{\Delta t}{2}} + \left\{F_c^G\right\}_{t+\frac{\Delta t}{2}} + \left\{F_c^G\right\}_{t-\frac{\Delta t}{2}} + \left\{F_r^G\right\}_{t+\frac{\Delta t}{2}} + \left\{F_r^G\right\}_{t-\frac{\Delta t}{2}} \tag{2.49}$$

After substituting all the known quantities at time (t-Δt/2) one obtains the above equation in the form (the vector { A_1 } contains values at time (t -Δt/2))

$$\left(\left[KC^G\right] + \frac{2}{\Delta t}\left[CP^G\right]\right)\left\{T^G\right\}_{t+\frac{\Delta t}{2}} = \left\{A_1\right\} + \left\{F_c^G\right\}_{t+\frac{\Delta t}{2}} + \left\{F_R^G\right\} \tag{2.50}$$

The vector $\{A_1\}$ is known at this point. The vectors $\{F_c^G\}_{t+\Delta/2}$ and $\{F_r^G\}_{t+\Delta/2}$ are to be evaluated using the nodal temperatures at time t+Δt/2. We can use an iteration procedure to solve the Eq. (2.50) for the nodal temperatures. In this procedure, we assume a nodal temperature vector $\{T^G\}$ at time t+Δt/2, which is same as the nodal temperature at time t-Δt/2. This assumed value is substituted on the right hand side of the Eq. (2.50). Then the Eq.(2.50) reduces to

$$\left(\left[KC^G\right] + \frac{2}{\Delta t}\left[CP^G\right]\right)\left\{T^G\right\}_{t+\frac{\Delta t}{2}} = \left\{A_2\right\} \tag{2.51}$$

where $\{A_2\}$ is now known. Solution of Eq. (2.51) will give us the unknown nodal temperature vector $\{T^G\}_{t+\Delta/2}$. The resultant nodal temperatures are compared with the assumed nodal temperatures and if the convergence criterion is not met, then for the next iteration the calculated nodal temperatures become the assumed nodal temperatures. The iterations continue till we get the converged transient nodal temperatures of the turbine blade. The transient nodal

temperatures are found in the airfoil cross-section at different heights of the turbine blade. Once the transient temperature distribution is known, the transient temperature gradients along the x and y directions at different heights can be calculated by using the following equation (2.52) for a twenty-noded element:

$$\{g^e\} = \begin{Bmatrix} \dfrac{\partial T}{\partial x} \\ \dfrac{\partial T}{\partial y} \end{Bmatrix} = [B^e] \begin{Bmatrix} T_1 \\ T_2 \\ T_3 \\ \cdot \\ \cdot \\ \cdot \\ T_{20} \end{Bmatrix} \tag{2.52}$$

2.4 ILLUSTRATION OF THEORY

The heat transfer process within a turbine blade was studied on a blade made of AISI 4140, which is a chromium alloy steel, and is used in the manufacturing of aircraft gas turbine blades. In order to carry out the finite element analysis of this turbine blade, the blade was divided into 35 curved, solid, C^0 continuity, quadratic, serendipity, twenty noded isoparametric elements as shown in Fig. 2.1. The convergence in the nodal temperatures was achieved by refining the time increment. A Fortran code was written in order to carry out the convergence studies. The convective heat transfer coefficient were assumed to vary with temperature of the blade. The values for these variations were obtained from Mukherjee (1978). All the material properties such as α, E, c, k, etc

of the blade in the present analysis were selected as a function of temperature and were obtained from (Cubberly, 1980). Table in APPENDIX D shows the values of these parameters at different temperatures.

2.5 TEMPERATURE GRADIENT DISTRIBUTION ACROSS THE AIRFOIL CROSS-SECTION AT DIFFERENT HEIGHTS OF THE TURBINE BLADE

Bahree (1987) has shown that the effect of radiative heat flux is quite significant at elevated temperatures as the radiative heat flux contains terms made up of higher powers of the nodal temperatures. Therefore all the results include the radiative terms.

Assuming the room temperature as the initial condition, one of the most important findings of this investigation was to observe the change in transient temperature and temperature gradients along the z-direction of the turbine blade modelled as a three-dimensional problem. Fig. 2.4 to Fig. 2.10 show the change in temperature variation in the nodes along z-axis at different times at different cross-sections of the turbine blade. From these graphs, it is clear that there is a change in temperature along the height of the blade. Fig. 2.11 to Fig. 2.15 show the temperature contours along different heights of the blade at time t = 150 sec. Fig. 2.16 to Fig. 2.20 show the variation of temperature gradients along the x and y directions at time t = 150 seconds as we go along the height of the blade. The careful study of these gradients is very important to understand the dynamics of the heat transfer process. An interesting observation can be made from these figures that the temperature gradient increases along the height of the blade which is in accordance with the direction of the heat flux, which is from the top to the bottom. This helps us to conclude that, in addition to the

thermal gradients along x and y axes of the blade, the thermal gradients along the height of the turbine blade are also very significant during the transient state and as such can not be neglected in calculating the overall stress distribution in the blade.

2.6 TRANSIENT THERMAL STRESS DETERMINATION - THE MATHEMATICAL MODEL

The next step in the heat transfer analysis is the calculation of thermal stresses caused by the temperature variation across the cross-section and along the height of the turbine blade.

The elemental stress is calculated using Hooke's law. Using this law, the elemental stress and strain vectors are related as given by [Segerlind, 1976]

$$\{\sigma^e\} = [D_1^e]\{\varepsilon^e\} - [D_1^e]\{\varepsilon_o^e\} \tag{2.53}$$

where

$\{\varepsilon^e\}$ is the elemental strain vector

$\{\varepsilon_o^e\}$ is the elemental initial strain vector

$\{\sigma^e\}$ is the elemental stress vector

$[D_1^e]$ is the material property matrix.

Stress components for thermal stresses analysis can be written as

$\{\sigma\}^T = [\sigma_{xx}, \sigma_{yy}, \sigma_{zz}, 0, 0, 0]$

Similarly, the strain components are

$\{\varepsilon\}^T = [\varepsilon_{xx}, \varepsilon_{yy}, \varepsilon_{zz}, 0, 0, 0]$

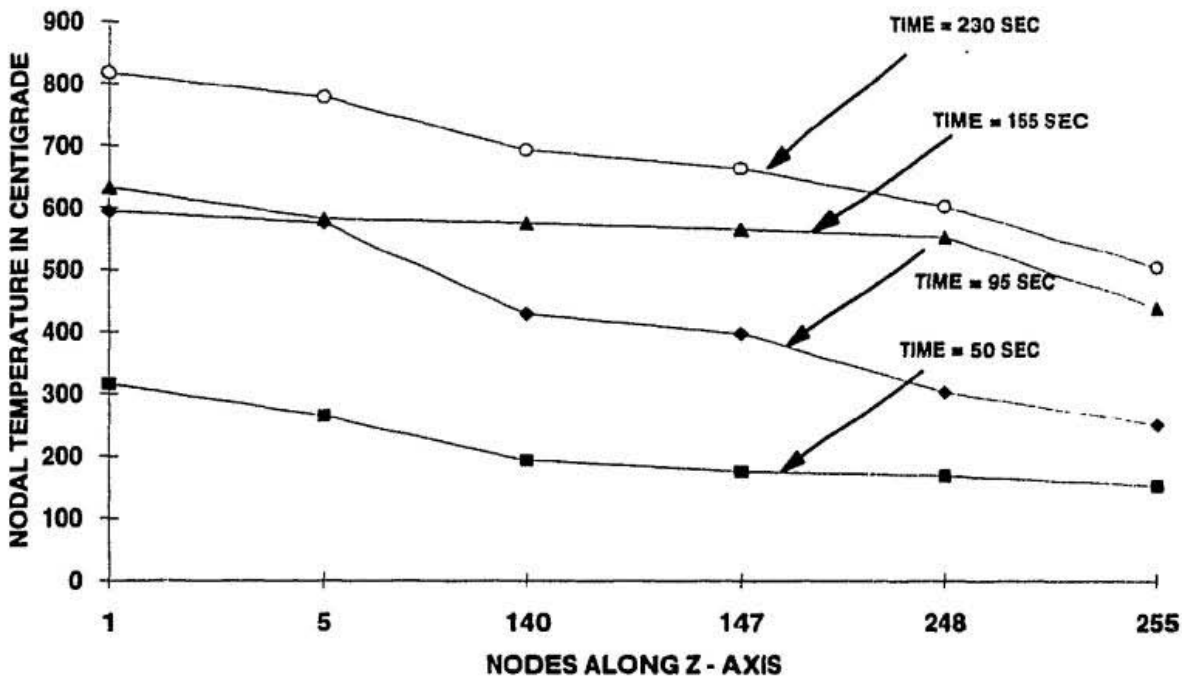

Fig. 2.4 NODAL TEMPERATURE VARIATION ALONG THE Z - AXIS AT LEADING EDGE

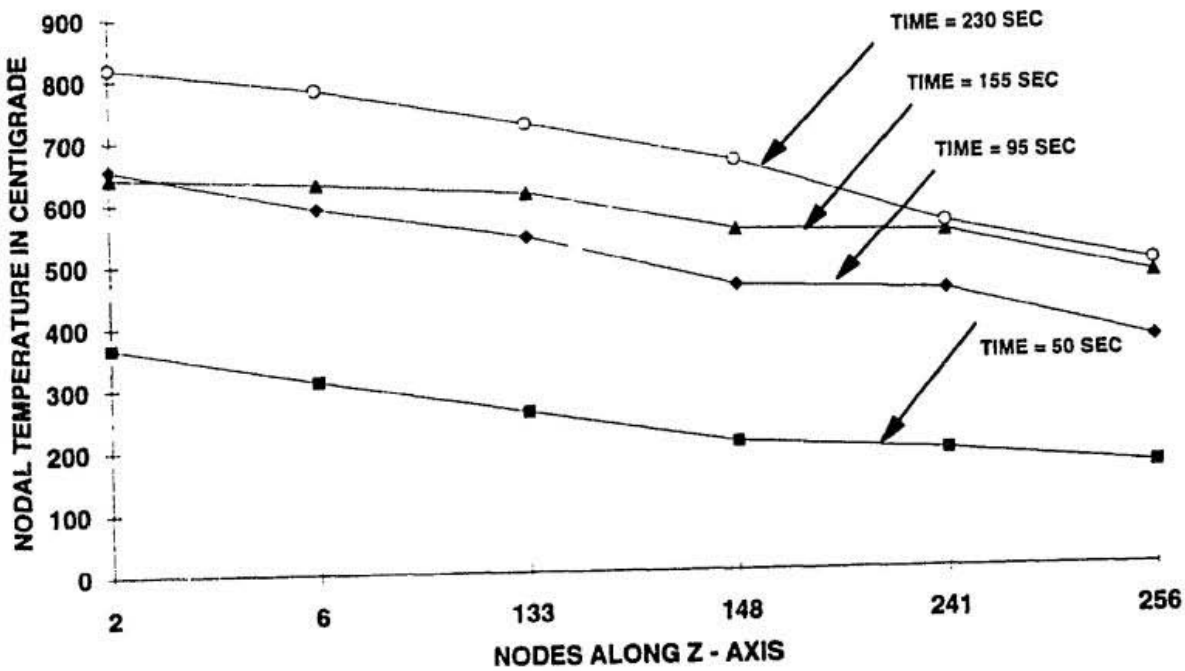

Fig. 2.5 NODAL TEMPERATURE VARIATION ALONG THE Z - AXIS AT 15 % CHORD LENGTH

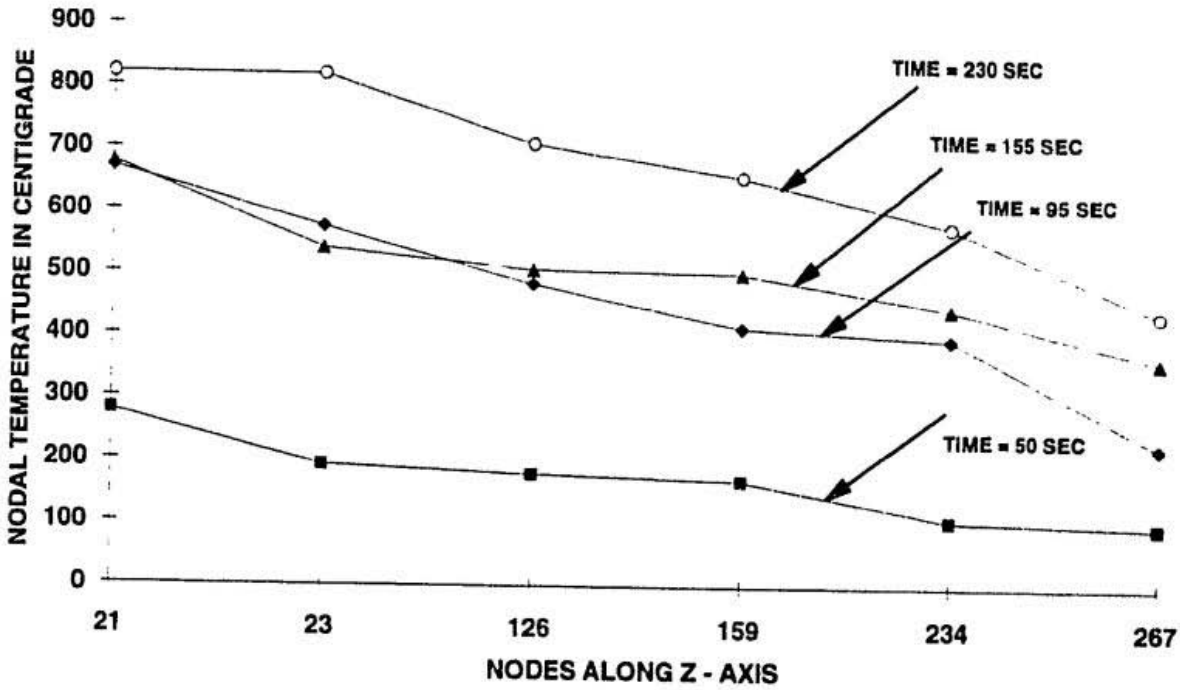

Fig. 2.6 NODAL TEMPERATURE VARIATION ALONG THE Z - AXIS AT 30 % CHORD LENGTH

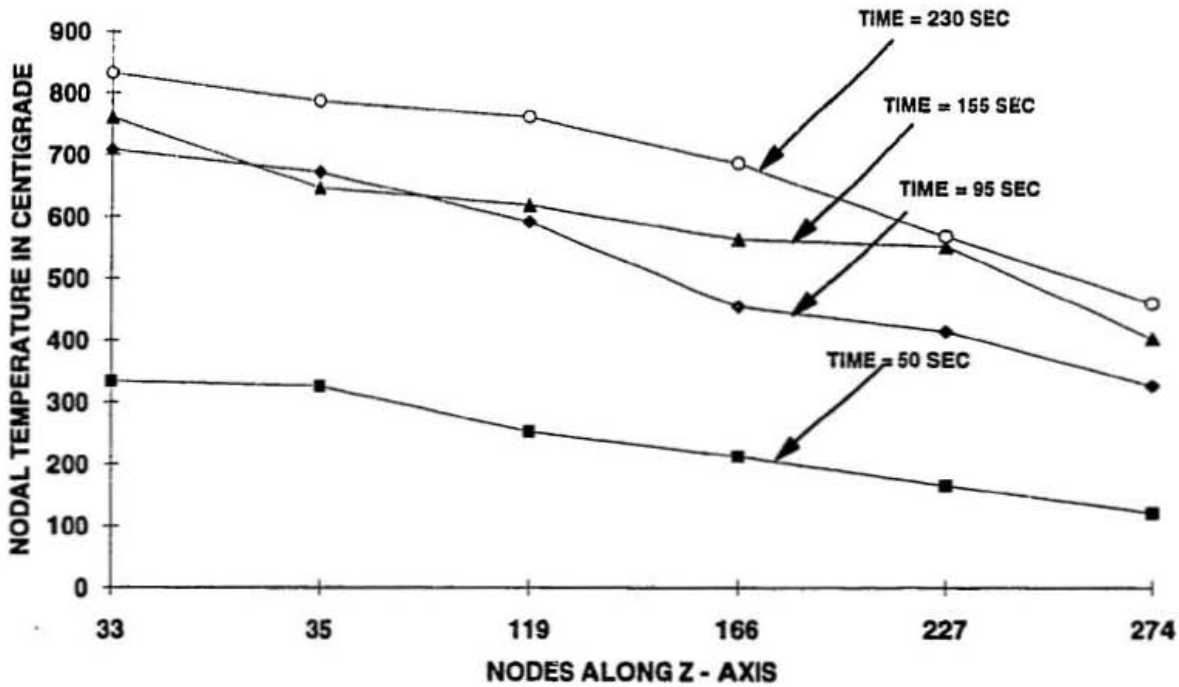

Fig. 2.7 NODAL TEMPERATURE VARIATION ALONG THE Z - AXIS AT 45 % CHORD LENGTH

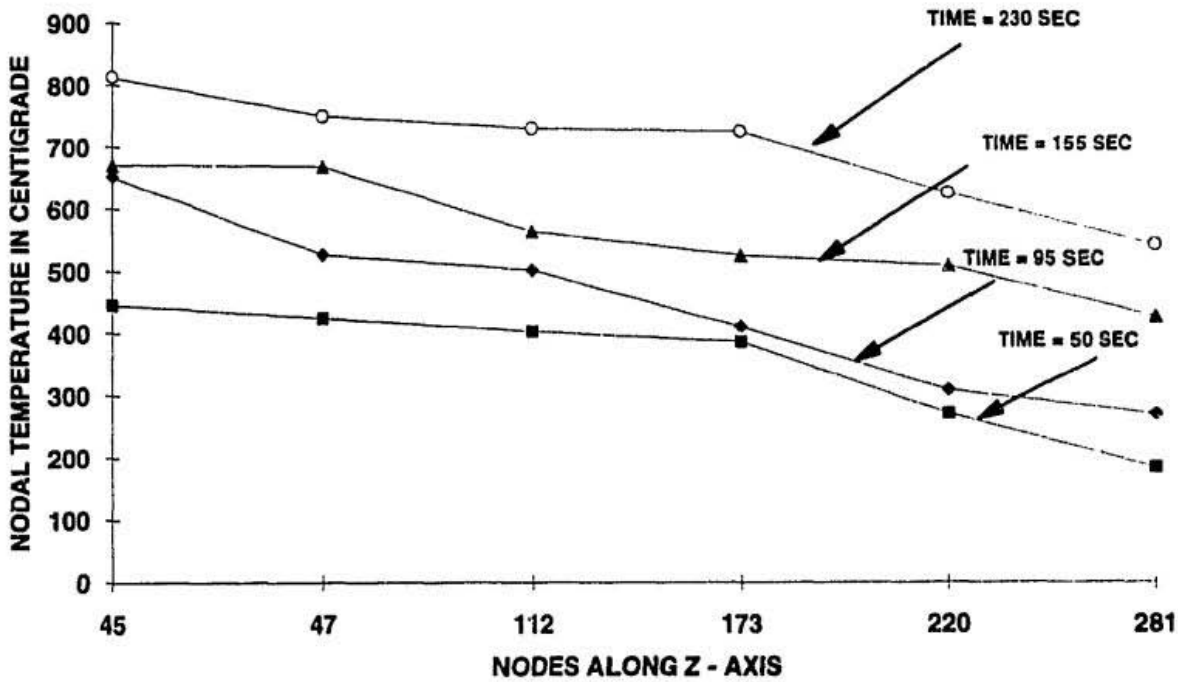

Fig. 2.8 NODAL TEMPERATURE VARIATION ALONG THE Z - AXIS AT 60 % CHORD LENGTH

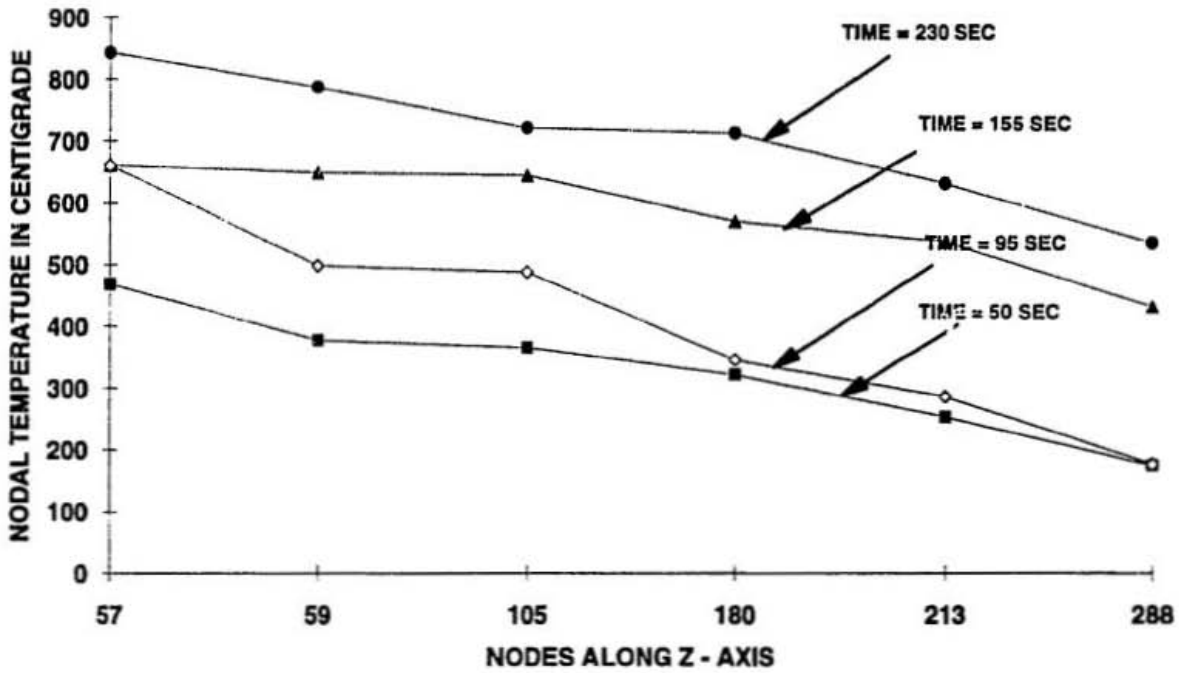

Fig. 2.9 NODAL TEMPERATURE VARIATION ALONG THE Z - AXIS AT 75 % CHORD LENGTH

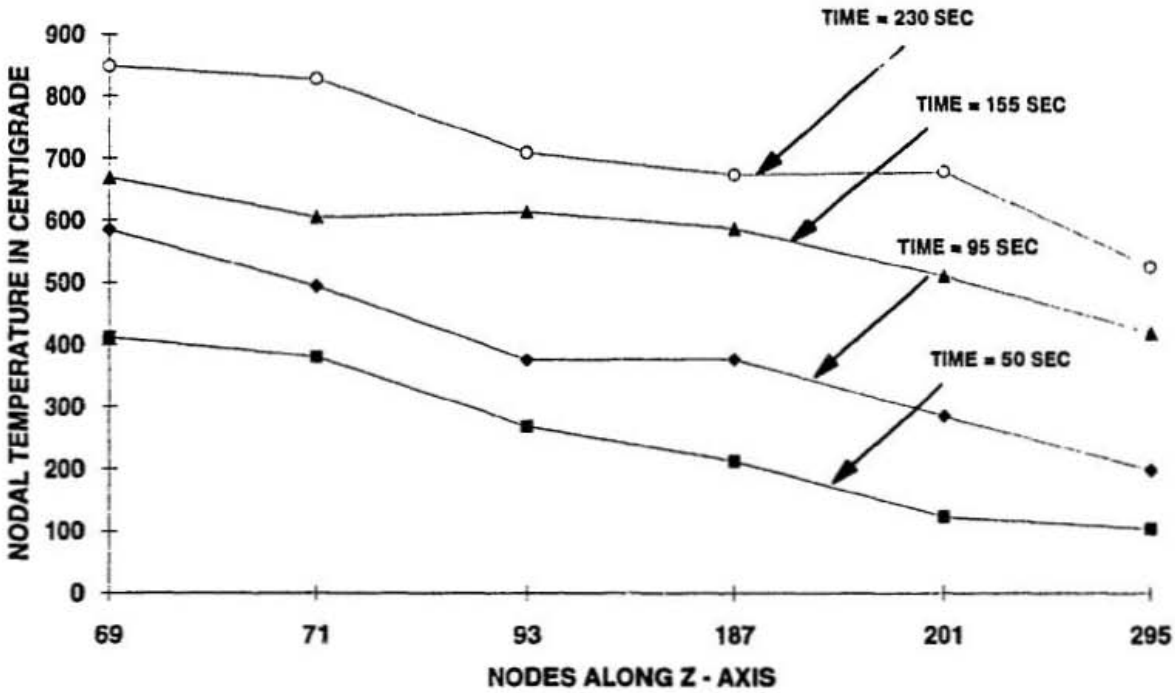

Fig. 2.10 NODAL TEMPERATURE VARIATION ALONG THE Z - AXIS AT TRAILING EDGE

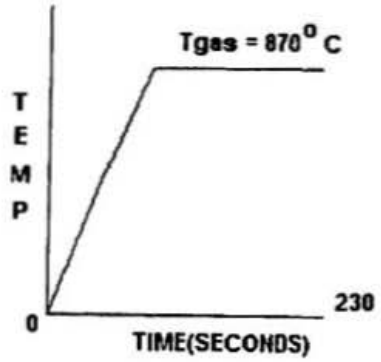

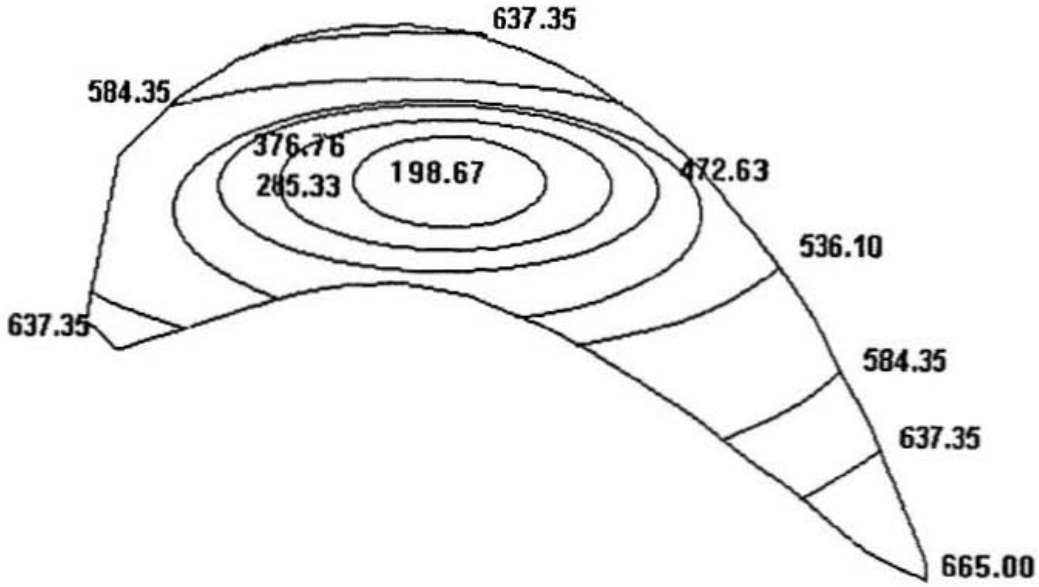

Fig. 2.11 TEMPERATURE CONTOURS ACROSS THE AIRFOIL SECTION AT t = 150 SEC (HEIGHT OF THE BLADE = 2.5 cm.)

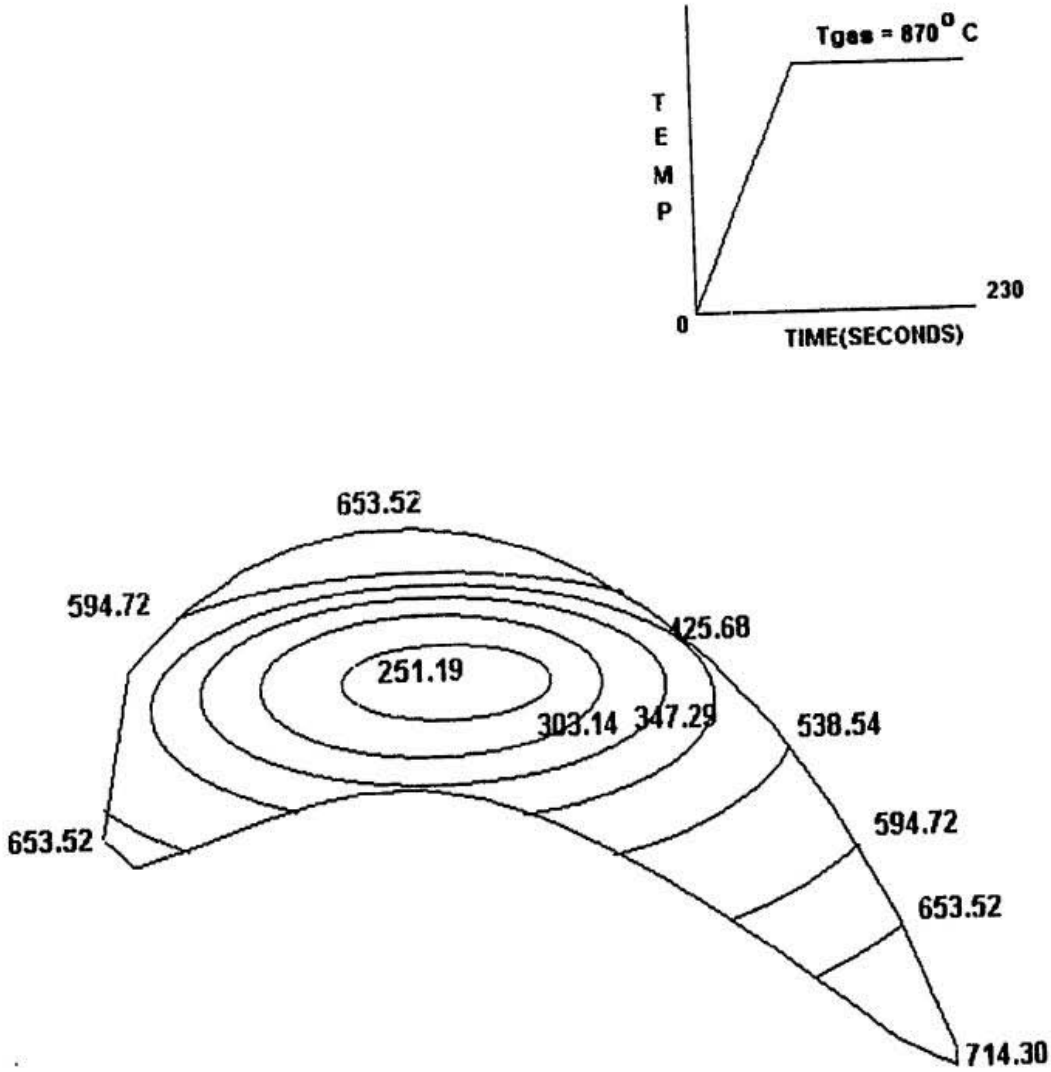

Fig. 2.12 TEMPERATURE CONTOURS ACROSS THE AIRFOIL SECTION AT t = 150 SEC (HEIGHT OF THE BLADE = 5.0 cm.)

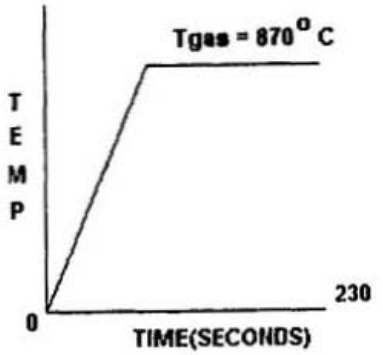

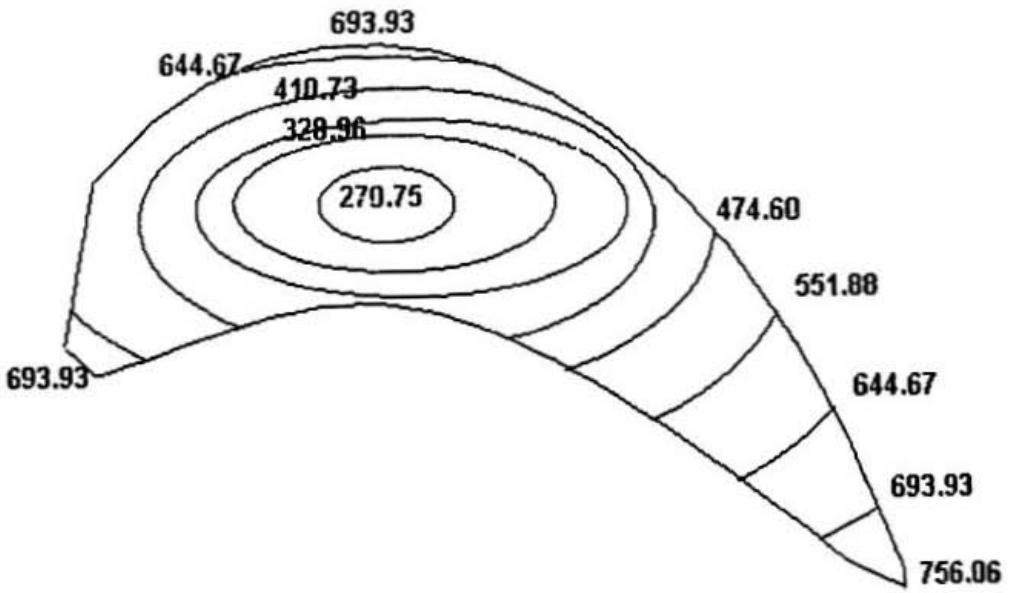

Fig. 2.13 TEMPERATURE CONTOURS ACROSS THE AIRFOIL SECTION AT t = 150 SEC (HEIGHT OF THE BLADE = 7.5 cm.)

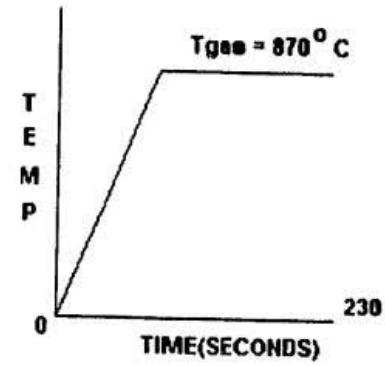

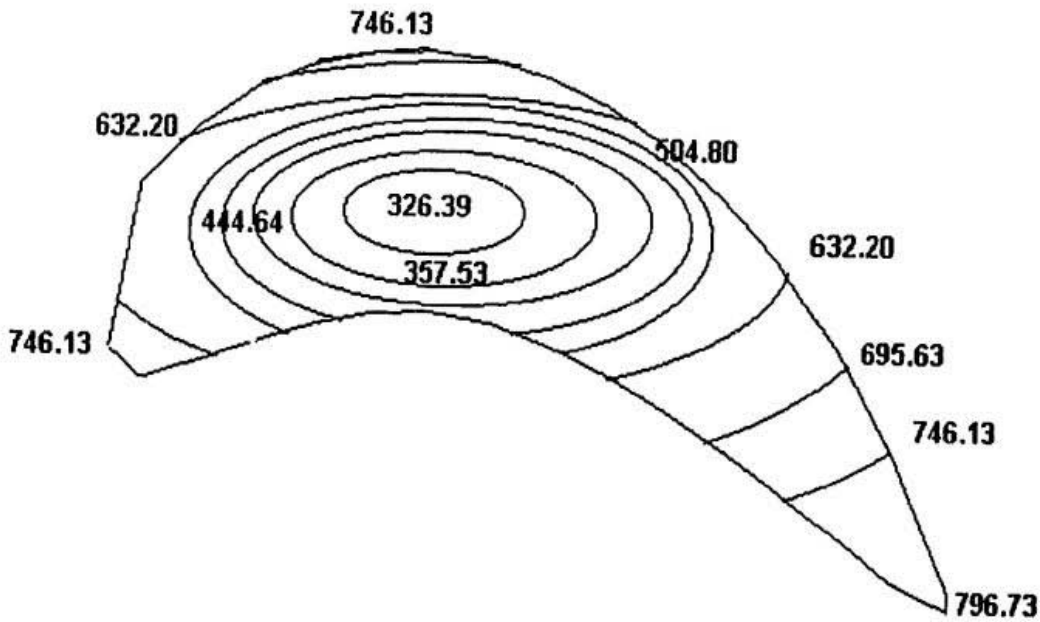

Fig. 2.14 TEMPERATURE CONTOURS ACROSS THE AIRFOIL SECTION AT t = 150 SEC (HEIGHT OF THE BLADE = 10.0 cm.)

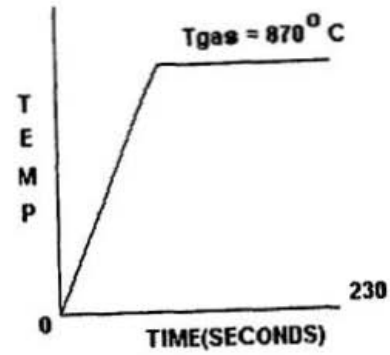

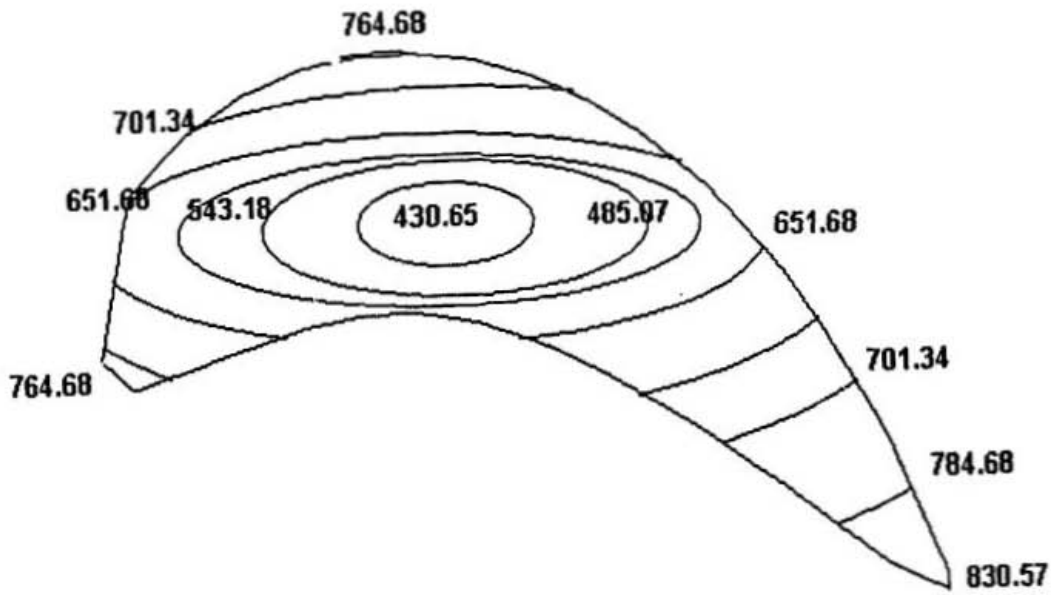

Fig. 2.15 TEMPERATURE CONTOURS ACROSS THE AIRFOIL SECTION AT t = 150 SEC (HEIGHT OF THE BLADE = 12.0 cm.)

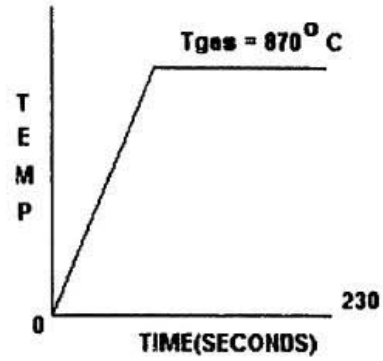

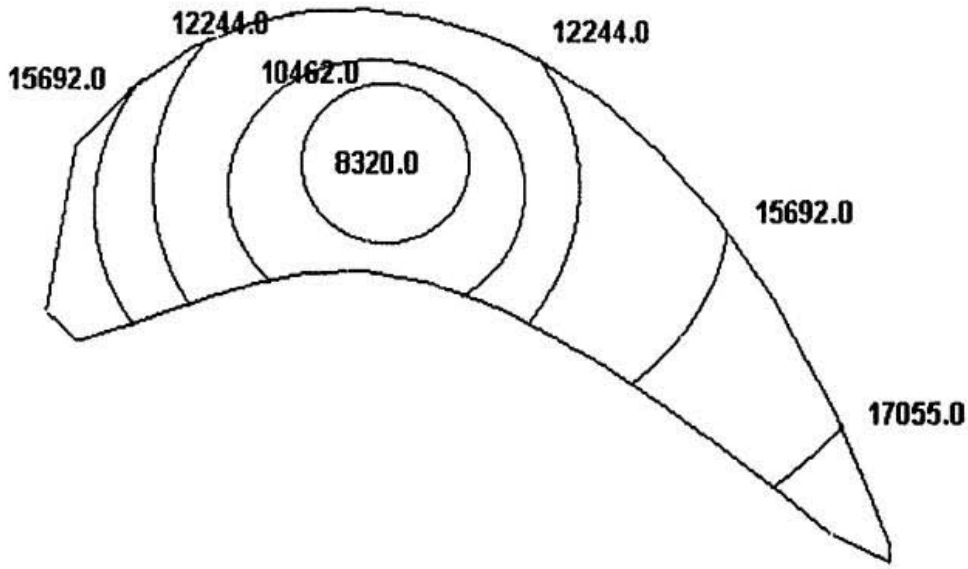

Fig. 2.16 TEMPERATURE GRADIENTS ACROSS THE BLADE CROSS-SECTION AT t = 150 SEC. (HEIGHT OF THE BLADE = 2.5 cm.)

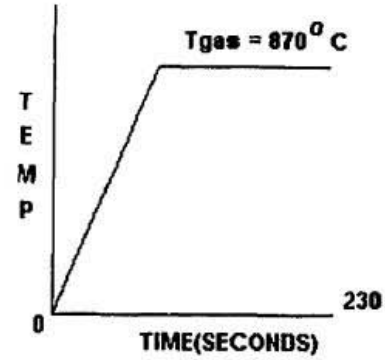

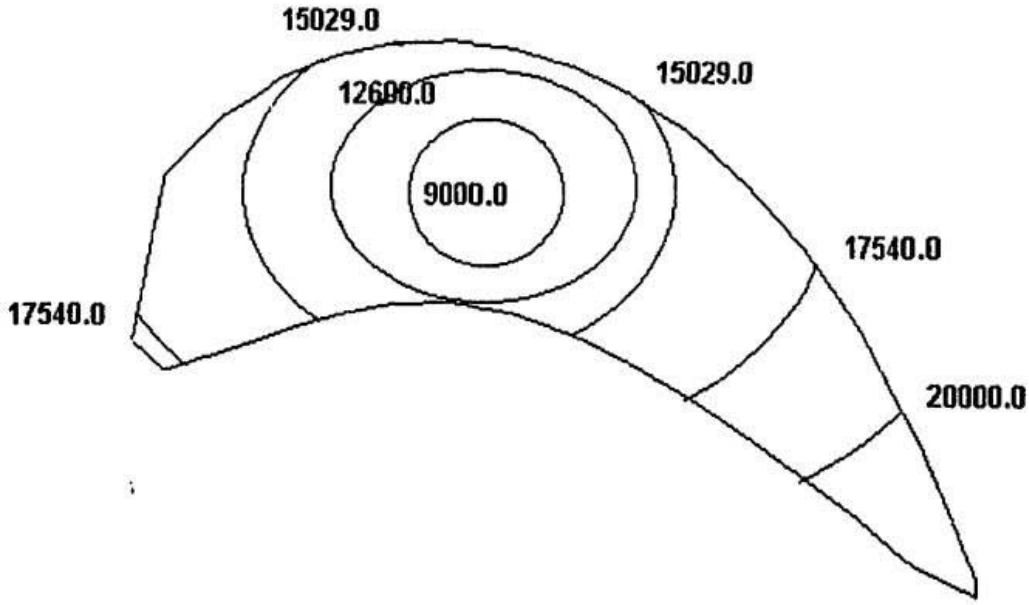

Fig. 2.17 TEMPERATURE GRADIENTS ACROSS THE BLADE CROSS-SECTION AT t = 150 SEC. (HEIGHT OF THE BLADE = 5.0 cm.)

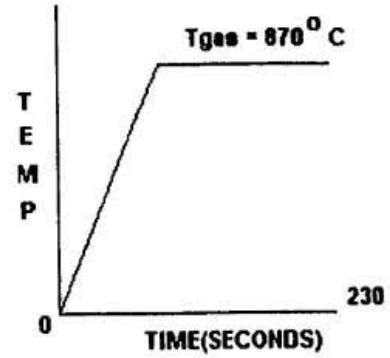

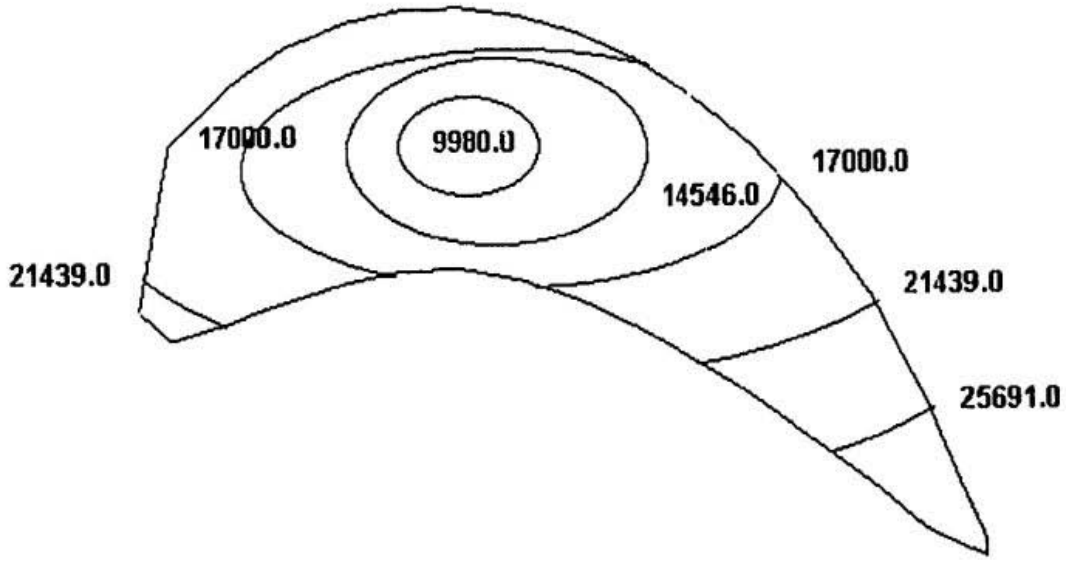

Fig. 2.18 TEMPERATURE GRADIENTS ACROSS THE BLADE CROSS-SECTION AT t = 150 SEC. (HEIGHT OF THE BLADE = 7.5 cm.)

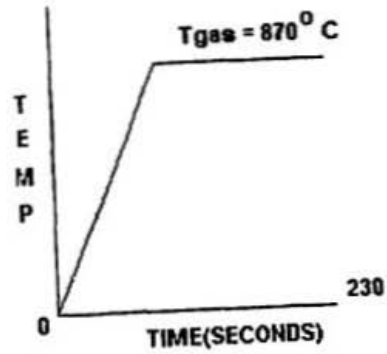

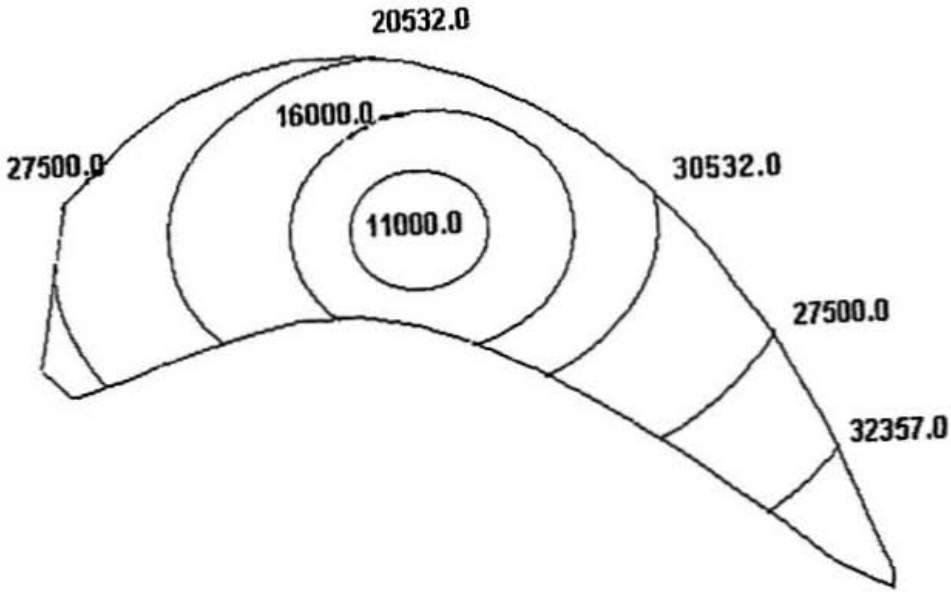

Fig. 2.19 TEMPERATURE GRADIENTS ACROSS THE BLADE CROSS-SECTION AT t = 150 SEC. (HEIGHT OF THE BLADE = 10.0 cm.)

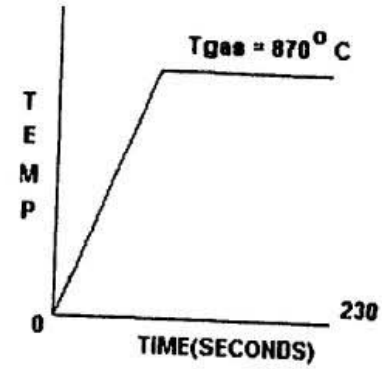

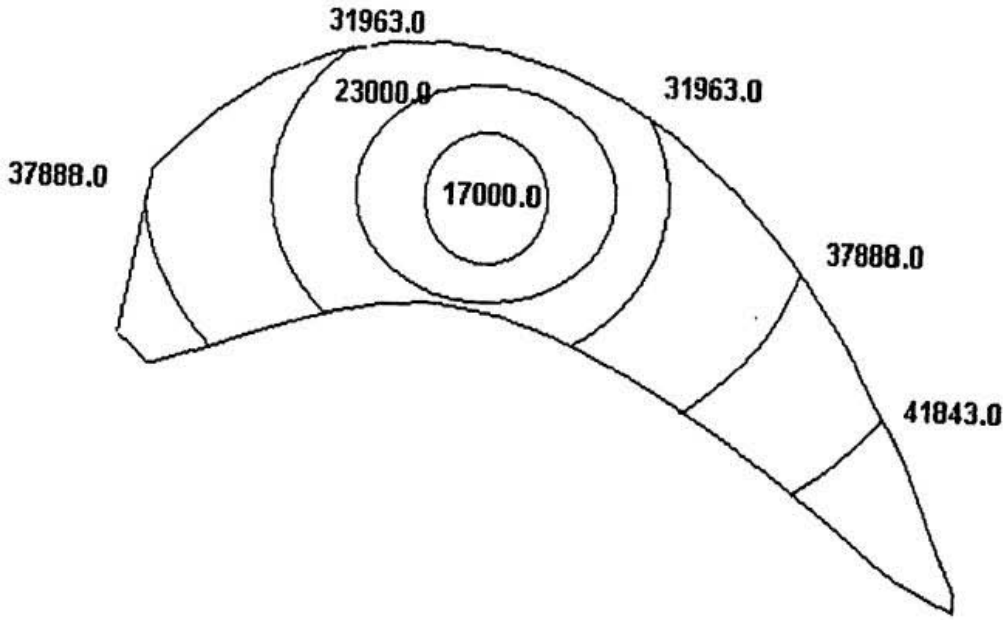

Fig. 2.20 TEMPERATURE GRADIENTS ACROSS THE BLADE CROSS-SECTION AT t = 150 SEC. (HEIGHT OF THE BLADE = 12.0 cm.)

In order to evaluate thermal stress analysis, we have to know the matrix $[B_1^e]$ which relates the strain in the element to the nodal displacements. The matrix $[B_1^e]$ for the stress analysis can be evaluated in the following way:

1. The strain vector in the global coordinate system can be related to the derivative of the displacement field as

$$\begin{Bmatrix} \varepsilon_{xx} \\ \varepsilon_{yy} \\ \varepsilon_{zz} \\ 0 \\ 0 \\ 0 \end{Bmatrix} = [P] \begin{Bmatrix} \frac{\partial u}{\partial x} \\ \frac{\partial u}{\partial y} \\ \frac{\partial u}{\partial z} \\ \frac{\partial v}{\partial x} \\ \frac{\partial v}{\partial y} \\ \frac{\partial v}{\partial z} \\ \frac{\partial w}{\partial x} \\ \frac{\partial w}{\partial y} \\ \frac{\partial w}{\partial z} \end{Bmatrix} \tag{2.54}$$

where the matrix [P] is given as

$$[P] = \begin{bmatrix} 1 & 0 & 0 & 0 & 0 & 0 & 0 & 0 & 0 \\ 0 & 0 & 0 & 0 & 1 & 0 & 0 & 0 & 0 \\ 0 & 0 & 0 & 0 & 0 & 0 & 0 & 0 & 1 \\ 0 & 1 & 0 & 1 & 0 & 0 & 0 & 0 & 0 \\ 0 & 0 & 0 & 0 & 0 & 1 & 0 & 1 & 0 \\ 0 & 0 & 1 & 0 & 0 & 0 & 1 & 0 & 0 \end{bmatrix} \tag{2.55}$$

$$6 \times 9$$

2. The vector containing derivatives of the displacement field in the global coordinate system is mapped to the vector containing derivatives of the displacement field in the local coordinate system as

$$\begin{Bmatrix} \frac{\partial u}{\partial x} \\ \frac{\partial u}{\partial y} \\ \frac{\partial u}{\partial z} \\ \frac{\partial v}{\partial x} \\ \frac{\partial v}{\partial y} \\ \frac{\partial v}{\partial z} \\ \frac{\partial w}{\partial x} \\ \frac{\partial w}{\partial y} \\ \frac{\partial w}{\partial z} \end{Bmatrix} = [Q] \begin{Bmatrix} \frac{\partial u}{\partial \xi} \\ \frac{\partial u}{\partial \eta} \\ \frac{\partial u}{\partial \zeta} \\ \frac{\partial v}{\partial \xi} \\ \frac{\partial v}{\partial \eta} \\ \frac{\partial u}{\partial \zeta} \\ \frac{\partial w}{\partial \xi} \\ \frac{\partial w}{\partial \eta} \\ \frac{\partial w}{\partial \zeta} \end{Bmatrix} \tag{2.56}$$

The matrix [Q] contains terms of the inverse of the Jacobian [J] and can be written as

$$[Q] = \begin{bmatrix} \underset{3 \times 3}{[J]^{-1}} & \underset{3 \times 3}{[0]} & \underset{3 \times 3}{[0]} \\ \\ \underset{3 \times 3}{[0]} & \underset{3 \times 3}{[J]^{-1}} & \underset{3 \times 3}{[0]} \\ \\ \underset{[3 \times 3]}{[0]} & \underset{[3 \times 3]}{[0]} & \underset{[3 \times 3]}{[J]^{-1}} \end{bmatrix} \tag{2.57}$$

The Jacobian matrix is formed by the chain rule of differential calculus as below:

$$\frac{\partial u}{\partial \xi} = \frac{\partial u}{\partial x}\frac{\partial x}{\partial \xi} + \frac{\partial u}{\partial y}\frac{\partial y}{\partial \xi} + \frac{\partial u}{\partial z}\frac{\partial z}{\partial \xi} \tag{2.58}$$

Therefore, the Jacobian is given as follows:

$$[J] = \begin{bmatrix} \frac{\partial x}{\partial \xi} & \frac{\partial y}{\partial \xi} & \frac{\partial z}{\partial \xi} \\ \frac{\partial x}{\partial \eta} & \frac{\partial y}{\partial \eta} & \frac{\partial z}{\partial \eta} \\ \frac{\partial x}{\partial \zeta} & \frac{\partial y}{\partial \zeta} & \frac{\partial z}{\partial \zeta} \end{bmatrix} \tag{2.59}$$

where J_{11} is given as:

$$J_{11} = \frac{\partial x}{\partial \xi} = \frac{\partial}{\partial \xi}\left([N_i]^e \right)\{x\}^e \tag{2.60}$$

3. The vector containing the derivatives of the displacement field in the local coordinate system can be related to the nodal displacement vector as

$$\begin{Bmatrix} \frac{\partial u}{\partial \xi} \\ \frac{\partial u}{\partial \eta} \\ \frac{\partial u}{\partial \zeta} \\ \frac{\partial v}{\partial \xi} \\ \frac{\partial v}{\partial \eta} \\ \frac{\partial u}{\partial \zeta} \\ \frac{\partial w}{\partial \xi} \\ \frac{\partial w}{\partial \eta} \\ \frac{\partial w}{\partial \zeta} \end{Bmatrix} = [R] \begin{Bmatrix} d_1 \\ d_2 \\ d_3 \\ \cdot \\ \cdot \\ \cdot \\ \cdot \\ \cdot \\ \cdot \\ \cdot \\ \cdot \\ \cdot \\ \cdot \\ \cdot \\ d_{60} \end{Bmatrix} \tag{2.61}$$

The matrix [R] contains the derivative of the interpolation functions with respect to the local coordinate system and this matrix can be represented as

$$
[R] = \begin{bmatrix}
\frac{\partial N_1}{\partial \xi} & 0 & 0 & \frac{\partial N_2}{\partial \xi} & 0 & 0 & \frac{\partial N_3}{\partial \xi} & \cdots \\
\frac{\partial N_1}{\partial \eta} & 0 & 0 & \frac{\partial N_2}{\partial \eta} & 0 & 0 & \frac{\partial N_3}{\partial \eta} & \cdots \\
\frac{\partial N_1}{\partial \zeta} & 0 & 0 & \frac{\partial N_2}{\partial \zeta} & 0 & 0 & \frac{\partial N_3}{\partial \zeta} & \cdots \\
0 & \frac{\partial N_1}{\partial \xi} & 0 & 0 & \frac{\partial N_2}{\partial \xi} & 0 & 0 & \cdots \\
0 & \frac{\partial N_1}{\partial \eta} & 0 & 0 & \frac{\partial N_2}{\partial \eta} & 0 & 0 & \cdots \\
0 & \frac{\partial N_1}{\partial \zeta} & 0 & 0 & \frac{\partial N_2}{\partial \zeta} & 0 & 0 & \cdots \\
0 & 0 & \frac{\partial N_1}{\partial \xi} & 0 & 0 & \frac{\partial N_2}{\partial \xi} & 0 & \cdots \\
0 & 0 & \frac{\partial N_1}{\partial \eta} & 0 & 0 & \frac{\partial N_2}{\partial \eta} & 0 & \cdots \\
0 & 0 & \frac{\partial N_1}{\partial \zeta} & 0 & 0 & \frac{\partial N_2}{\partial \zeta} & 0 & \cdots
\end{bmatrix}_{9 \times 60} \tag{2.62}
$$

Therefore, the $[B_1^e]$ matrix for an element can be expressed as

$$
\underset{[6 \times 60]}{\left[B_1^e\right]} = \underset{[6 \times 9]}{[P]} \; \underset{[9 \times 9]}{[Q]} \; \underset{[9 \times 60]}{[R]} \tag{2.63}
$$

The materials property matrix $[D_1]$ for a three-dimensional isotropic material is given by

$$[D_t] = \frac{E(1-\nu)}{(1+\nu)(1-\nu)} \begin{bmatrix} 1 & \frac{\nu}{(1-\nu)} & \frac{\nu}{(1-\nu)} & 0 & 0 & 0 \\ \frac{\nu}{(1-\nu)} & 1 & \frac{\nu}{(1-\nu)} & 0 & 0 & 0 \\ \frac{\nu}{(1-\nu)} & \frac{\nu}{(1-\nu)} & 1 & 0 & 0 & 0 \\ 0 & 0 & 0 & \frac{1-2\nu}{2(1-\nu)} & 0 & 0 \\ 0 & 0 & 0 & 0 & \frac{1-2\nu}{2(1-\nu)} & 0 \\ 0 & 0 & 0 & 0 & 0 & \frac{1-2\nu}{2(1-\nu)} \end{bmatrix} \tag{2.64}$$

The initial strain vector for a thermal load is

$$\varepsilon_o = \alpha \, \Delta T_{av} \begin{Bmatrix} 1 \\ 1 \\ 1 \\ 0 \\ 0 \\ 0 \end{Bmatrix} \tag{2.65}$$

The turbine blade material is subjected to thermal expansion and the thermal force vector generated as a result of this expansion is written as follows:

$$\{f^{(e)}\} = \frac{\alpha\ V^e\ E\ (\Delta T_{av})}{1-2\ \nu}\ [\ B_1\ ] \begin{Bmatrix} 1 \\ 1 \\ 1 \\ 0 \\ 0 \\ 0 \end{Bmatrix} \tag{2.66}$$

Just like before (as in Eq 2.44) one would have to obtain the global stiffness matrix $[KS^G]$ and the global force vector $\{F^G\}$ (the equations will be linear here) and write the equations for any time t as

$$[KS^G]\ \{d^G\} = \{F^G\} \tag{2.67}$$

The solution of this system will yield the displacements d_1, d_2,... etc. The stresses within any element will then be obtained using Eqs. (2.53), (2.54), (2.56) and (2.61). The modulus of elasticity E in Eq. (2.64), and the coefficient of thermal expansion α in Eq. (2.65) are evaluated at the average temperature of the element. The T_{av} is the average temperature of the twenty nodes of an element. ΔT_{av} is the difference in T_{av} at any instant of time and T_{av} initially when there is a stress free state. The elemental temperatures obtained from the analysis before thus help us to calculate the thermal stress σ_{xx}, σ_{yy}, and σ_{zz} using Eq. (2.53). These stresses at different instants of time are shown in Figs. 2.21 to 2.23. It is clear from these figures that stresses along x and y directions are also significant and thus must be included in the design analysis of the turbine blade. It was also observed that with the present heating path, the maximum stress curve for σ_{zz} would

exceed unity as shown in Fig. 2.23 and as such would be an infeasible heating path. In order that maximum stress curve does not exceed the value of unity, the heating path has to be modified so that the maximum stresses remain below the yield stress throughout the heating period(Fig. 2.24). These stresses have been normalized with respect to the yield stress, σ_{yield}. This yield stress is a function of temperature and therefore the normalizing values would be different at different instants of time. From the stress-time graph, one can clearly observe that the peak stress occurs at time t = 200 seconds. The stresses in these figures increase to a maximum value and then decrease because different points in the blade undergo differential rise in temperature to a maximum value and then the entire blade is expected to reach a steady state temperature given sufficient time. During the steady state, the thermal stresses would be zero because ΔT from the reference state at two instants of time in the steady state will be the same for any element. These results show that σ_{xx} and σ_{yy} are not negligible as compared to σ_{zz}. This is due to the three-dimensional variation of the temperatures.

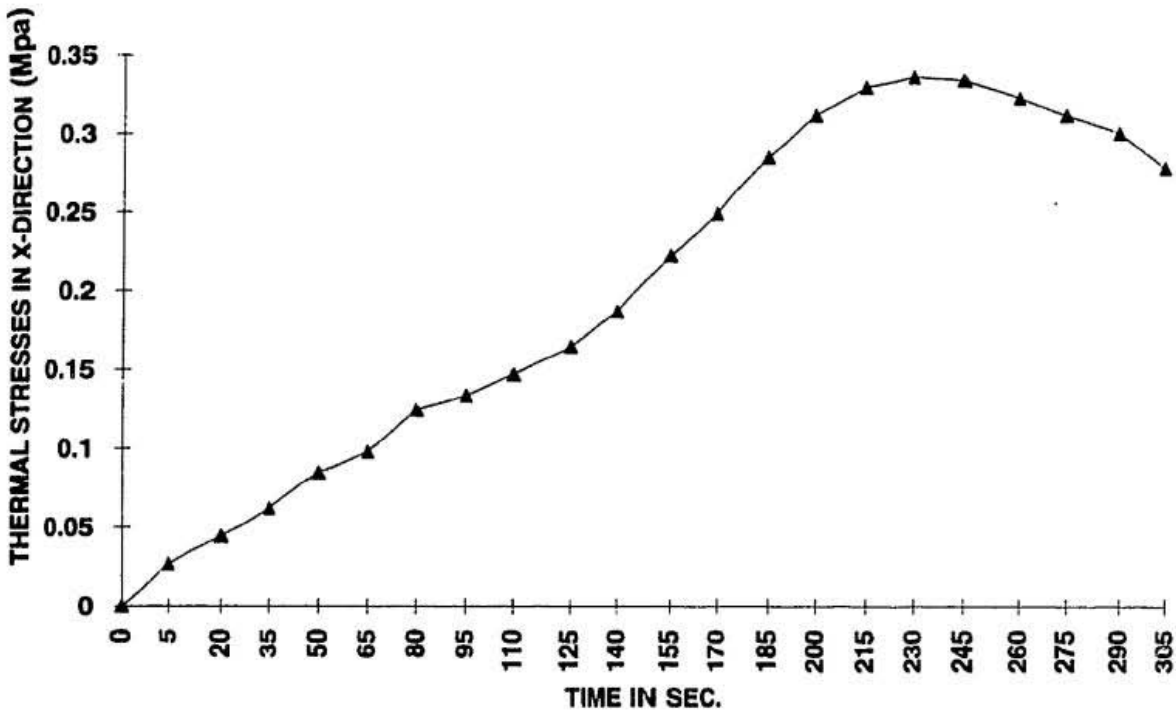

Fig. 2.21 TRANSIENT THERMAL STRESS (σ_{xx}) DISTRIBUTION IN THE BLADE

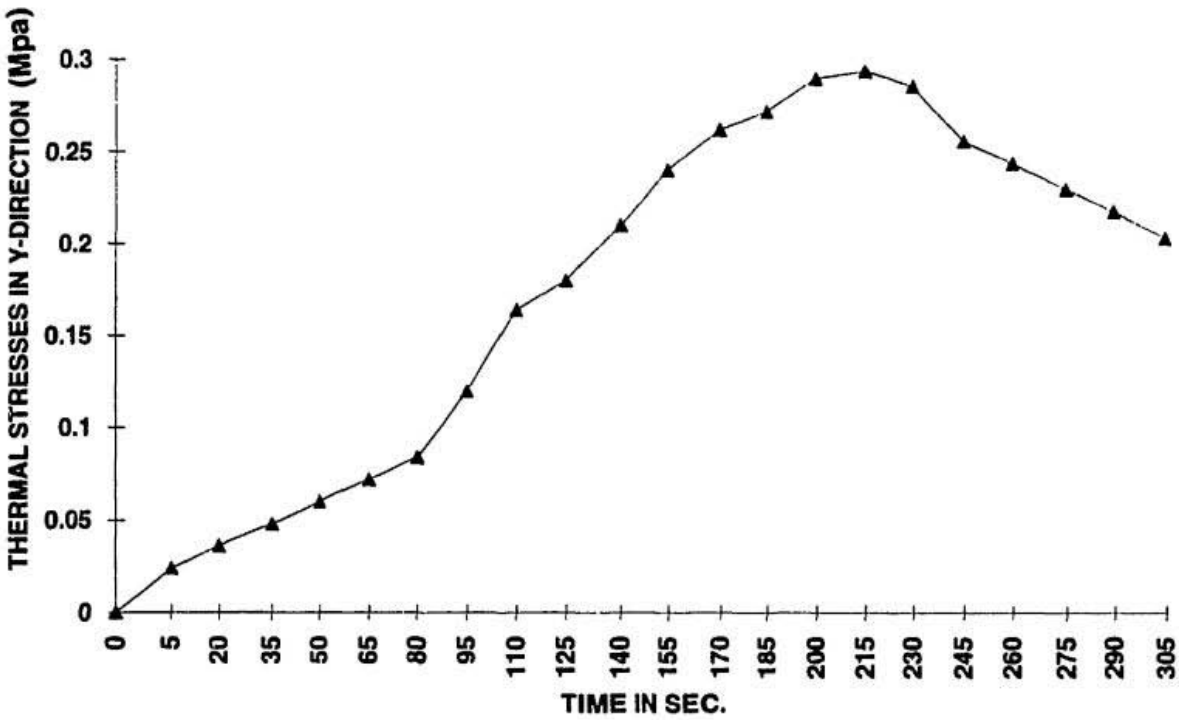

Fig. 2.22 TRANSIENT THERMAL STRESS (σ_{yy}) DISTRIBUTION IN THE BLADE

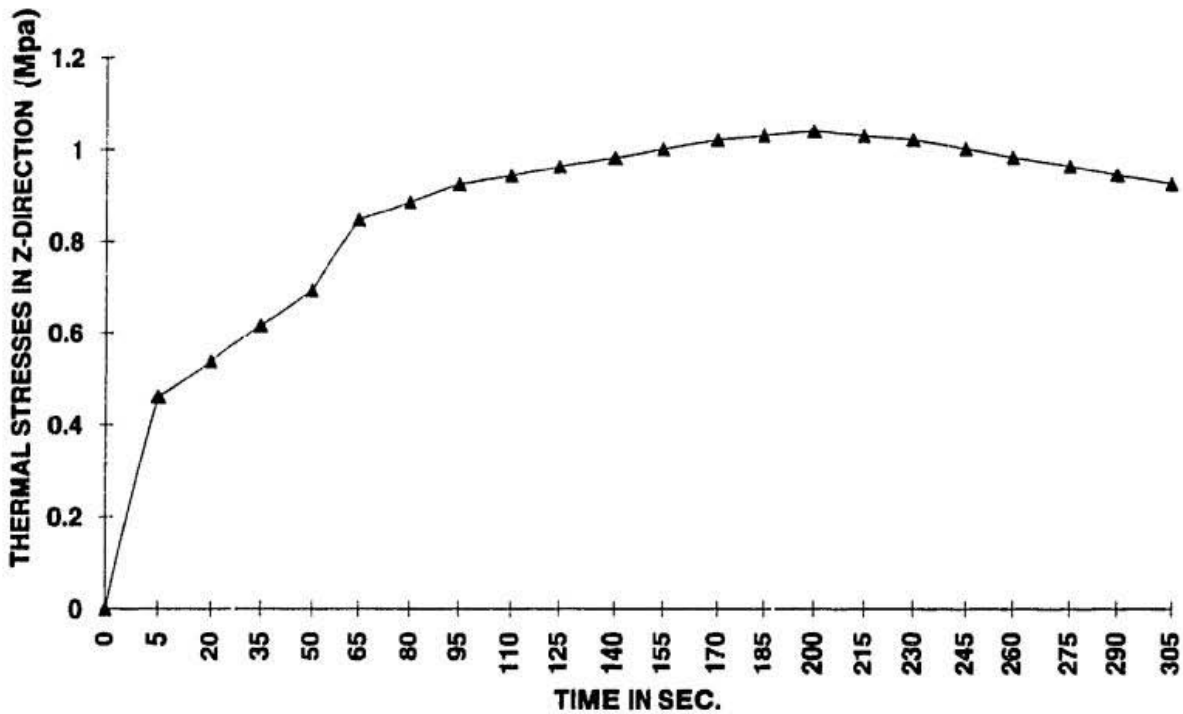

Fig. 2.23 TRANSIENT THERMAL STRESS (σ_{zz}) DISTRIBUTION IN THE BLADE

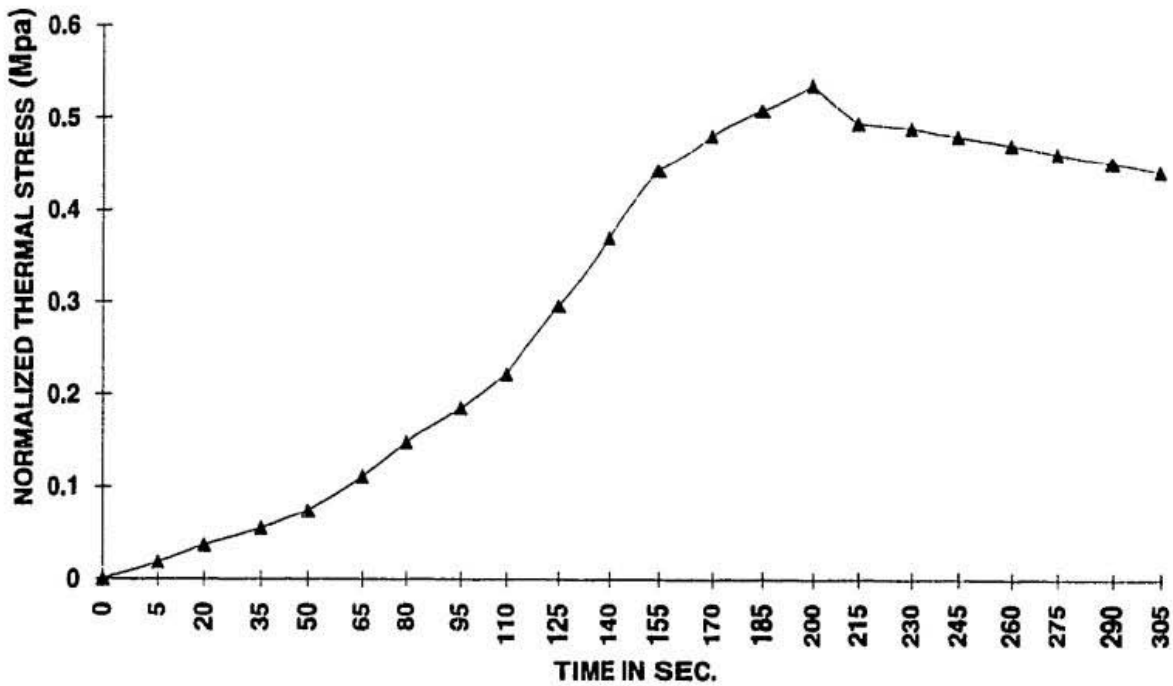

Fig. 2.24 TRANSIENT THERMAL STRESS (σ_{zz}) DISTRIBUTION IN THE BLADE FOR THE FEASIBLE HEATING RATE OF 24° C/SEC AT DIFFERENT INSTANTS OF TIME

2.7 CONCLUSION

The main objective of the investigation done in this chapter was to determine the transient temperature distribution, temperature gradient distributions and the thermal stresses in a turbine blade modelled as a three-dimensional non-linear finite element problem. The observation made from the study done in this chapter clearly shows that a significant temperature gradients exist along the height of the blade which are very essential in the performance of an accurate analysis of the temperature and thermal stress distribution in a turbine blade.

CHAPTER 3

FREE VIBRATION ANALYSIS

3.1 INTRODUCTION

The free vibration analysis of the turbine blade has been a challenging area to the engineers for a long time. Before designing a turbine blade, it is very essential to know its undamped natural frequencies and there are various reasons for it. Right from the start and until it comes to a constant operating speed, the rotor goes through the various blade natural frequencies. In order to avoid resonance, the steady state operating speed should not match with the system natural frequencies. Also, as the temperature of the turbine blade changes with time, there is a change in the material properties of the turbine blade. This change in the material property of the turbine blade is reflected in the change in the conventional stiffness $[K_s]$ matrix of the blade and this causes a change in the natural frequencies of the turbine blade. There is also a significant change in the natural frequencies because of the variational effect of stress stiffness matrix $[K_\sigma]$ which is non-linear in nature and is caused by the rotation of the turbine blade.

The present investigation is to study the combined effects of the two non-linearities on the natural frequencies of the turbine blade. The mathematical model for the study of the vibration analysis of the turbine blade is formulated using curved, three -dimensional, C^0 continuity, serendipity, twenty-noded isoparametric finite elements. This type of element is chosen because of its versatility in accurately mapping the complex geometry of the turbine blade. The blade is basically an airfoil cross-section, being asymmetric,

pre-twisted and having taper along its length. The two sections of the blade along its length are shown in Fig. 3.1.

3.2 MATHEMATICAL FORMULATION

The finite element analysis of the blade was done by dividing it into 35 elements, as shown in Fig 2.1. These elements are curved, solid, C^0 continuity, serendipity, twenty-noded isoparametric finite elements. Such type of an element was chosen because it gives a non-linear displacement field, which in turn takes care of the non-linear geometry of the turbine blade. The element chosen was a C^0 continuity element because the degrees of freedom at the nodes of the element are translational in nature along all the three axes. Hence, by selecting the degrees of freedom for displacements at the nodes along all the three axes, one can get the other modes of vibration also. Also, in case of isoparametric elements, the generalised coordinates and the generalised displacements are related to the nodal coordinates and nodal displacements respectively by the same shape function. The striking feature of the isoparametric elements is that they make use of a special coordinate system (ξ, η, ζ) as shown in Fig. 2.3. The shape functions are defined for the variation of the local coordinate system from +1 to -1. Therefore, we can have: $\xi = \pm 1$; $\eta = \pm 1$; and $\zeta = \pm 1$. The shape functions $[N_i]$, for the 20-noded isoparametric element can be expressed as (Zienkiewic ., 1971):

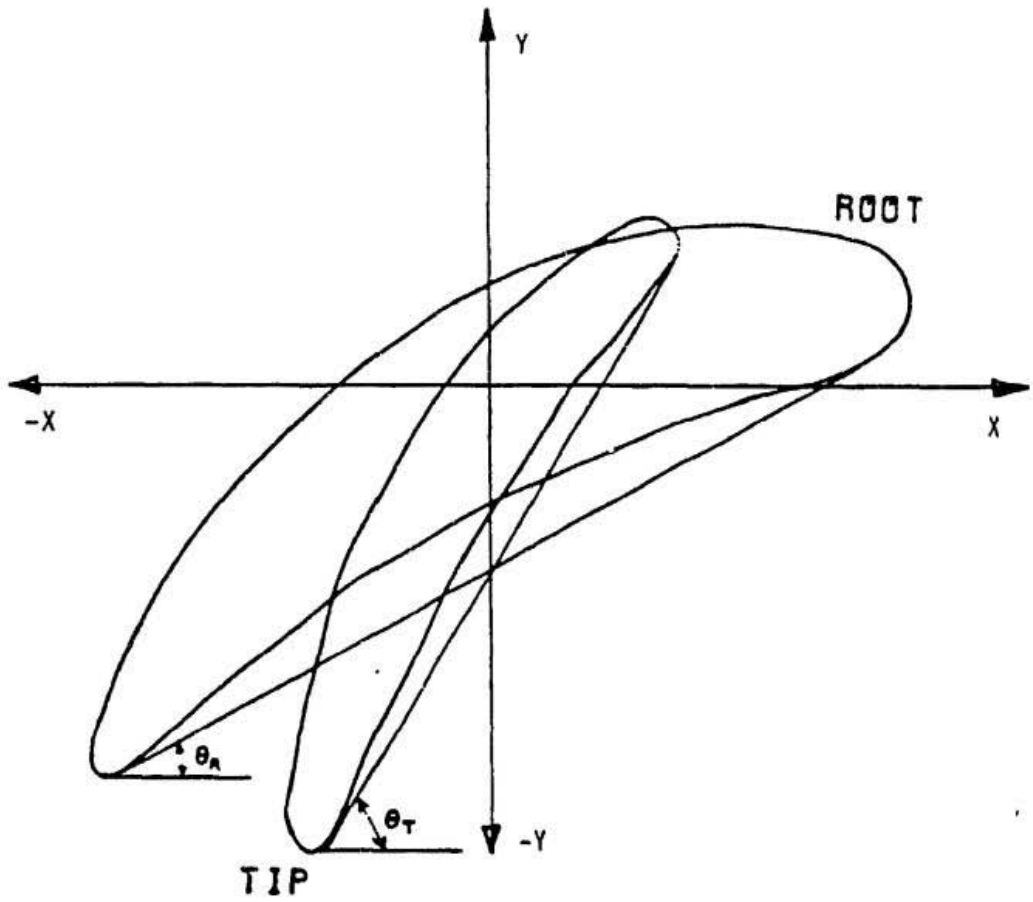

Fig 3.1 TURBINE BLADE AIRFOIL CROSS - SECTION AT THE ROOT AND THE TIP[Bahree, 1987]

Corner Nodes

$$N_i = \frac{1}{8}(1 + \xi\,\xi_i)(1 + \eta\,\eta_i)(1 + \zeta\,\zeta_i)(\xi\,\xi_i + \eta\,\eta_i + \zeta\,\zeta_i - 2) \qquad (3.1)$$

The details of Eq. (3.1) are given in APPENDIX A.

Typical Mid-side nodes

$$N_i = \frac{1}{4}(1 - \xi^2)(1 + \eta\,\eta_i)(1 + \zeta\,\zeta_i) \qquad (3.2)$$

for the case when $\xi_i = 0$, $\eta_i = \pm 1$, and $\zeta_i = \pm 1$. The subscript i stands for the ith node of the twenty-noded element in Eqs. (3.1) and (3.2).

Similarly one can write the equations corresponding to Eq. (3.2) as shown in APPENDIX B.

The mathematical formulation is arrived in the following way:

1. The local displacement vector {u, v, w} of a point in the element is related to nodal displacement vector {d} through matrix [N]:

$$\begin{Bmatrix} u \\ v \\ w \end{Bmatrix} = [N]\,\{d\} \qquad (3.3)$$

or

$$\begin{Bmatrix} u \\ v \\ w \end{Bmatrix} = \begin{bmatrix} N_1 & 0 & 0 & N_2 & 0 & 0 & N_3 & 0 & 0 & \dots & N_{20} & 0 & 0 \\ 0 & N_1 & 0 & 0 & N_2 & 0 & 0 & N_3 & 0 & \dots & 0 & N_{20} & 0 \\ 0 & 0 & N_1 & 0 & 0 & N_2 & 0 & 0 & N_3 & \dots & 0 & 0 & N_{20} \end{bmatrix} \begin{Bmatrix} u_1 \\ v_1 \\ w_1 \\ u_2 \\ v_2 \\ w_2 \\ \cdot \\ \cdot \\ \cdot \\ u_{20} \\ v_{20} \\ w_{20} \end{Bmatrix} \tag{3.4}$$

2. The global coordinate vector {x, y, z} at the same point in the element is related to nodal local coordinates {c} through $[\bar{N}]$ as

$$\begin{Bmatrix} x \\ y \\ z \end{Bmatrix} = [\overline{N}] \{c\} \tag{3.5}$$

or

$$\begin{Bmatrix} x \\ y \\ z \end{Bmatrix} = \begin{bmatrix} N_1 & 0 & 0 & N_2 & 0 & 0 & N_3 & 0 & 0 & \dots & N_{20} & 0 & 0 \\ 0 & N_1 & 0 & 0 & N_2 & 0 & 0 & N_3 & 0 & . & 0 & N_{20} & 0 \\ 0 & 0 & N_1 & 0 & 0 & N_2 & 0 & 0 & N_3 & \dots & 0 & 0 & N_{20} \end{bmatrix} \begin{Bmatrix} x_1 \\ y_1 \\ z_1 \\ x_2 \\ y_2 \\ z_2 \\ . \\ . \\ . \\ x_{20} \\ y_{20} \\ z_{20} \end{Bmatrix} \quad (3.6)$$

where

u, v, w are generalized displacements along global X, Y, and Z axes,

x, y, z are generalized coordinates along global X, Y, and Z axes,

{d} is nodal displacement vector,

{c} is nodal coordinate vector,

[N]and [$\bar{N}$] are shape function matrices which are the same for isoparametric elements, and both [N] and [$\bar{N}$] are functions in terms of ξ, η, and ζ.

The eigenvalues and eigenvectors of the system are obtained from the stiffness and the mass matrices which are described below

3.2.1 $[K_s^e]$ ELEMENTAL CONVENTIONAL STIFFNESS MATRIX - THE MATHEMATICAL FORMULATION

This stiffness matrix which depends upon the elastic properties of the turbine blade is given by the following relationship:

$$\left[K_s^e\right] = \int_v \left[B_1^e\right]^T \left[D_1\right] \left[B_1^e\right] dv \tag{3.7}$$

In order to formulate $[K_s^e]$, we have to know the matrix $[B_1^e]$ which relates the strain in the element to the nodal displacements and the material property matrix $[D_1]$. The matrix $[B_1^e]$ for the stress analysis can be evaluated in the same way as explained in the Eq. (2.54) to Eq. (2.63).

The materials property matrix $[D_1]$ for a three-dimensional isotropic material is same as given by Eq. (2.64).

Thus, elemental stiffness matrix can be expressed as

$$\left[K_s^e\right] = \int_v [B_1]^T [D_1] [B_1] dv = \int_v [B_1]^T [D_1] [B_1] \, dx \, dy \, dz \tag{3.8}$$

The $[K_s^e]$ matrix in terms of ξ, η, and ζ can be expressed as

$$\left[K_s^e\right] = \int_v [B_1]^T [D_1] [B_1] |J| \, d\xi \, d\eta \, d\zeta \tag{3.9}$$

where $|J|$ is the determinant of Jacobian matrix [J].

Since the local coordinates ξ, η, and ζ vary from -1 to +1, for the isoparametric formulation, the Eq. (3.9) can also be expressed as

$$\left[K_s^e\right] = \int_{-1}^{+1}\int_{-1}^{+1}\int_{-1}^{+1} [B_1]^T [D_1] [B_1] |J| \, d\xi \, d\eta \, d\zeta \tag{3.10}$$

The matrix $[K_s^e]$ is evaluated numerically by making use of Gaussian quadrature. Because of the quadratic polynomial used for each side of the twenty-noded element, the expression for the elemental matrix is also quadratic. Therefore, for a general second degree polynomial $\Phi = a + b\xi + c\xi^2$, two Gauss points will give an accurate solution. This gives rise to 8 Gauss points within each element which is adequate to integrate each element of the matrix $[K_s^e]$.

Therefore,

$$\left[K_s^e\right] = \sum_{i=1}^{2}\sum_{j=1}^{2}\sum_{k=1}^{2} W_i \, W_j \, W_k \, [B_1(\xi,\eta,\zeta)]^T [D_1] [B_1(\xi,\eta,\zeta)] |J(\xi,\eta,\zeta)| \tag{3.11}$$

where W_i, W_j, and W_k are corresponding weighting functions in the ξ, η, and ζ directions respectively.

3.2.2 $[K_\sigma^e]$ ELEMENTAL STRESS STIFFNESS MATRIX - THE MATHEMATICAL FORMULATION

We define another elemental matrix $[K^e_\sigma]$ that accounts for the change in potential energy associated with rotation of volume elements under load. This matrix is called the stress stiffness matrix. It is independent of material properties and depends only on the element's geometry, the displacement field, and state of stress. APPENDIX E explains how this matrix comes into the overall picture and why it is important to include this matrix in the present analysis.

The most important thing in deriving the mathematical formulation for elemental

Stress Stiffness Matrix $[K^e_\sigma]$, for a complicated geometry (as in our case), is to make sure that both linear and non-linear terms have been included. Thus, a general expression for Elemental Stress Stiffness Matrix $[K^e_\sigma]$ is derived as follows:

Strains can be written as

$$\{ \varepsilon \} = \{ \varepsilon_L \} + \{ \varepsilon_{NL} \} \tag{3.12}$$

where $\{\varepsilon_L\}$ is the strain linear in the displacement derivatives and the higher order terms give rise to $\{\varepsilon_{NL}\}$, the non-linear strains. The strain energy U is stored as a result of constant stresses $\{\sigma_o\}$ acting through strains $\{\varepsilon\}$ and is given as:

$$\int_v \{ \varepsilon \}^T \{ \sigma_o \} dv = \int_v \{ \varepsilon_L \}^T \{ \sigma_o \} dv + \int_v \{ \varepsilon_{NL} \}^T \{ \sigma_o \} dv \tag{3.13}$$

or

$$U = U_L + U_{NL}$$

APPENDIX E explains that $[K_\sigma]$ is produced by stresses acting through displacements associated with higher-order contributions to strain.

Therefore the $[K_\sigma]$ is extracted from U_{NL} as follows:

Expressions for strain are written in conventional notation as

$$\varepsilon_x = u_{,x} + \frac{1}{2}(u^2_{,x} + v^2_{,x} + w^2_{,x}) \tag{3.14}$$

and

$$\gamma_{xy} = u_{,y} + v_{,x} + (u_{,x}u_{,y} + v_{,x}v_{,y} + w_{,x}w_{,y}) \tag{3.15}$$

The terms within the parenthesis give rise to $\{\varepsilon_{NL}\}$ where x, y, z are global directions.

In order to formulate $[K_\sigma]$, we define the following:

$\{\delta\} = [G]\{d\}$ where

$\{d\}$ is the nodal displacement vector as described before. We can also write

$\{\delta\} = \{u_{,x}, u_{,y}, u_{,z}, v_{,x}, v_{,y}, v_{,z}, w_{,x}, w_{,y}, w_{,z}\}$

where $u_{,x}$, $u_{,y}$, and $u_{,z}$ are $\partial u/\partial x$, $\partial u/\partial y$, and $\partial u/\partial z$ respectively.

Differentiating shape functions in [N] give us the coefficients in [G] given by Eq. (2.62).

We define one more matrix here which is

$$[\,Q_1\,] = \begin{bmatrix} u_{,x} & 0 & 0 & v_{,x} & 0 & 0 & w_{,x} & 0 & 0 \\ 0 & u_{,y} & 0 & 0 & v_{,y} & 0 & 0 & w_{,y} & 0 \\ 0 & 0 & u_{,z} & 0 & 0 & v_{,z} & 0 & 0 & w_{,z} \\ u_{,y} & u_{,x} & 0 & v_{,y} & v_{,x} & 0 & w_{,y} & w_{,x} & 0 \\ 0 & u_{,z} & u_{,y} & 0 & v_{,z} & v_{,y} & 0 & w_{,z} & w_{,y} \\ u_{,z} & 0 & u_{,x} & v_{,z} & 0 & v_{,x} & w_{,z} & 0 & w_{,x} \end{bmatrix} \tag{3.16}$$

Therefore Eq. (3.13) can be written as

$$\{\,\varepsilon\,\} = \{\,\varepsilon_L\,\} + \{\,\varepsilon_{NL}\,\} = \{\,\varepsilon_L\,\} + \frac{1}{2}\,[\,Q_1\,]\,[\,G\,]\,\{d\} \tag{3.17}$$

Displacements u, v, and w are functions of x, y, z where x, y, and z is the position of a point in the continuum in the unstrained configuration. Therefore $\{\varepsilon\}$ is called Lagrangian strain and $\{\varepsilon\} = 0$ for any rigid-body motion, no matter how large is the rotation or the displacement (Cook, 1981).

The vector $\{\sigma_0\}$ is defined as

$$\{\sigma_o\} = \{\sigma_{xo}, \sigma_{yo}, \sigma_{zo}, \tau_{xyo}, \tau_{yzo}, \tau_{zxo}\} \tag{3.18}$$

Combining Eqs. (3.13), (3.17) and (3.18), we get

$$U_{NL} = \frac{1}{2}\{d\}^T \int_v [\,G\,]^T [\,Q_1\,]^T \{\sigma_o\}\, dv = \frac{1}{2}\{d\}^T \int_v [\,G\,]^T \begin{bmatrix} [s] & 0 & 0 \\ 0 & [s] & 0 \\ 0 & 0 & [s] \end{bmatrix} \{\delta\}\, dv \tag{3.19}$$

where

$$[\,Q\,]^T \{\sigma_o\} = \begin{bmatrix} [s] & 0 & 0 \\ 0 & [s] & 0 \\ 0 & 0 & [s] \end{bmatrix} \{\delta\} \tag{3.20}$$

[9 X 6] [6 X 1] [9 X 9] [9 X 1]

and

$$[\,s\,] = \begin{bmatrix} \sigma_{xo} & \tau_{xyo} & \tau_{zxo} \\ \tau_{xyo} & \sigma_{yo} & \tau_{yzo} \\ \tau_{zxo} & \tau_{yzo} & \sigma_{zo} \end{bmatrix} \tag{3.21}$$

[3 X 3]

Thus elemental stress stiffness matrix is given as

$$[\,K_\sigma^e\,] = \int_v [G]^T \begin{bmatrix} [s] & 0 & 0 \\ 0 & [s] & 0 \\ 0 & 0 & [s] \end{bmatrix} [G] dv \tag{3.22}$$

The element stress stiffness matrix $[K_\sigma^e]$ is a symmetric matrix like the conventional stress

stiffness matrix $[K_s]$ and the global $[K_\sigma]$ is obtained by the usual assembly of elemental $[K_\sigma^e]$ matrices.

3.2.3 $[M^e]$ ELEMENTAL MASS MATRIX - THE MATHEMATICAL FORMULATION

The elemental mass matrix for the system is given by:

$$[M^e] = \int_v [N]^T \rho \, [N] dv \tag{3.23}$$

where [N] is the shape function matrix,

ρ is the material density.

In terms of local coordinate system ξ, η, and ζ, the Eq. (3.34) can be represented as

$$[M^e] = \int_{-1}^{+1} \int_{-1}^{+1} \int_{-1}^{+1} [N]^T \, \rho \, [N] \, |J| \, d\xi \, d\eta \, d\zeta \tag{3.24}$$

Using Gauss quadrature, the elemental expression for $[M^e]$ can be written as

$$[M^e] = \sum_{i=1}^{2} \sum_{j=1}^{2} \sum_{k=1}^{2} W_i \, W_j \, W_k \, [N(\xi,\eta,\zeta)]^T \, [N(\xi,\eta,\zeta)] \, | \, J(\xi,\eta,\zeta) \, | \tag{3.25}$$

3.3 FREE VIBRATION ANALYSIS

The global stiffness matrix $[K^G]$ obtained from assembling global $[K_s^G]$ and global $[K_\sigma^G]$, and global mass matrix $[M^G]$ were evaluated after assembling the elemental stiffness and mass matrices respectively. The natural frequencies were found by solving the following equation for the eigenvalue problem:

$$[K^G]\{x\} - \lambda [M^G]\{\ddot{x}\} = 0 \tag{3.26}$$

Figs. 3.4 to 3.10 show the variation of first five natural frequencies of the turbine blade both without and with the inclusion of stress stiffness matrix $[K_\sigma]$ to the conventional matrix $[K_s]$ at different rotor speeds. It is clear from these graphs that there is a significant change in the frequency of the turbine blade by including stress stiffness matrix. Because of the change in the frequency there is also a change in the actual resonance of the system. Fig. 3.11 and 3.12 show the projected and actual resonance for first and second natural frequencies. Frequencies beyond second are of only academic interest because the maximum speed at which the rotor operates does not go beyond 4000 rpm.

3.4 EFFECT OF TEMPERATURE VARIATION ON THE NATURAL FREQUENCIES OF THE BLADE

One of the objectives of the present investigation was to show the effect of various factors on the natural frequencies of the turbine blade. Besides the effect of stress stiffness matrix, it was observed that the frequencies of the turbine blade also changed with the change in the temperature. This is due to the change in the elastic properties of the blade which resulted a change in the stiffness matrix of the system. The heating path chosen for finding the effect of change in temperature on frequency was the one which put the yield stress below one as shown in Fig. (2.24). Figs. 3.13 to 3.17 show the variation of first five natural frequencies of the turbine blade at different instants of time during the heating process. It is very clear from these figures that as the material is heated, the frequencies start decreasing due to a decrease in the value of the modulus of elasticity of the material of the turbine blade. If the effect of stress stiffness matrix is

not included, then the frequencies decrease only with increase in temperature of the turbine blade. The frequencies increase due to large deflections and , at the same time, these decrease due to increased temperature due to lowering of E, the modulus of elasticity. Thus, it is clear from these figures that there is a significant change in the natural frequencies in the transient state and is thus an important factor to be taken into account while designing a turbo blade. Therefore, the frequency analysis of the turbine blade must include the combined effect of

i) inclusion of the stress stiffness matrix to the conventional matrix and

ii) change in the material properties of the blade resulting in change in overall stiffness matrix of the turbine blade due to change in temperature in the transient phase.

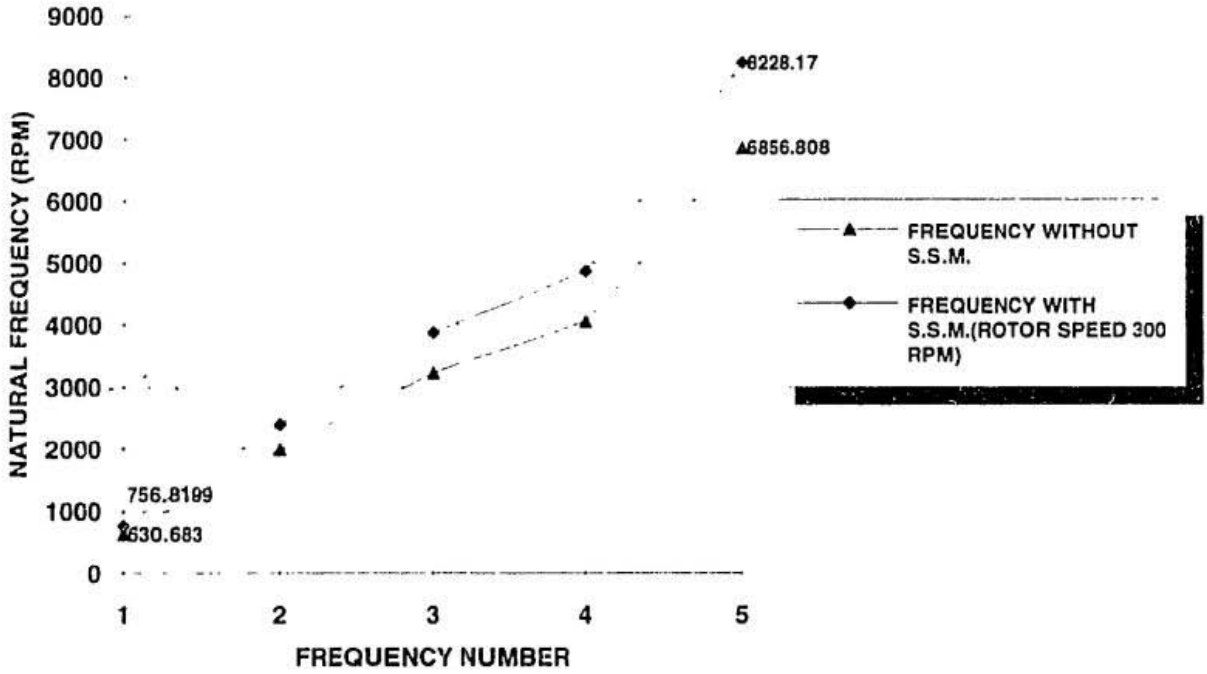

Fig. 3.2 VARIATION OF FIRST FIVE NATURAL FREQUENCIES OF TURBINE BLADE AT ROTOR SPEED OF 300 RPM

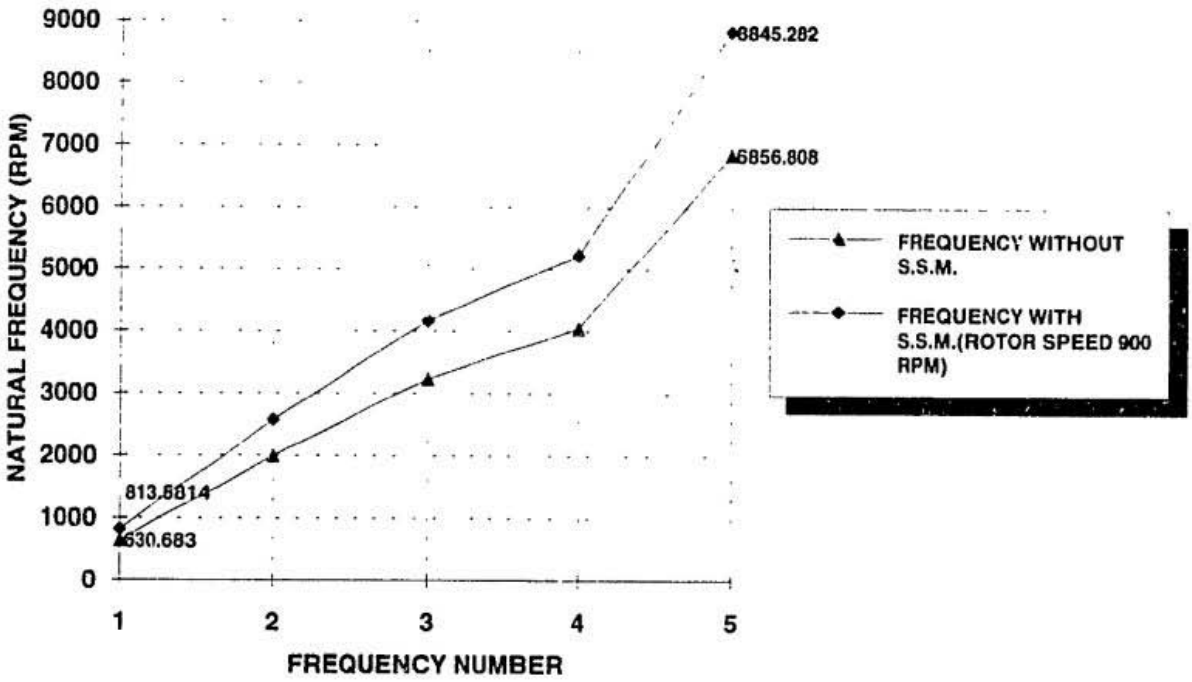

Fig. 3.3 VARIATION OF FIRST FIVE NATURAL FREQUENCIES OF TURBINE BLADE AT ROTOR SPEED OF 900 RPM

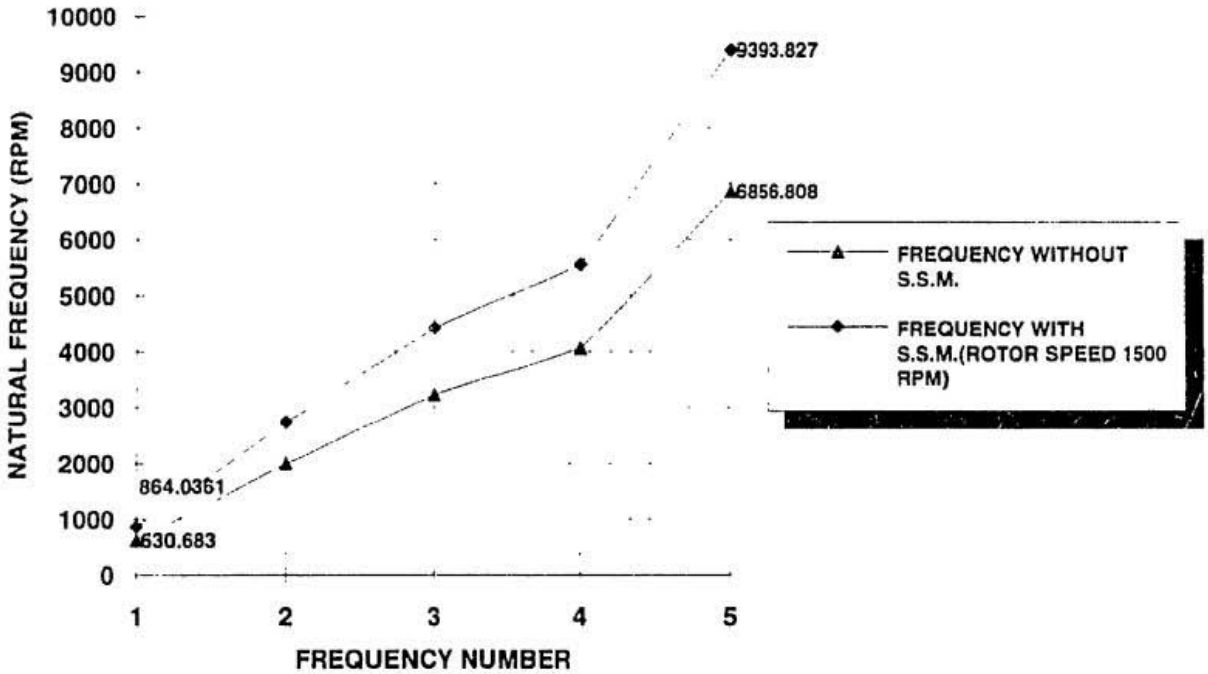

Fig. 3.4 VARIATION OF FIRST FIVE NATURAL FREQUENCIES OF TURBINE BLADE AT ROTOR SPEED OF 1500 RPM

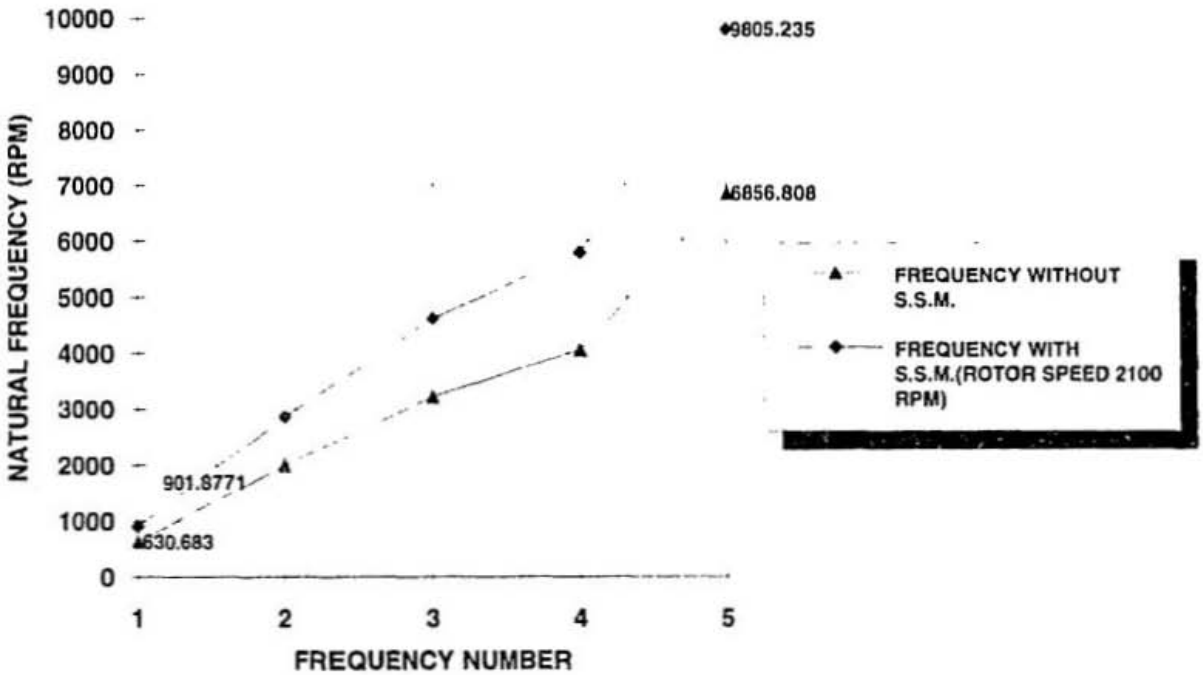

Fig. 3.5 VARIATION OF FIRST FIVE NATURAL FREQUENCIES OF TURBINE BLADE AT ROTOR SPEED OF 2100 RPM

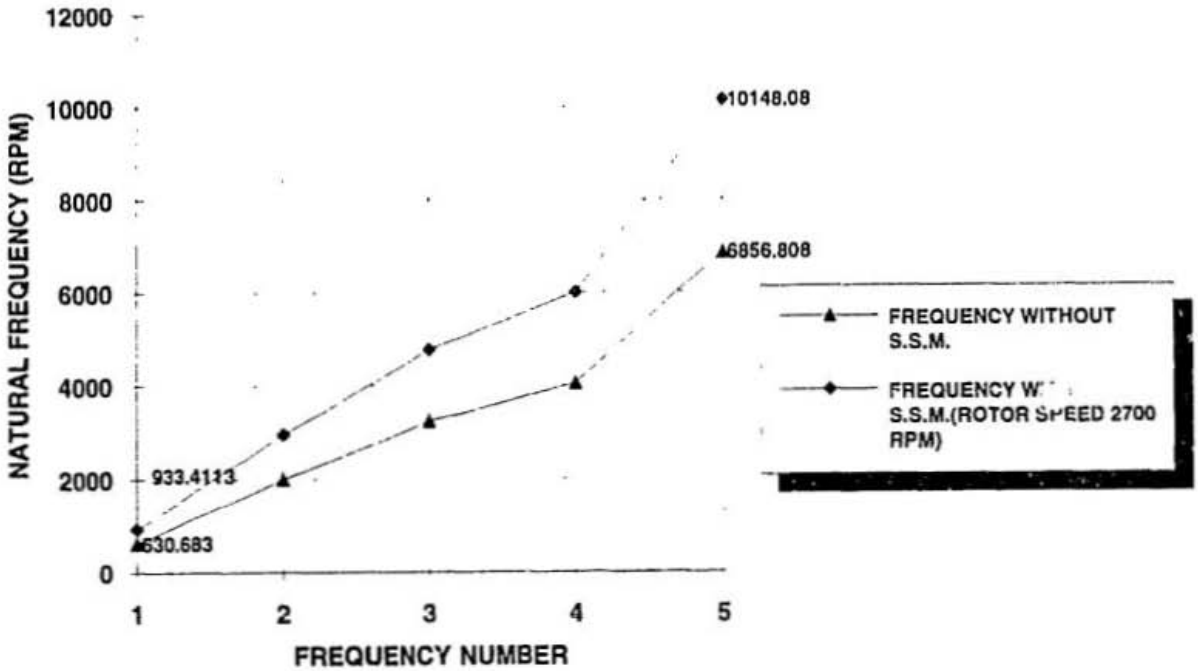

Fig. 3.6 VARIATION OF FIRST FIVE NATURAL FREQUENCIES OF TURBINE BLADE AT ROTOR SPEED OF 2700 RPM

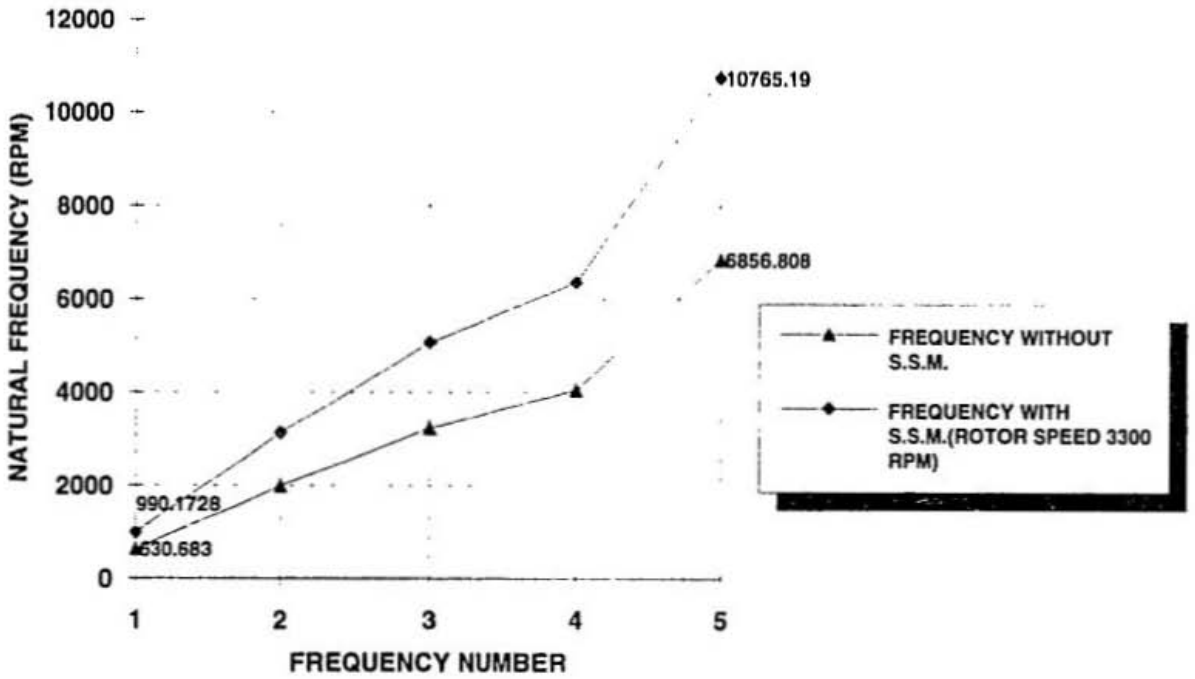

Fig. 3.7 VARIATION OF FIRST FIVE NATURAL FREQUENCIES OF TURBINE BLADE AT ROTOR SPEED OF 3300 RPM

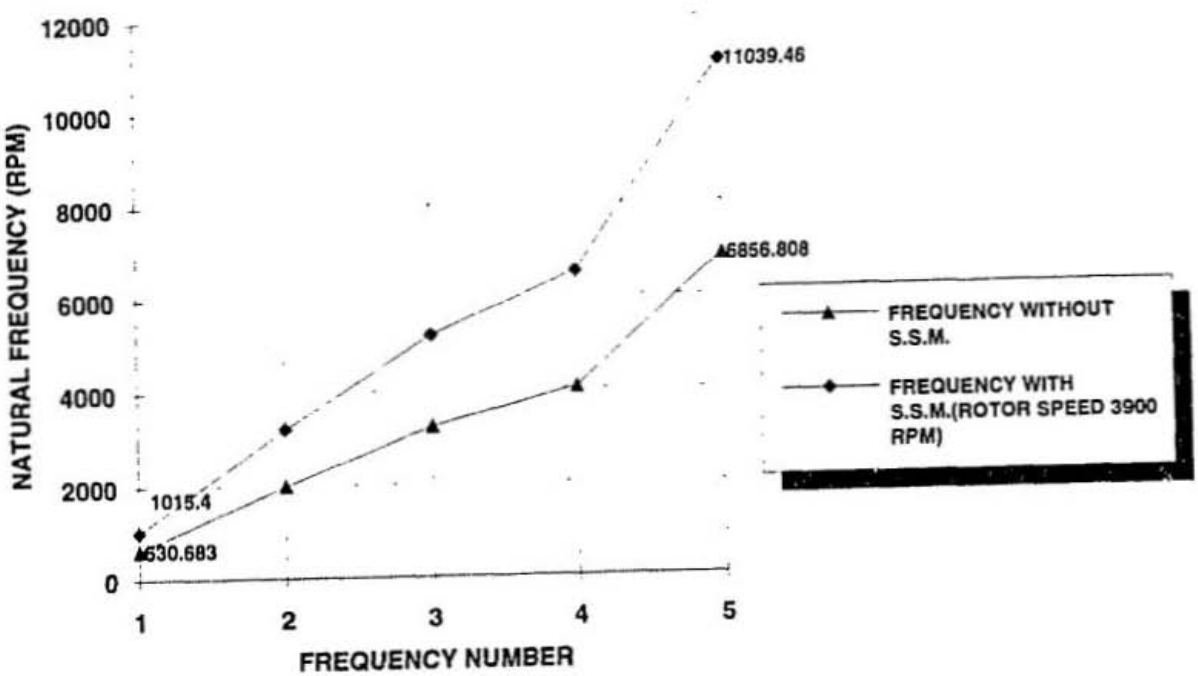

Fig. 3.8 VARIATION OF FIRST FIVE NATURAL FREQUENCIES OF TURBINE BLADE AT ROTOR SPEED OF 3900 RPM

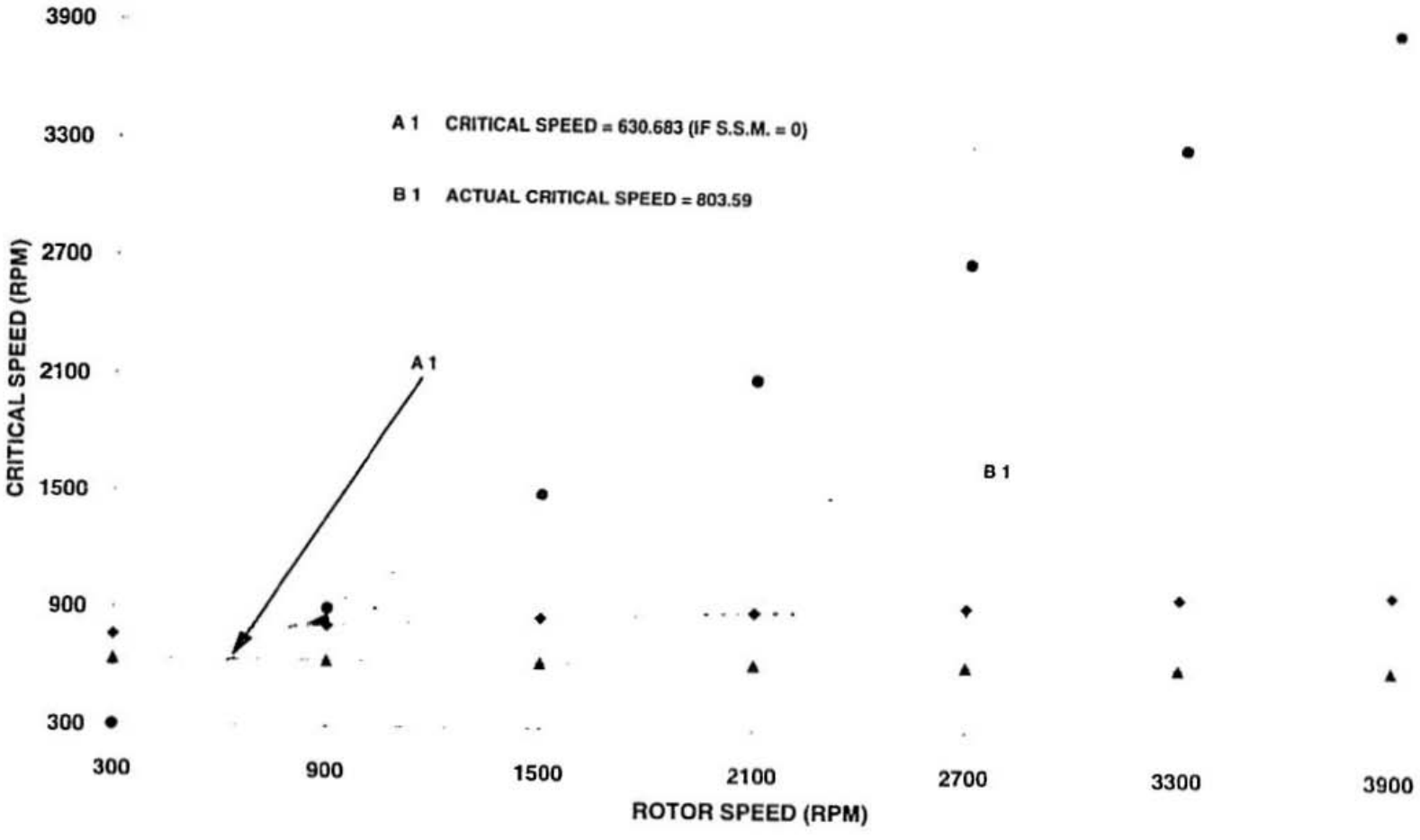

Fig. 3.9 COMPARISON OF FIRST ACTUAL CRITICAL SPEED WITH FIRST PROJECTED CRITICAL SPEED USING STRESS STIFFNESS MATRIX

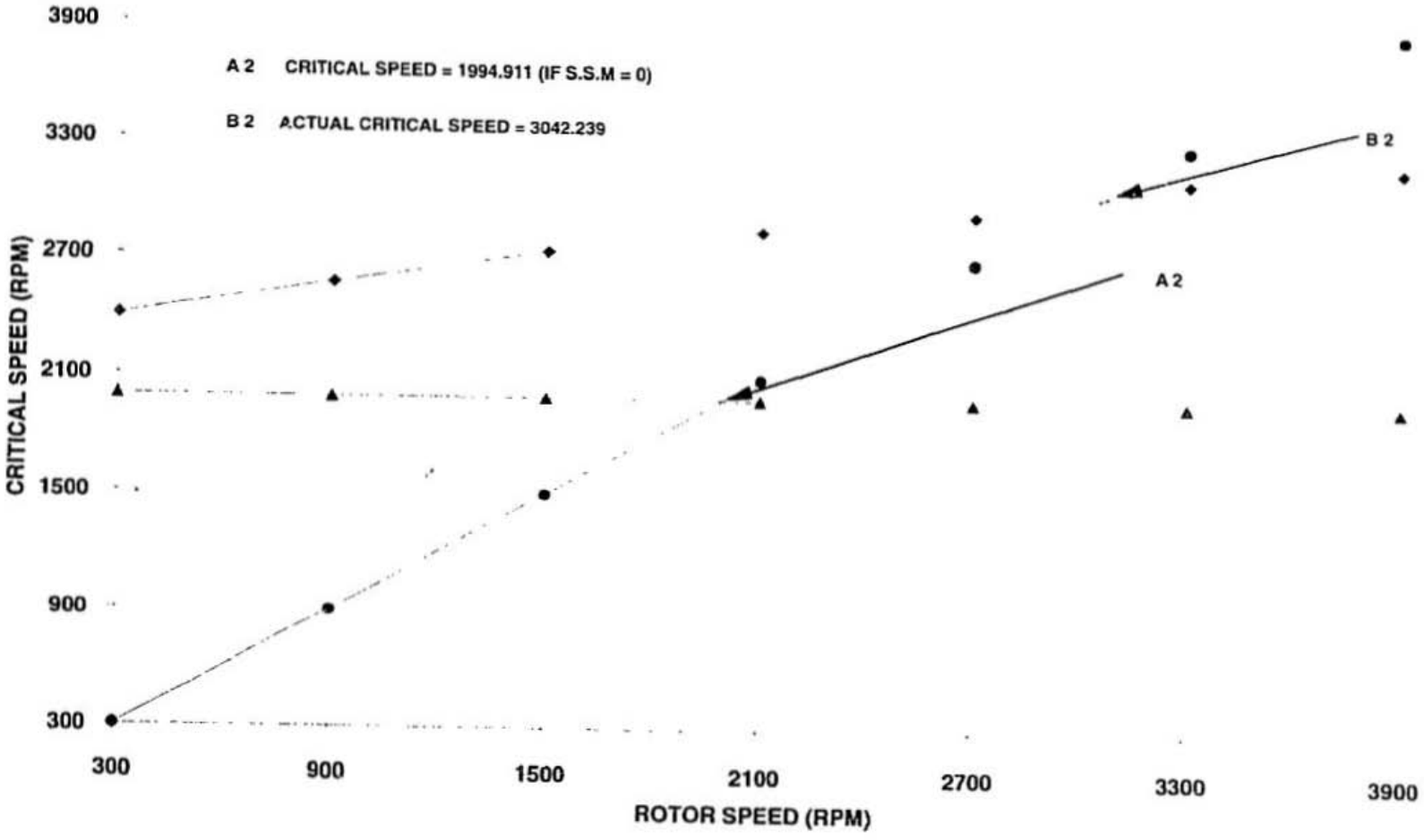

Fig. 3.10 COMPARISON OF SECOND ACTUAL CRITICAL SPEED WITH SECOND PROJECTED CRITICAL SPEED USING STRESS STIFFNESS MATRIX

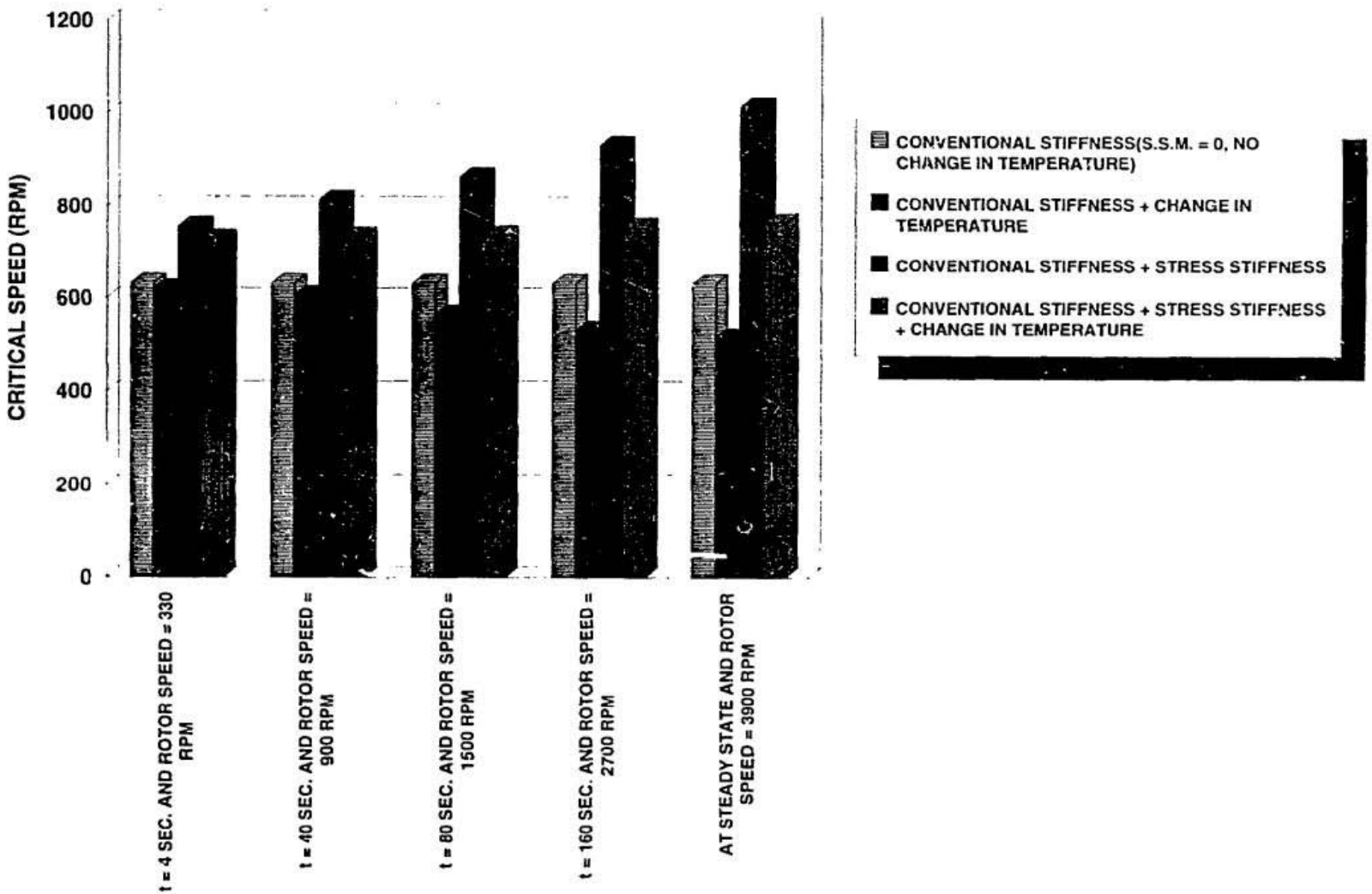

Fig. 3.11 COMPARISON OF FIRST CRITICAL SPEED OBTAINED FROM VARIOUS METHODS

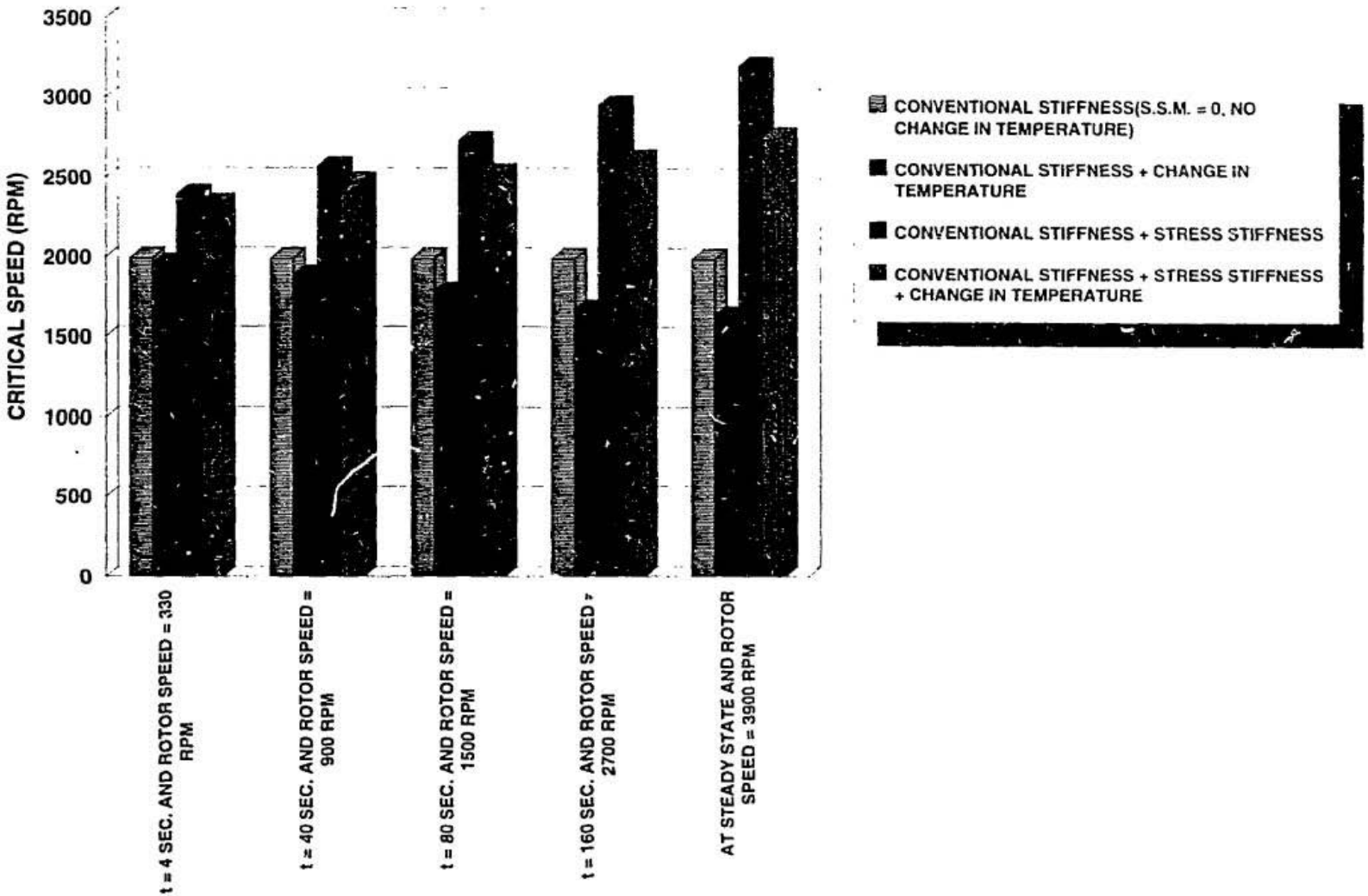

Fig. 3.12 COMPARISON OF SECOND CRITICAL SPEED OBTAINED FROM VARIOUS METHODS

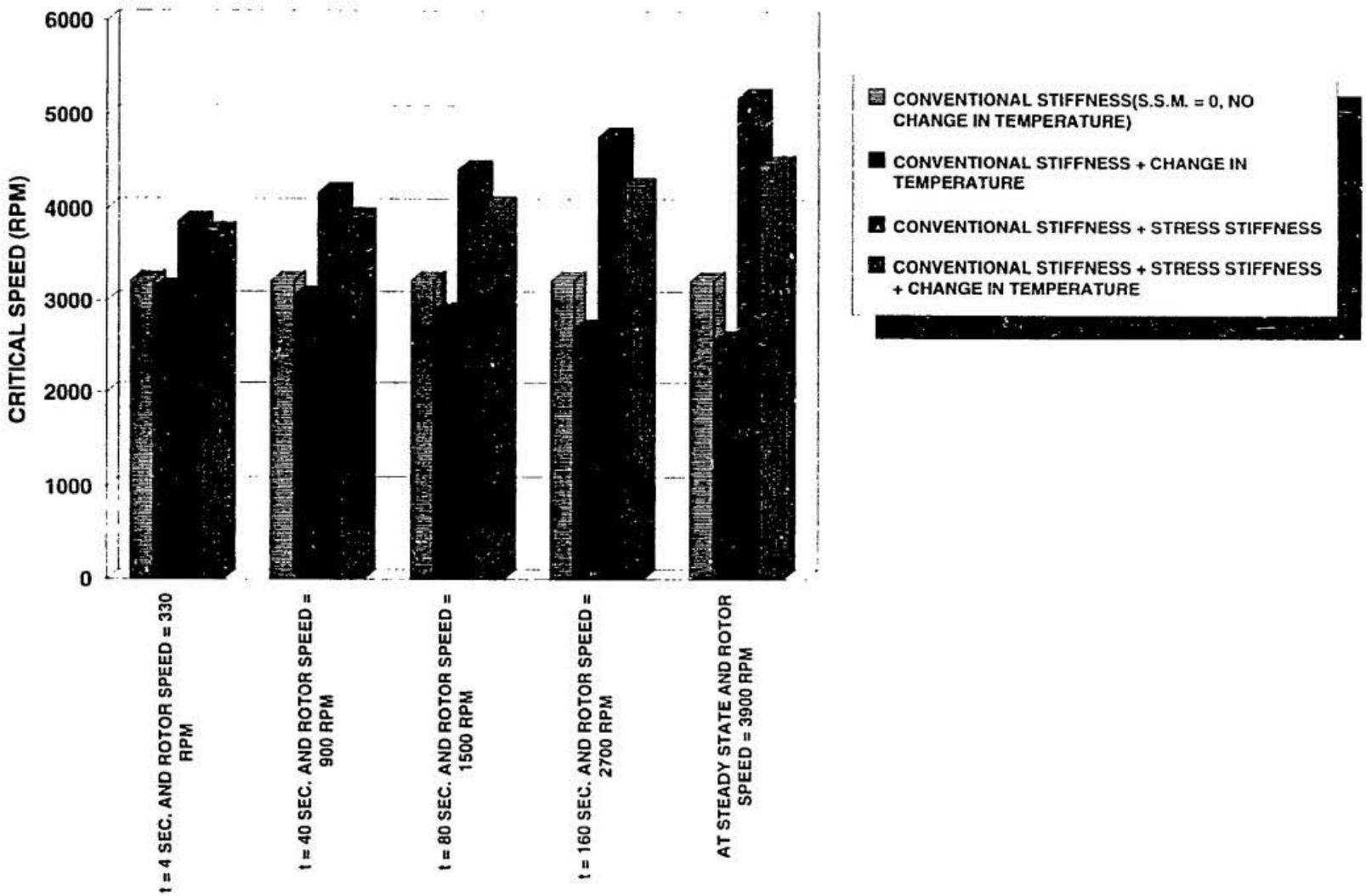

Fig. 3.13 COMPARISON OF THIRD CRITICAL SPEED OBTAINED FROM VARIOUS METHODS

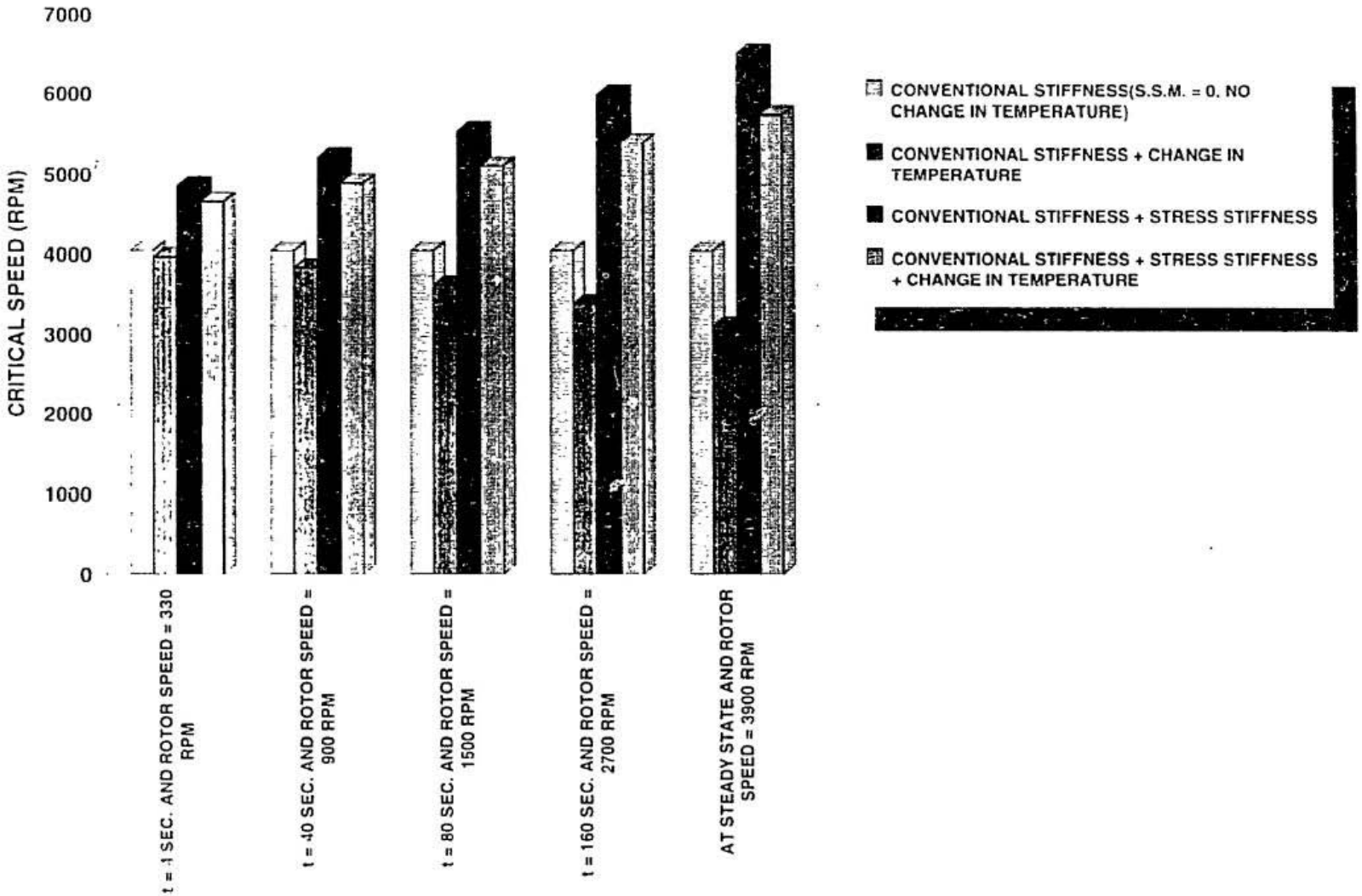

Fig. 3.14 COMPARISON OF FOURTH CRITICAL SPEED OBTAINED FROM VARIOUS METHODS

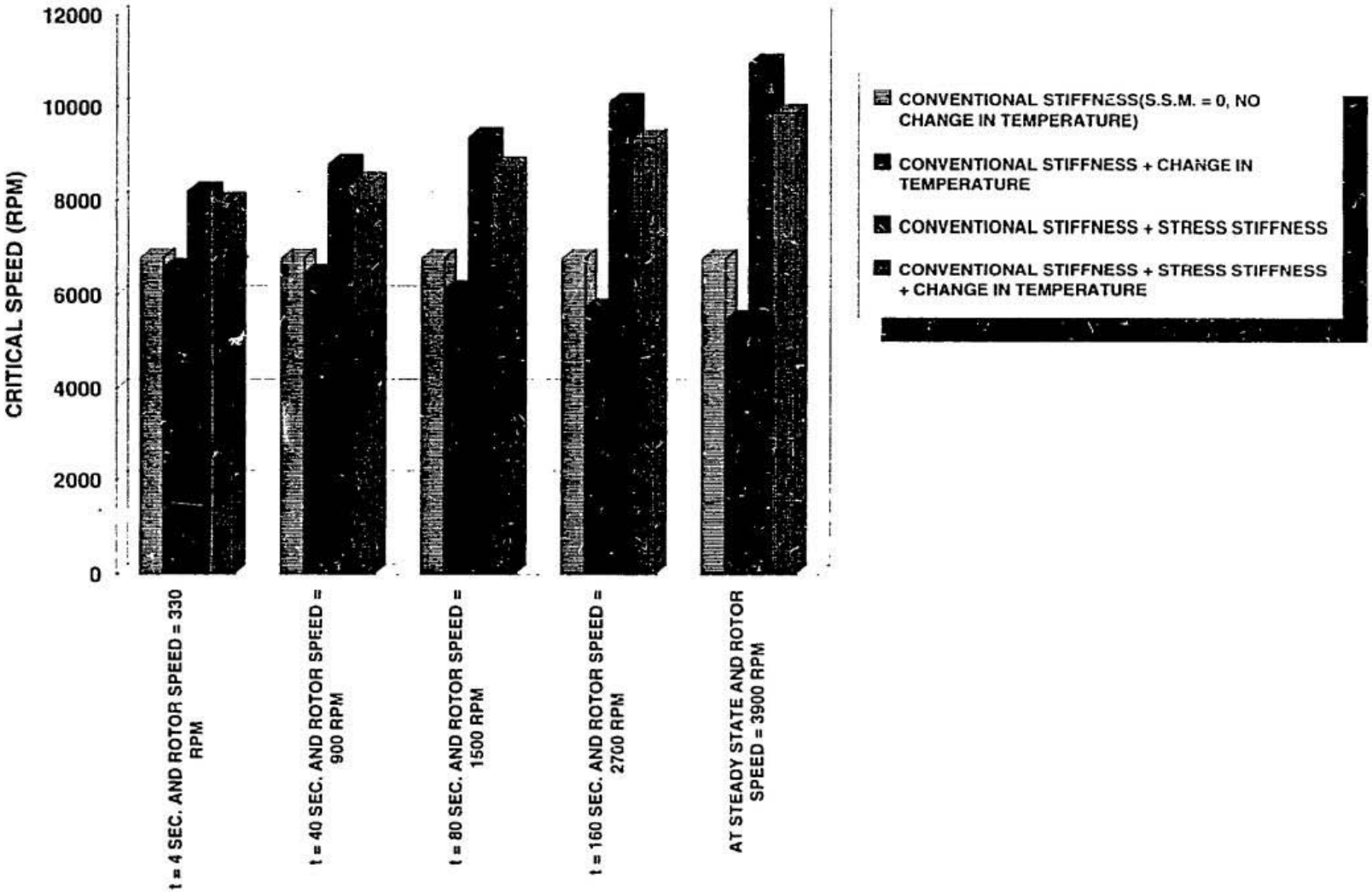

Fig. 3.15 COMPARISON OF FIFTH CRITICAL SPEED OBTAINED FROM VARIOUS METHODS

3.5 CONCLUSIONS

In this chapter, the eigenvalues and eigenvectors for the blade were found by discretizing of the turbine blade into finite elements. The turbine blade had a height of 12 cm. and was discretized into 35 elements with 7 elements across the cross-section and 5 layers along the height. The dynamics of the system was represented by 308 nodes and 924 degrees of freedom. The natural frequencies of the turbine blade were calculated after taking into account the effect of including stress stiffness matrix to the conventional stiffness matrix and the effect of change in the material properties of the turbine blade with the change in temperature and it was observed that inclusion of these two factors resulted in a significant change in the natural frequency of the turbine blade.

CHAPTER 4

TRANSIENT STRESS ANALYSIS

& FATIGUE LIFE ESTIMATION

4.1 INTRODUCTION

The present chapter deals with the transient stress analysis due to thermal, vibratory, and centrifugal loading on the blade. Primarily, there are three different reasons for the existence of the transient conditions of operation. They are due to: (a) unsteady flow conditions on the blade arising out of gas admission to the stator, (b) rising gas temperature till it reaches to steady-state, and (c) acceleration and deceleration of the rotor during starting and shutting operations of the machine. Under the transient conditions of gas admission, the blade experiences variable magnitudes of excitation forces. The resulting stresses may be high and can lower the life cycle of the blade. These stresses, however, can be minimized by good operating procedures. The present investigation studies the separate and collective effect of transient conditions arising out of thermal, vibratory, and centrifugal stress conditions. The transient conditions of operation that exist during the machine start-up and shut-down conditions generate resonant stresses at certain rotor speeds. The forces due to gas pressure are assumed to be distributed along the entire length of the blade. The actual magnitude of the pressure distribution would depend upon the type and operating conditions of the turbine. As has been seen in the Chapter 3 that the overall stiffness matrix [K] changes due to a change in the stress stiffness matrix $[K_\sigma]$ which changes as a result of change in the

deflection of the turbine blade. In order to economize on the CPU time, the stress stiffness matrix $[K_\sigma]$ is computed as the average value of $[K_\sigma]$ at 12 different speeds near the critical speed zone of the turbine blade. In addition, the value of E also changes due to the change in the temperature of the turbine blade. This value of E has also been kept constant as a first approximation towards saving on the CPU time for calculating the vibratory stresses(Bahree, 1987). The boundary conditions at the root of the blade correspond to zero deflection for the applicable nodes. This averaging approximates the linearization of the system.

4.2 TRANSIENT RESPONSE OF A ROTOR BLADE DUE TO NOZZLE EXCITATION FORCES

The equations of motion for a damped system can be expressed as

$$[M^G]\{\ddot{x}\} + [C^G]\{\dot{x}\} + [K^G]\{x\} = \{F(t)^G\} \tag{4.1}$$

The response of each mode is found by decoupling the global equation of motion given in Eq. (4.1). The procedure for decoupling the equations of motion is given below. Introducing a state vector

$$\{y\} = \left\{\frac{\{\dot{x}\}_s}{\{x\}_s}\right\} \tag{4.2}$$

Eq. (4.1) can be reduced to a set of simultaneous first-order equations which are expressed as:

$$[AA]\{\dot{y}\} + [BB]\{y\} = \{EE\} \tag{4.3}$$

where

$$[AA] = \left[\begin{array}{c|c} \underset{(n\times n)}{[0]} & \underset{(n\times n)}{[M^G]} \\ \hline \underset{(n\times n)}{[M^G]} & \underset{(n\times n)}{[C^G]} \end{array}\right] \tag{4.4}$$

$$[BB] = \left[\begin{array}{c|c} \underset{(n\times n)}{[-M^G]} & \underset{(n\times n)}{[0]} \\ \hline \underset{(n\times n)}{[0]} & \underset{(n\times n)}{[K^G]} \end{array}\right] \tag{4.5}$$

and

$$\{EE\} = \left\{\begin{array}{c} \underset{(n\times 1)}{\{0\}} \\ \hline \underset{(n\times 1)}{\{F^G\}} \end{array}\right\} \tag{4.6}$$

The damped natural frequencies are then found by finding the eigenvalues of the dynamical matrix [H] which can be expressed as

$$[H] = -[AA]^{-1}[BB] \tag{4.7}$$

The dynamical matrix of the transposed system will be

$$[H^*] = -[A^T]^{-1} [B] \tag{4.8}$$

Eq. (4.3) can be transformed using the relation

$$\{y\} = [\phi]\{z\} \tag{4.9}$$

where $[\Phi]$ is the modal matrix of the system defined in Eq. (4.3).

Substituting Eq. (4.9) into Eq. (4.3) and premultiplying by $[\Phi^*]^T$, we obtain

$$[\phi^*]^T [AA] [\phi] \{\dot{z}\} + [\phi^*]^T [BB] [\phi] \{z\} = [\phi^*]^T \{EE\} \tag{4.10}$$

This leads to the diagonalization of the global mass and stiffness matrices respectively. Thus the entire system is expressed by individual single degree of freedom systems by decoupling the equations of motion.

In case of mass-orthonormalization of the matrix of eigenvectors, the Eq. (4.1) can be written as

$$\{\ddot{q}\} + 2\zeta\omega_n \{\dot{q}\} + \omega_n^2 \{q\} = \{QF\} \tag{4.11}$$

For individual modes, Eq. (4.11) can be expressed as

$$\ddot{q}_k(t) + 2\zeta_k\omega_{n_k}\dot{q}_k(t) + \omega_{n_k}^2 \ddot{q}_k(t) = QF_k(t) \tag{4.12}$$

where k represents the mode number.

The present investigation models the nozzle excitation force as a sinusoidal pulse as a superposition of two sine waves with a delay of time t_1. Consequently, there will be two types of responses; one for time $t < t_1$ (due to first wave) and second for time $t > t_1$ (due to both waves), as shown in Fig. (4.1). Now, we will consider a rotor blade excited by a force $F(\omega,t)$. Since the frequency

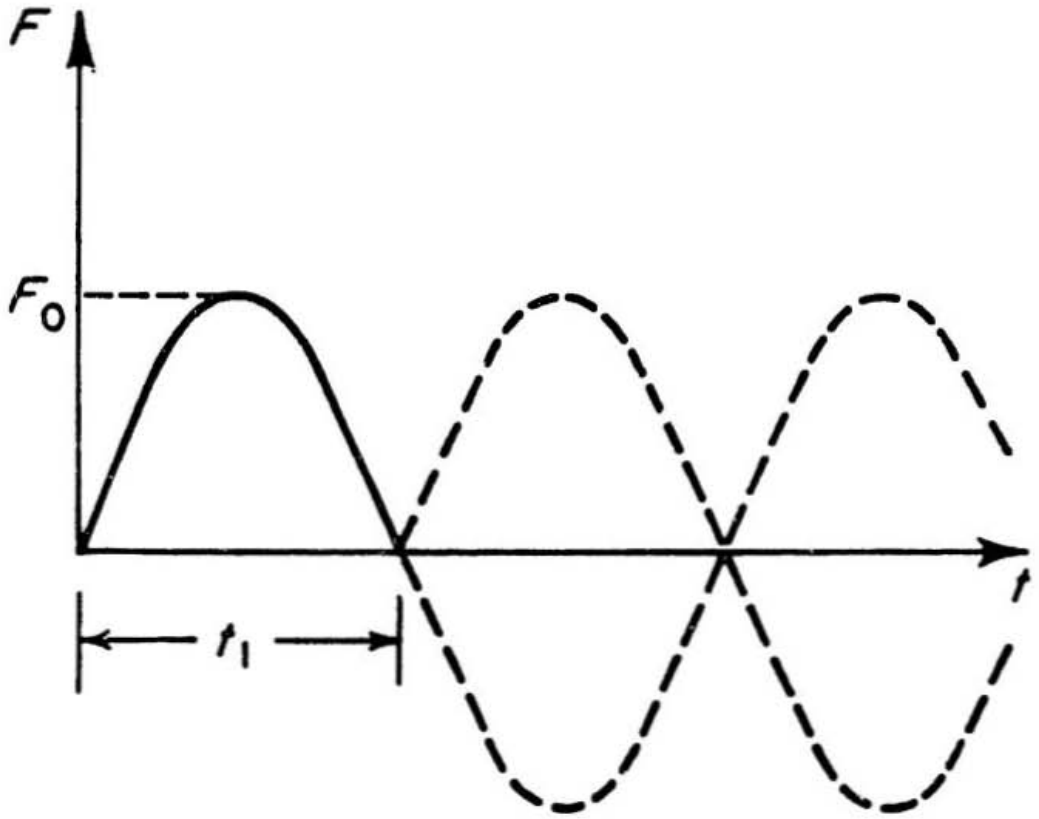

Fig. 4.1 REPRESENTATION OF THE NOZZLE EXCITATION FORCES AS A SINUSOIDAL PULSE

is time dependent, we have

$$\omega = \omega_o + \alpha t \tag{4.13}$$

where

ω_o = angular velocity

α = angular acceleration, and

ω = instantaneous angular velocity

The excitation force for sinusoidal pulse is

$$F = F_o \, Sin(\omega t) \tag{4.14}$$

The response of each mode can be calculated as follows:

$$\ddot{x} + \omega_n^2 x = \frac{F_o}{m} \, Sin(\omega t) \tag{4.15}$$

Since $\omega = \pi / t_1$, we have

$$\ddot{x} + \omega_n^2 x = \frac{F_o}{m} \, Sin\left[\frac{\pi}{t_1} t\right] \tag{4.16}$$

The general solution for Eq. (4.16) is

$$x(t) = A \, Sin(\omega_n t) + B \, Cos(\omega_n t) + \frac{\frac{F_o}{m} \, Sin\left[\frac{\pi}{t_1} t\right]}{\left[\omega_n^2 - \left[\frac{\pi}{t_1}\right]^2\right]} \tag{4.17}$$

The initial conditions are

$$For\ x(0) = \dot{x}(0) = 0, we\ get$$

$$B = 0\ and\ A = \frac{-\frac{F_o}{m}\left[\frac{\pi}{t_1}\right]}{\omega_n\left[\omega_n^2 - \left[\frac{\pi}{t_1}\right]^2\right]} \tag{4.18}$$

Since $\omega_n = 2\pi/\tau$, we can write

$$\frac{\pi}{t_1\ \omega_n} = \frac{\pi}{t_1}\frac{\tau}{2\pi} = \frac{\tau}{2\ t_1} \tag{4.19}$$

Therefore Eq. (4.17) becomes

$$x(t) = \frac{F_o}{m}\left\{\frac{\frac{-\pi}{t_1}Sin\ (\omega_n t)}{\omega_n\left[\omega_n^2 - \left[\frac{\pi}{t_1}\right]^2\right]} + \frac{Sin\left[\pi\frac{t}{t_1}\right]}{\omega_n^2 - \left[\frac{\pi}{t_1}\right]^2}\right\} \tag{4.20}$$

or

$$x(t) = \frac{\frac{F_o}{m}}{\left[\left[\frac{2\pi}{\tau}\right]^2 - \left[\frac{\pi}{t_1}\right]^2\right]}\left\{-\frac{\tau}{2t_1}Sin\ \left[2\pi\frac{t}{\tau}\right] + Sin\left[\pi\frac{t}{t_1}\right]\right\} \tag{4.21}$$

The Eq. (4.21) is the response for the time $t < t_1$.

For time $t > t_1$, the solution above is added with t replaced by $(t - t_1)$. The response in

that case will be as:

$$x(t) = \frac{\frac{F_o}{m}}{\left[\left(\frac{2\pi}{\tau}\right)^2 - \left(\frac{\pi}{t_1}\right)^2\right]} \left\{ -\frac{\tau}{2t_1} Sin\left[2\pi\frac{t-t_1}{\tau}\right] + Sin\left[\pi\frac{t-t_1}{t_1}\right]\right\} \quad (4.22)$$

or

$$x(t) = \frac{\frac{F_o}{m}}{\left(\omega_n^2 - \omega^2\right)} \left\{ -\frac{\tau}{2t_1} Sin\left(\omega_n\,(t-t_1)\right) + Sin\left(\omega(t-t_1)\right)\right\}$$

(4.23)

The gas forces have been calculated from the circulation and the lift over the airfoil. The circulation over the airfoil is given by

$$\Gamma = c\int_0^{\pi} \gamma(\theta)\sin\theta d\theta$$

$$= 2V_\infty c\int_0^{\pi} \{A_0(1 + \cos\theta) + \Sigma A_n \sin n\theta \sin\theta\} d\theta$$

$$= 2V_\infty c\left\{\pi A_o + \frac{1}{2}\pi A_1\right\} \quad (4.24)$$

where

$V_\infty = 718.05$ m/sec.

$c = 0.07$

$A_0 = 0.40151$

$A_1 = 0.08146$

A_0 and A_1 are Glauert constants for a thin cambered airfoil.

The lift L is thus calculated as

$$L = \pi c \rho_\infty V_\infty^2 (2A_0 + A_1) \tag{4.25}$$

where $\rho = 2.89$. F_0 was 10 % of the value of the lift obtained in Eq. (4.25).

4.3 TRANSIENT RESPONSE DUE TO CENTRIFUGAL FORCE

The radial location of the element with reference to the axis of rotation of the rotor shaft causes the centrifugal forces in the turbine blade. The centrifugal force is given as:

$$F_c = m\ \omega^2\ (R + z) \tag{4.26}$$

where

m = the mass of the element

R = radius of the rotor disk

z = distance from the root to the centre of gravity of element.

This force acts at the centre of gravity and such can be replaced by eight equivalent forces each of which act at the corner and mid nodes. Also, these centrifugal forces are time variant because ω in Eq. (4.26) is a variable which is calculated from Eq. (4.14).

For calculating the dynamic response due to the centrifugal forces, the forcing function corresponding to the Eq. (4.19) is given as

$$F_c = (R + z)\ (\alpha t)^2\ m \tag{4.27}$$

by assuming $\omega_0 = 0$ in Eq. (4.13).

The modal response is given by:

$$q_k\ (\ t\ ) = \frac{1}{\omega_{dk}} \int_0^t (R + z)\ (\alpha t)^2\ m\ e^{(-\xi_k\ \omega_{nk}\ (t\ -\ \tau))}\ \mathrm{Sin}(\omega_{dk}\ (t\ -\ \tau))d\tau \tag{4.28}$$

where ω_{nk} = natural frequency of kth mode

ω_{dk} = damped natural frequency of kth mode

The solution for this equation can be written as(Weast, 1975):

$$q_k\ (\ t\ ) = \frac{(R + z)}{\omega_{dk}}\ \alpha^2\ \mathrm{Sin}\ (\ \omega_{dk}\ t\ )\ e^{(-\xi_k\ \omega_{nk}\ t\ )}$$

$$\left[e^{(\xi_k\ \omega_{nk}\ \tau)} \sum_{r=0}^{2} \frac{(-1)^r\ 2!\ (\tau)^{(2-r)}}{\left(\xi_k^2\ \omega_{nk}^2 + \omega_{dk}^2\right)^{\frac{r+1}{2}}\ (2\ -r)\ !}\ \mathrm{Cos}\left(\omega_{dk}\ \tau - (r\ +1)\ \tan^{(-1)}\left(\frac{\omega_{dk}}{\xi_k\ \omega_{nk}}\right)\right)\right]_0^t$$

$$-\ \frac{(\ R\ +z\ )\ \alpha^2}{\omega_{dk}}\ \mathrm{Cos}(\ \omega_{dk}\ t\ )\ e^{(-\xi_k\ \omega_{nk}\ t\ )} \tag{4.29}$$

$$\left[e^{(\xi_k \omega_{nk}\ \tau)} \sum_{r=0}^{2} \frac{(\ -1)^r\ 2!\ (\ \tau\ )^{(2-r)}}{\left(\xi_k^2\ \omega_{nk}^2 + \omega_{dk}^2\right)^{\frac{r+1}{2}}\ (\ 2\ -r\ )!}\ \mathrm{Sin}\left(\ \omega_{dk}\ \tau - (\ R\ +1\ )\ \tan^{(-1)}\left(\frac{\omega_{dk}}{\xi_k \omega_{nk}}\right)\right)\right]_0^t$$

To calculate the response one has to decouple the equations of motion using the matrix of eigenvectors in the same fashion as shown from Eq. (4.1) to Eq. (4.12).

4.4 VIBRATORY STRESSES

The dynamic loading on the turbine blade is caused by nozzles placed at regular intervals along the periphery of the rotor. For the purpose of calculating the vibratory stresses, the turbine blade is divided into 35 twenty-noded elements shown in Fig. (2.4). Defining $\{\gamma\}$ and $\{x\}$ as elemental strains and displacements, from the total response of the turbine blade due to nozzle excitations, the strains in each element are obtained from the isoparametric finite element formulation as

$$\underset{6 \times 1}{\{\gamma\}} = \underset{6 \times 60}{[B_1]} \; \underset{60 \times 1}{\{x\}} \tag{4.30}$$

and the dynamic stresses are calculated as

$$\underset{6 \times 1}{\{\sigma\}} = \underset{6 \times 6}{[D_1]} \; \underset{6 \times 1}{\{\gamma\}} \tag{4.31}$$

The vibratory stresses were calculated using Eqs. (4.30) and (4.31). The results obtained are shown in Fig. 4.2. This figure shows that the peak stresses occur at the critical speeds.

4.5 CENTRIFUGAL STRESSES

Similar procedure was applied to find centrifugal stresses at different rotor speeds.

In this case response was obtained using Eq. (4.29). The Fig. (4.3) shows that centrifugal stresses increase as the rotor speed increases. This follows from the fact that the normal acceleration increases with the increase in the angular velocity.

4.6 THERMAL STRESSES

The temperature distribution for the three-dimensional turbine blade finite element model was obtained from Eqs. (2.1) to (2.52). The thermal stress distribution was found from this temperature distribution using Eqs. (2.53) to (2.67). It was also established in the Chapter 2 that if gas temperature is raised from room temperature to 870° C instantaneously, the thermal stresses in the blade for that particular heating rate exceed the yield stress as shown in Fig. (4.4). This problem is solved by increasing the gas temperature in stages; first to 400° C, then to 870° C and finally maintaining the gas temperature at 870° C. The thermal stresses for this heating path were then calculated and found to be within the yield stress limit. These stresses are shown in Fig. (4.5).

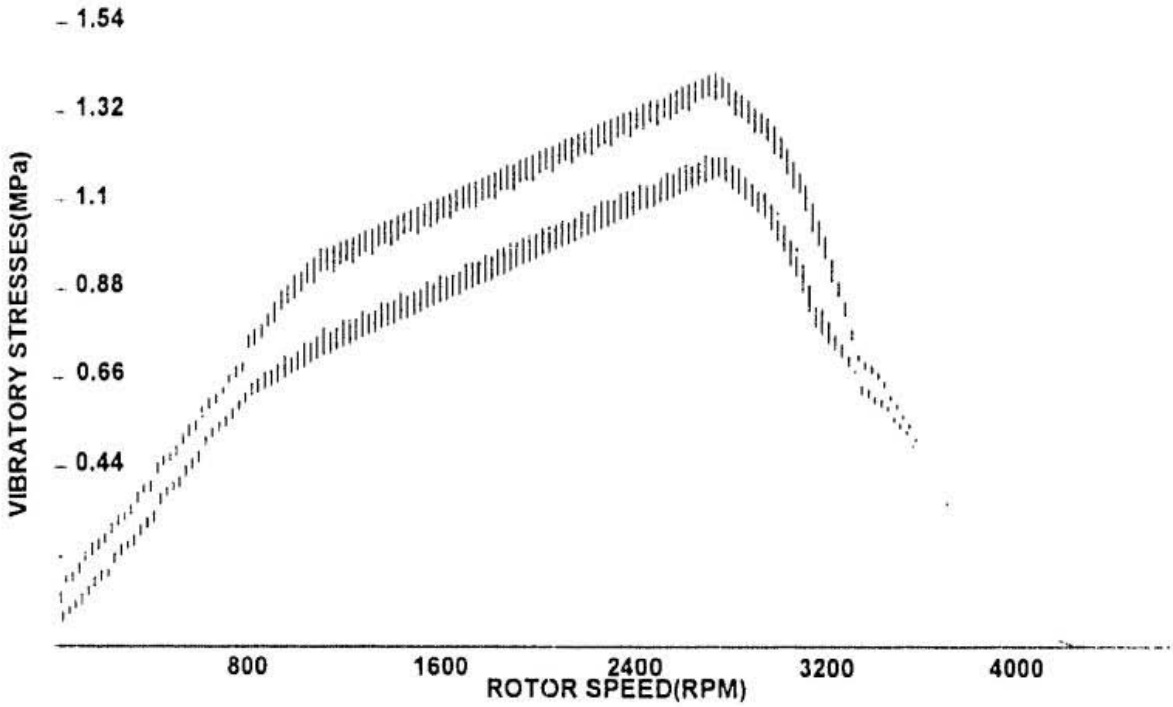

Fig. 4.2 VIBRATORY STRESSES AT VARIOUS ROTOR SPEEDS

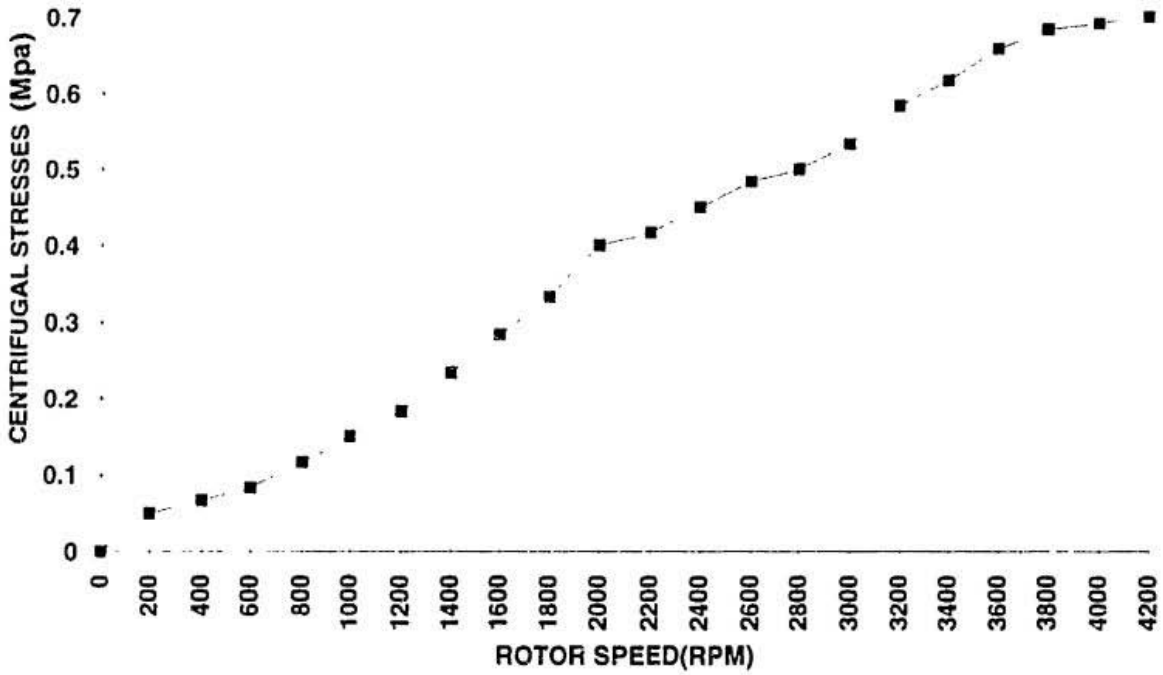

Fig. 4.3 CENTRIFUGAL STRESSES AT VARIOUS ROTOR SPEEDS

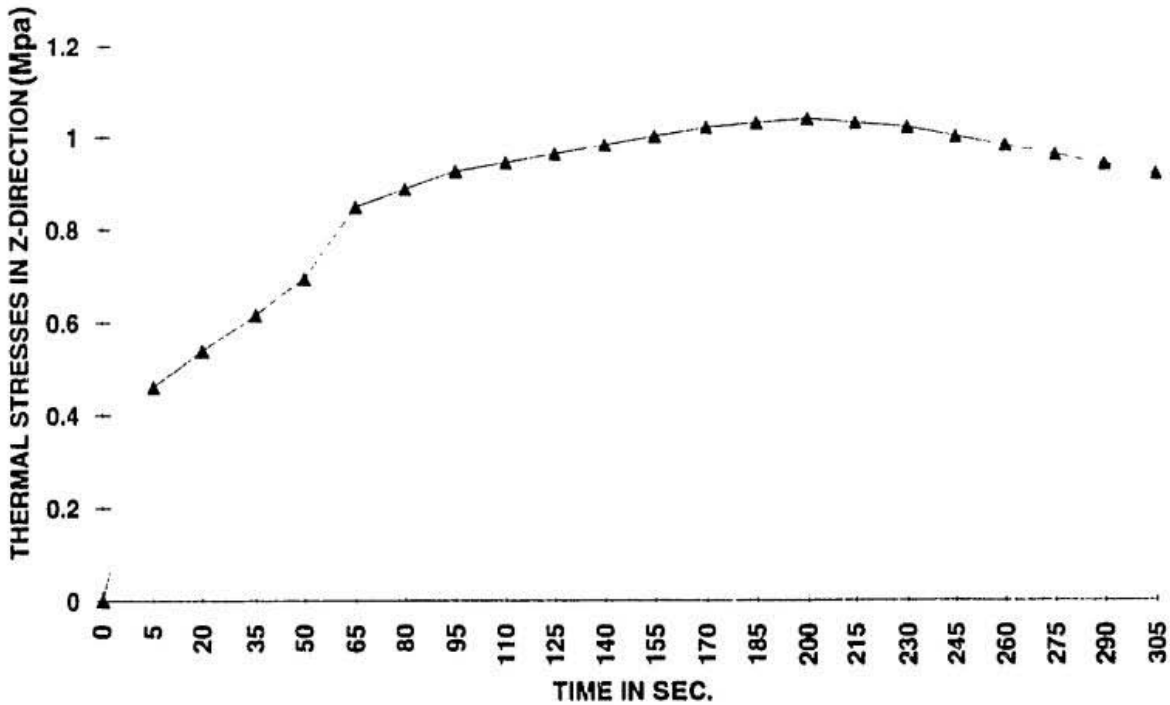

Fig. 4.4 THERMAL STRESSES AT VARIOUS TIMES

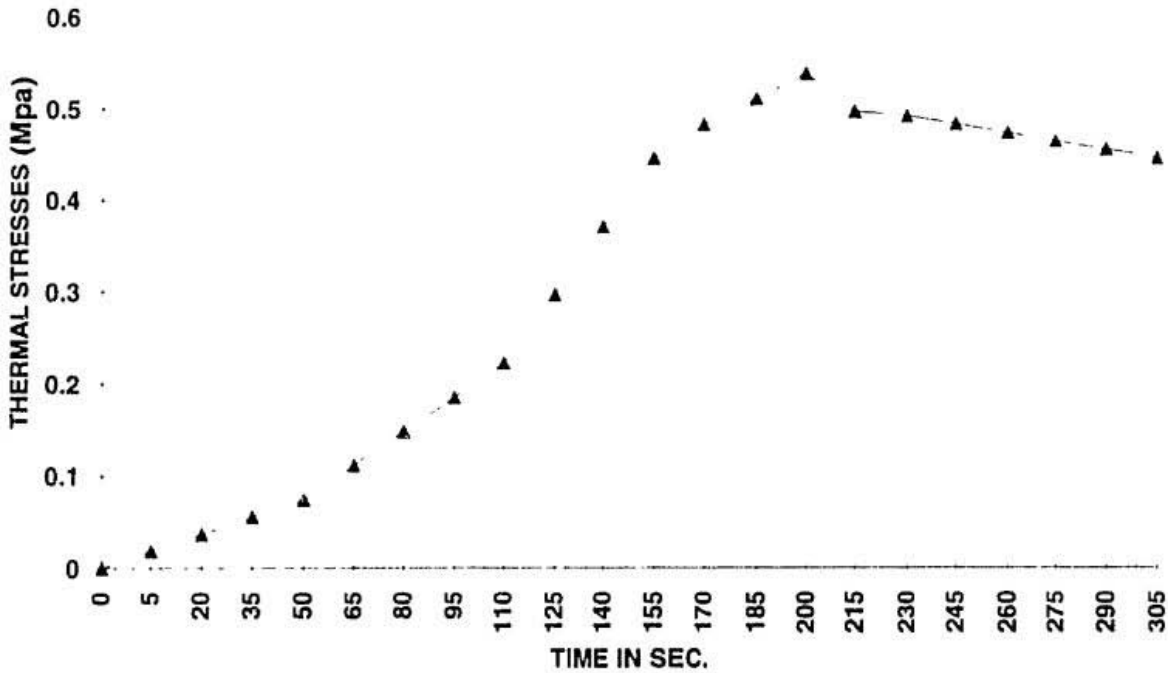

Fig. 4.5 TRANSIENT THERMAL STRESS (σ_{zz}) DISTRIBUTION IN THE BLADE FOR THE FEASIBLE HEATING RATE OF 24° C/SEC AT DIFFERENT INSTANTS OF TIME

4.7 STRESS ANALYSIS OF BLADE DUE TO COMBINED EFFECTS

From the Figs. 4.2 to 4.5, one can determine the critical instants of time from the stress point of view. The thermal stresses are maximum at time t = 200 sec., and then these stresses decrease slowly with time. At time t = 200 sec. when the rotor speed is 2900 rpm, centrifugal stresses are also high and are still increasing with increase in rotor speed. An interesting feature is that the vibratory stresses show their peak at time t = 204 sec. when rotor speed is about 3000 rpm. From these observations, it is clear that between time t = 200 sec. and t = 205 sec., and between rotor speeds of 2800 rpm and 3200 rpm, all the three types of stresses are at their peak. All the stresses mentioned here are normalized stresses(normalizing factor is the yield stress). By selecting a feasible heating path for thermal stresses, the normalized thermal stresses are kept below one. Also the centrifugal stresses can be kept within the safe limit by operating the rotor at a speed within 4000 rpm. However, in case of vibratory stresses, we see normalized stresses going beyond one. From all these discussions, one can conclude that, in addition to vibratory and centrifugal stresses, the thermal stresses are also quite important in the design of the blade. In the design of an actual turbine blade, the transient forces have to be exactly known, and, therefore, the actual design would involve at first the summation of all the stresses at any instant of time, and then finding the global maxima of these types of combined stresses as the time varies. To do this, the stresses are added up and the principal stresses in each element of the turbine blade are obtained by solving the following cubic equation given by Timoshenko and Goodier (1970):

$$S^3 - (\sigma_x + \sigma_y + \sigma_z) S^2 + (\sigma_x \sigma_y - \sigma_y \sigma_z + \sigma_x \sigma_z - \tau_{yz}^2 - \tau_{xz}^2 - \tau_{xy}^2) S$$

$$- (\sigma_x \sigma_y \sigma_z + 2 \tau_{yz} \tau_{xz} \tau_{xy} - \sigma_x \tau_{yz}^2 - \sigma_y \tau_{xz}^2 - \sigma_z \tau_{xy}^2) = 0 \qquad (4.32)$$

Solving the Eq. (4.32) will give the three principal stresses as σ_1, σ_2, and σ_3. In order to know the state of stress in each element of the turbine blade, the design stress (σ_d) is found using distortion energy theory. The σ_d is given by the following equation:

$$\sigma_d = \frac{1}{\sqrt{2}} \left[(\sigma_1 - \sigma_2) + (\sigma_2 - \sigma_3) + (\sigma_3 - \sigma_1) \right]^{1/2} \qquad (4.33)$$

This stress σ_d comprises of both mean and alternating stresses arising from thermal, centrifugal, and vibratory stresses. This gives us a clear picture about the stress history of the turbine blade and their effect on fatigue life of the turbine blade which is discussed in next article.

4.8 FATIGUE LIFE ESTIMATION

The present investigation makes use of the fatigue failure surface line by Bagci(1981). Fig. (4.6) shows the failure surface and the Bagci line where the mean stress is represented by σ_m. This fatiguo line gives the fatigue design of machine elements subjected to cyclic combined stresses having non-vanishing stress as in the present case. It is reported to fit the most recent fatigue data well and defines the two design zones, namely, the zone of fatigue failure experiencing brittle fracture and

the zone of failure due to yielding in one, and thus, providing a unified fatigue design equation for machine members.

Bagci's fatigue failure surface line is of fourth order and is given by

$$\sigma_{af} = \sigma_e \left(1 - \left\{ \frac{\sigma_{mf}}{\sigma_y} \right\}^4 \right) \tag{4.34}$$

where

σ_{af} = failure value of alternating stress

σ_e = endurance limit

σ_{mf} = failure value of mean stress

σ_y = yield stress for the material

The endurance limit σ_e of the actual blade may be lower than the endurance limit σ_e' of the standard rotating fatigue specimen due to a number of factors discussed below.

The factors are accounted for by using

$$\sigma_e = R_f \, \sigma_e' \tag{4.35}$$

where the endurance limit modifying factor

$R_f = k_a \, k_b \, k_c \, k_d \, k_e \, k_f$

with

k_a = surface factor

= 0.46 for the turbine blade material with tensile strength of 1183 MPa

k_b = size factor

= 1.00 for the thickness dimension ($d \leq 7.6$ mm.) of the root-section of the turbine blade

k_c = reliability factor

= .86

k_d = temperature factor

= 3100/(2400 + 9T) for T > 70° C. Therefore for T = 435° C, k_d = 0.50

k_e = stress concentration factor

= 1/(1 + q(k_t - 1)), q is the notch sensitivity factor, where k_t is the factor which depends on the geometric values of the member. For a notch of 0.2 cm. radius, q = 0.85, k_t = 2.6 which gives k_e = 0.424.

k_f = miscellaneous factor

= 1.0 (assuming the blade to be undamaged).

Therefore, R_f = 0.46 X 1.0 X 0.86 X 0.50 X 0.424 X 1.0 = 0.084

Using

σ_u(ultimate stress) = 1183 MPa

σ_y(yield stress) = 855 MPa

σ_e(endurance limit) = 591 MPa, and

from the values detailed above, the following stresses for the material can be calculated: using Eq. (4.27).

σ_{af}(alternating failure stress) = 49.686 MPa

σ_{mf}(mean failure stress) = 89.4348 MPa

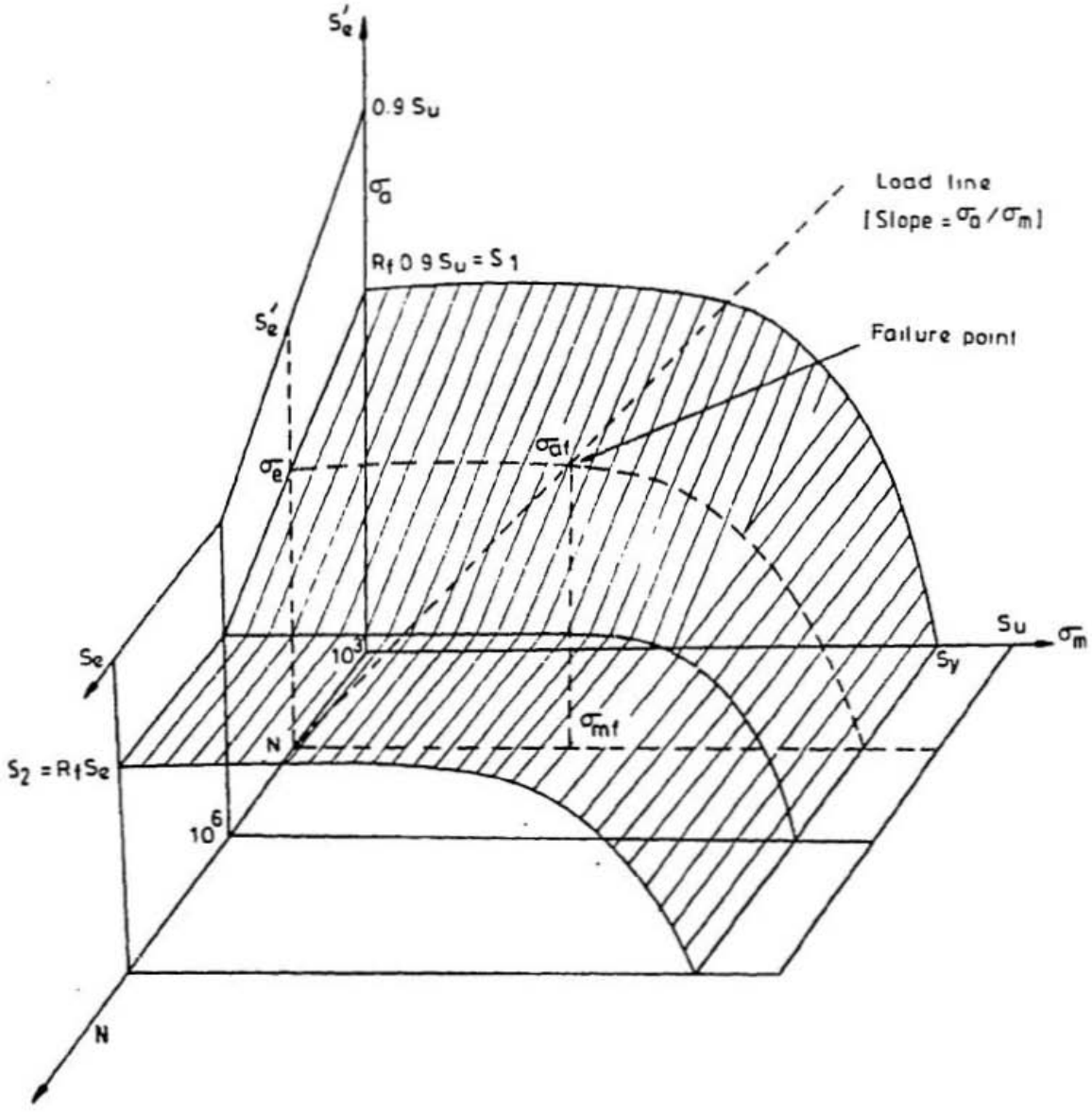

Fig. 4.6 FATIGUE FAILURE SURFACE DEFINED BY BAGCI LINE

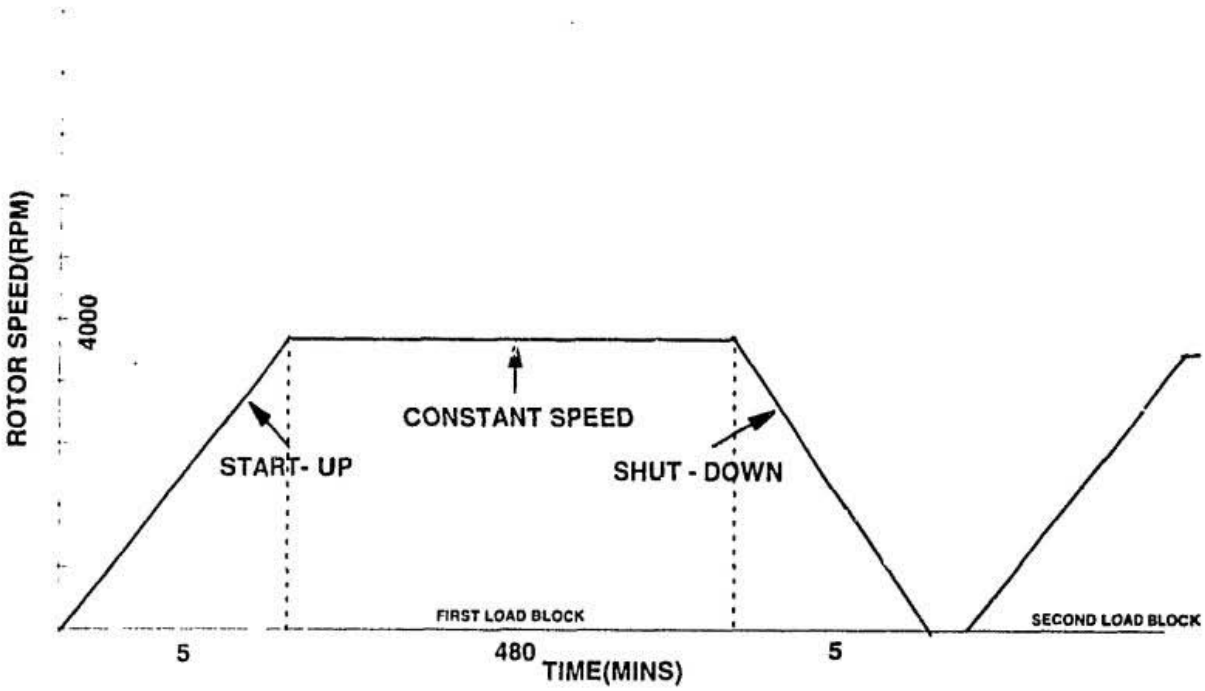

Fig. 4.7 BLADE LOADING PATTERN

4.9 CUMULATIVE FATIGUE DAMAGE

The turbine blades discussed in the present investigation are assumed to be operating in a machine at an acceleration rate of 800 rpm/min and working for 8 hours (480 minutes) at 4000 rpm. Fig. (4.7) gives blade loading pattern If the blade was to operate at 4000 rpm without being ever shut down, the blade will have infinite life However, that is not the case due to the actual blade loading pattern shown in Fig. 4.7. The turbine blade is excessively stressed while passing through resonant rotor speeds, both during start-up and shut-down, in each load block. Since it was established before that the resonant stresses would be between 2800 rpm and 3200 rpm at time t = 200 sec, a check of the stress levels experienced between these two rotor speeds and at these particular time instants were made. In order to calculate the fatigue damage, the calculations of the stress amplitudes between 2800 rpm and 3200 rpm were made. The peak alternating stresses within this speed zone are shown in Fig. (4.8). From these graphs, it is clear that the resonant stresses lie above the failure value and the fatigue damage would be caused to the blade. For the estimation of fatigue damage, the resonant peaks are divided into 11 stress blocks. The rotor speeds and the corresponding stress levels are shown Table 4.1. The number of cycles N to failure is obtained by locating the load point on the failure surface and the number of cycles, n, experienced n is obtained from calculating the cycles in each stress blocks. Thus fatigue damage is obtained as a ratio of n/N.

The total fatigue damage during start-up in each stress block as can be seen in Table 4 1 is $\Sigma\ n/N = 25 \times 10^{-5}$

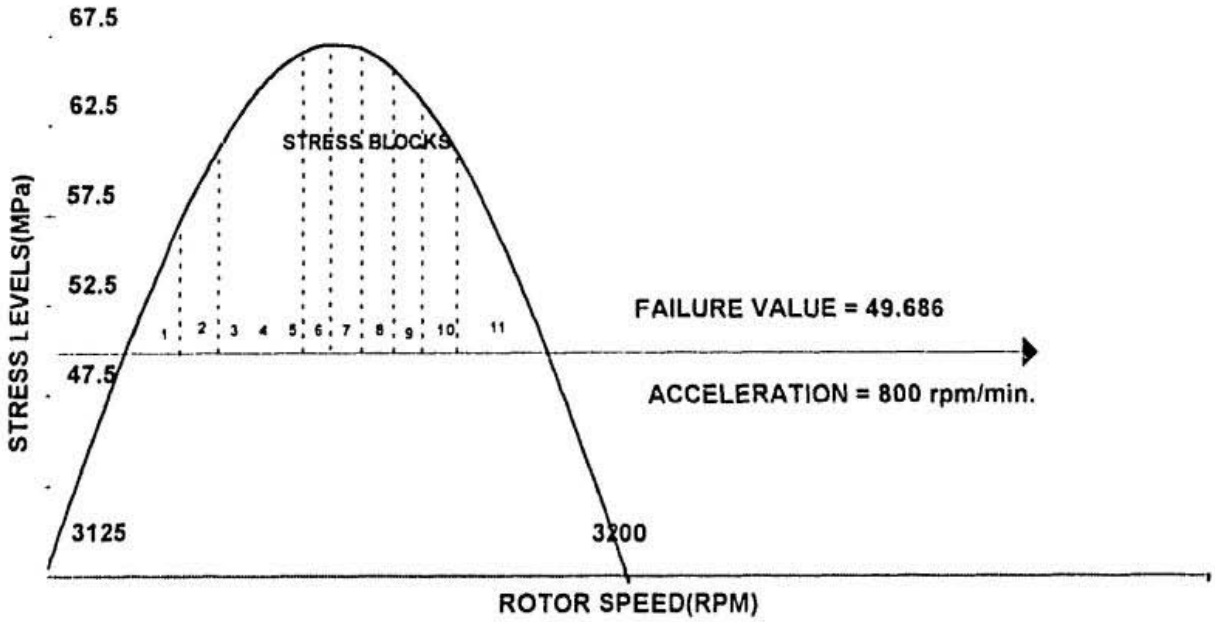

Fig. 4.8 MAGNIFIED STRESS LEVELS BETWEEN 3100-3200 RPM DURING START-UP AT ROTOR ACCELERATION OF 800 RPM/MIN.

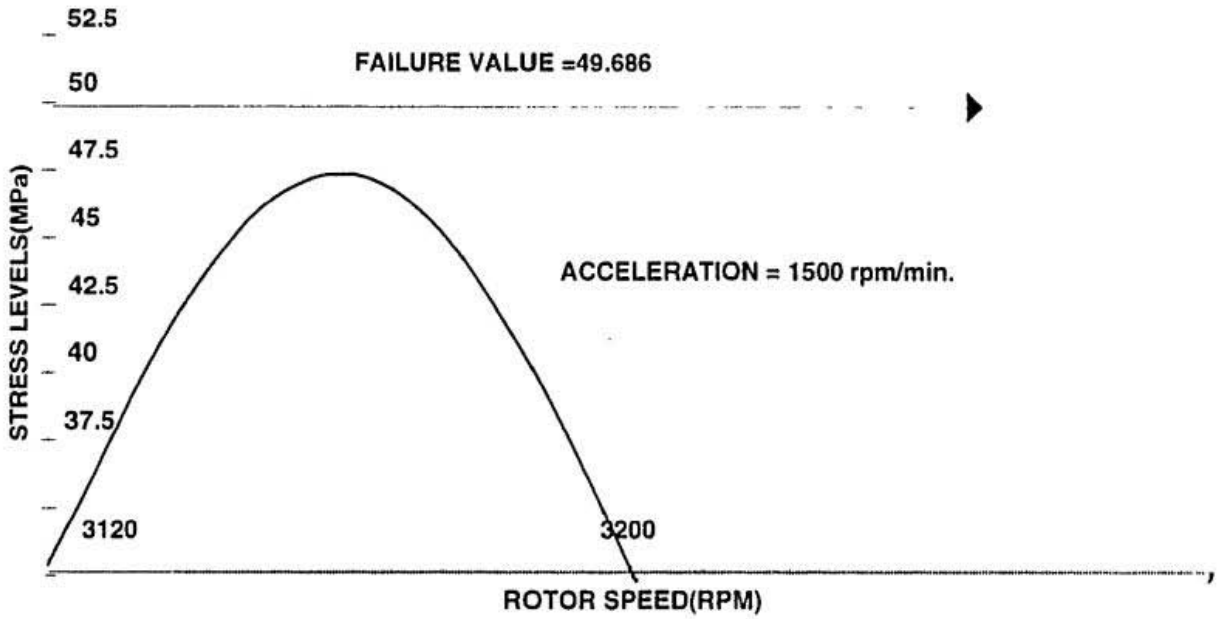

Fig. 4.9 MAGNIFIED STRESS LEVELS BETWEEN 3100-3200 RPM DURING START-UP AT ROTOR ACCELERATION OF 1500 RPM/MIN.

STRESS BLOCK NUMBER(DURING START - UP)	ALTERNATING STRESS(Pa)	MEAN SPEED(RPM)	CYCLES TO FAILURE(N)	CYCLES EXPERIENCED(n)	FATIGUE DAMAGE(n/N *10*(-5))
1	52500000	2800	1605000	23	1.433021807
2	53650000	2840	1665000	23	1.381381381
3	55800000	2880	1350000	22	1.62962963
4	58650000	2920	975000	27	2.769230769
5	64500000	2960	449000	27	6.013363029
6	63500000	3000	456500	13	2.847754655
7	61600000	3040	585000	20	3.418803419
8	58500000	3080	1105500	21	1.899592944
9	54500000	3120	1400000	25	1.785714286
10	52500000	3160	1605000	20	1.246105919
11	50500000	3200	1906300	20	1.049152809
STRESS BLOCK NUMBER(DURING SHUT - DOWN)					
1	52447399	2800	1765000	22	1.246458924
2	53590000	2840	1832000	20	1.091703057
3	55744500	2880	1490000	21	1.409395973
4	58596500	2920	1075200	18	1.674107143
5	64435000	2960	493950	19	3.846543172
6	63437600	3000	502200	19	3.783353246
7	61534800	3040	643750	25	3.883495146
8	57914500	3080	1215060	20	1.646009251
9	54440000	3120	1540500	12	0.778967868
10	52447399	3160	1766000	23	1.302378256
11	50445900	3200	2096390	13	0.620113624
TOTAL FATIGUE DAMAGE DURING START UP	0.000254738				
TOTAL FATIGUE DAMAGE DURING SHUT DOWN	0.000212825				
TOTAL FATIGUE DAMAGE DURING START-UP AND SHUT-DOWN	0.000467563	=46*10**(-5)			

Table 4.1 STRESS-BLOCK APPROXIMATION OF FATIGUE DAMAGE FOR START-UP AND SHUT DOWN OPERATION

In this table the fatigue damage during the shut-down is

$\Sigma\, n/N = 21 \times 10^{-5}$

The total fatigue damage due to start-up and shut-down in each load block is thus given as

$25 \times 10^{-5} + 21 \times 10^{-5} = 46 \times 10^{-5}$.

Similar calculations with different acceleration were done. A new value of acceleration (1500 rpm/min) of blade rpm was found to be safe as the peak of the resonant stresses obtained for the rotor speed zone between 2800 rpm and 3200 rpm, were found to be below the failure value indicating no fatigue damage caused to the blade. Fig. 4.9 shows the peak alternating stress levels for a value of 1500 rpm/min. The total blade fatigue life is given by applying Miner's rule:

$$\frac{1}{46 \times 10^{-5}} = 2.173 \times 10^{3} \text{ load blocks}$$

4.10 CONCLUSIONS

In spite of the fact that various design procedures for preventing failure of turbine blades due to fatigue are being used, there is yet no indication that a satisfactory situation exists with reference to basic data that will lead to establishing sound procedures in this regard. This is because of the fact that blade fatigue is a multi-dimensional problem and as such, has been undergoing continuous investigations for long time. However, the approach discussed in the present investigation can be used effectively to identify the time instants and rotor speeds which can cause fatigue damage due to start-up and shut-down operations.

CHAPTER 5

CONCLUSIONS AND RECOMMENDATIONS

5.1 A BRIEF DISCUSSION ABOUT THE INVESTIGATION AND THE CONCLUSIONS

The objective of this investigation was to find the fatigue life of turbine blades due to combined effects of thermal and vibratory loadings. This was achieved by separately carrying out the heat transfer and vibration analysis of a blade and then adding the effects due to each of these. The heat transfer analysis was done using non-linear finite element analysis in three-dimensions. The non-linearity was due to change in material properties of the blade with temperature. The transient temperatures obtained from the heat transfer analysis were then used in the calculation of the temperature gradients and transient thermal stresses. The dynamic analysis was done at first, for finding the undamped natural frequencies of the turbine blade. These free vibration studies included the effect of the non-linearity in the stiffness matrix caused by the rotation of the turbine blade. The effect of change in the frequencies arising from the change in the material properties of the blade with temperature were also studied. Thereafter, the vibratory stresses due to (a) the nozzle excitation and (b) the centrifugal stresses at different rotor speeds were calculated. Finally, the total effect of all the three different types of stresses (transient thermal, centrifugal, and vibratory due to the nozzle excitation) on the fatigue life of the turbine blade was studied. The mathematical model for both the heat transfer and the vibratory analysis was formulated using curved, solid, C^0 continuity, quadratic, serendipity, twenty noded isoparametric finite elements.

The studies carried out in this investigation, therefore, helps one to draw the following conclusions:

1. In addition to temperature gradients along the cross-section of the blade, there exists a significant gradient along the z-direction as well.
2. In addition to stresses in z-direction, there are significant stresses in x and y directions as well, which are due to the three-dimensional temperature distribution.
3. The thermal stresses are maximum at time t = 200 sec. These stresses decrease slowly with time.
4. The transient thermal stress distribution in the blade can be limited well within yield stress for the feasible heating rate of 24° C/sec.
5. The solid isoparametric finite element can be successfully used to accurately predict the three-dimensional temperature distribution.
6. The effect of including the stress stiffness matrix along with the conventional matrix makes a significant change in the natural frequencies of the blade.
7. The blade natural frequencies also vary quite significantly during the transient period.
8. The kinematic equations can be successfully used to model the nozzle excitation forces as a sinusoidal pulse.
9. The centrifugal stresses increase with increase in rotor speed.
10. The vibratory stresses show their peak at time t = 204 sec. when the rotor speed is about 3000 rpm.
11. Between time t = 200 sec. and t = 205 sec., and between rotor speeds of 2800

rpm and 3200 rpm, all the three types of stresses are at their peak.

12. In addition to vibratory and centrifugal stresses, the thermal stresses are also quite important in the design of the blade.

13. The turbine blade is excessively stressed while passing through resonant rotor speeds both during start-up and shut-down in each load block.

14. A new value of acceleration (1500 rpm/min) of blade was found to be safe as the peak of the resonant stresses obtained for the rotor speed zone between 2800 rpm and 3200 rpm, were found to be below the failure value indicating no fatigue damage caused to the blade.

5.2 LIMITATIONS OF THE PRESENT INVESTIGATION AND RECOMMENDATIONS FOR FUTURE WORK

1. The calculations for non-linear temperature distribution were done assuming surrounding gases to be at uniform temperature while the gas temperatures in practice are not so. The present finite element model can be amended to include the effect of non-uniform gas temperature distribution around the blade.

2. The creep under high temperature conditions was not taken into account.

3. Fatigue being a multi-facet problem, data collection on broad blade-operational aspects is essential for definition of a specific fatigue problem.

4. The dynamic response was calculated keeping viscous damping as a function of rotor speed. The non-linearity in the damping due to dry-friction damping at the root of the blade, where it is attached to the rotor disk, should also be taken into

account.

REFERENCES

1. **Akin, J.E.**, 1982. "Application and Implementation of Finite Element Methods", Academic Press Inc. (London) Ltd., pp. 65-77.

2. **Allen, J.M.**, 1982(April). "Effect of Temperature Dependent Mechanical Properties on Thermal Stresses in Cooled Turbine Blades", Journal of Engineering for Power, Trans. ASME, Vol. 104, pp. 349-353.

3. **Bagci, C.**, 1981. "Fatigue Design of Machine Elements Using Bagci Line Defining the Fatigue Surface Line (Mean Stress Diagram)", Mechanism and Machine Theory, 16, No. 4, p. 339.

4. **Bahree, R.**, 1987. "Analysis and Design of Rotor Blades Due to the Transient Thermal and Vibratory Loads", M. Eng thesis, Memorial university of Newfoundland.

5. **Banerji, J.R. and Williams, F.W.**, 1985. "Exact Bernoulli-Euler Dynamic Stiffness Matrix for a Range of Tapered Beams", Intl. J. of Numerical Methods in Engineering, Vol. 21, pp. 2289.

6. **Bogov, I.A.**, 1978. "Influence of Turbine Blade Airfoil and Root Thickness Variation

along the Blade on its Thermal Stress State", Energomashinostroenie, No. 8, pp. 10--12.

7. **Boyce, P. Maherwan**, 1982. "Gas Turbine Engineering Handbook", Gulf Publishing Company.

8. **Collins, J.A.**, 1981. "Failure of Materials in Mechanical Design", John Wiley.

9. **Cook, R.D.**, 1981. "Concepts and Applications of Finite Element Analysis", John Wiley and Sons Inc., pp. 13-121.

10. **Cravalho E.G. and Smith, J.L. Jr.**, 1981. "Engineering Thermodynamics", Pitman Publishing Inc.

11. **Csanady, G.T.**, 1964. "Theory of Turbomachines", McGraw-Hill Book Company.

12. **Cubberly, W.H.**, 1980. "ASM Metals Reference Book, American Society for Metals", Metals Park, Ohio, Ed. 9, Vol. 3, pp. 248-249.

13. **Daniels, L.D. and Browne, W.B.**, 1981. "Calculation of Heat Transfer Rates to Gas Turbine Blades", Int. Journal of Heat and Mass Transfer, Vol. 24, No. 5, pp. 871-879.

14. **Dewey, R.P. and Rieger, N.F.**, 1982. "Survey of Steam Turbine Blade Failures", Proc. EPRI Workshop on Steam Turbine Reliability, Boston, MA.

15. **Dimarogonas, A.D. and Paipetis, S.A.**, 1983. "Analytic Methods in Rotor Dynamics", Applied Science Publishers.

16. **Faires, V.M.**, 1970. "Thermodynamics", The Macmillan Company, London.

17. **Gryaznov, B.A., Zaslotskya, L.A., Konoplyanikov, E.G., and Mitchenko, E.I.**, 1979(Sept.). "Experimental Verification of Finite Element Caiculation of the Thermal Stress of Gas Turbine Blades", Probl. Procn., No. 9, pp. 34-37.

18. **Gupta, A.K.**, 1985. "Vibration of Tapered Beams", J. of Structural Engineering, ASCE, Vol. 111, pp. 19.

19. **Guyan, R.J.**, 1965. "Reduction of Stiffness and Mass Matrices", AIAAJ, Vol. 3, No. 2, pp. 380.

20. **Hartog, D.**, 1956. "Mechanical Vibrations", McGraw-Hill Book Company.

21. **Heywood, R.B.**, 1962. "Designing Against Fatigue", Chapman and Hall.

22. **Hosny, A.N.**, 1973. "Propulsion Systems", University of South Carolina.

23. **Houghton E.L. and Brock A.E.**, 1970. "Aerodynamics for Engineering Students", Edward Arnold (Publishers) Ltd.

24. **Huebner H.B. and Thornton, E.A.**, 1982. "The Finite Element Method for Engineers", John Wiley & Sons.

25. **Hutchinson, J.R. and Zillmer, S.D.**, 1986. "On the Transverse Vibration of Beams of Rectangular Cross-Section", J. of Applied Mechanics, ASME, Vol. 53, p 278.

26. **Juvenal, R.C.**, 1967. "Engineering Considerations of Stress, Strain, and Strength", McGraw-Hill.

27. **Juvinall, R.C.**, 1983. "Fundamentals of Machine Component Design", John Wiley & Sons, 1983.

28. **Littler, D.J.**, 1969(Sept.). "Thermal Stresses and Thermal Fatigue", Proceedings of the Int. Conference held at Berkeley Castle, Gloucestershire, England, pp. 374-386.

29. **Mabie, H.H. and Rogers, C.B.**, 1974. "Transverse Vibrations of a Doubly Tapered Cantilever Beam with an End Mass and End Support", J. of Acou. Soc.America, Vol. 55, pp. 986.

30. **Maya, T., Katsumata, I., and Itoh, M.**, 1978. "A study of Thermal Fatigue Life Prediction of Air-Cooled Turbine Blades", ASME Paper No. 78-GT-63.

31. **Meirovitch, Leonard.**, 1975. "Elements of Vibration Analysis", McGraw-Hill, Inc.

32. **Mohanty, A.K., Raghavachar, T.S., and Nanda, R.S.**, 1977. "Heat Transfer from Rotating Short Radial Blades", Int. Journal of Heat and Mass Transfer, Vol. 20, pp. 1417-1425.

33. **Mukherjee, D.K.**, 1978. "Stresses in Turbine Blades Due to Temperature and Load Variation", ASME Paper No. 78-GT-158.

34. **Nagarajan, P. and Alwar, R.S.**, 1984. "A three Dimensional Approach to Blade Packet Vibrations", J. of Sound and Vibration, Vol. 95(3), pp. 295-303.

35. **Ramamurthy, V. and Balasubramaniam, P.**, 1984(Aug.). "Analysis of Turbomachine Blades - A Review", Sh. V.B., pp. 7.

36. **Rao, J.S. and Vyas, N.S.**, 1985. "Response of Steam Turbine Blades Subjected to Distributed Harmonic Nozzle Excitation", 3rd Int. Modal Analysis Conference, Orlando, Florida, 1985, pp. 618-626.

37. **Rao, J.S.**, 1981. "Turbomachine Blade Vibration", Wiley Eastern Ltd.

38. **Rao, J.S. and Carnegie, W.**, 1970. "Solution of the Equation of Motion of Coupled Bending-Torsion Vibrations of Turbine Blades by the Method Ritz-Galerkin", Int. J. of Mech. Sci., Vol. 12, pp. 875.

39. **Rao, J.S.**, 1983. "Single Blade Dynamics", Session Proc. Tech. Comm. on Rotordynamics, Sixth IFToMM Congress, New Delhi, pp. 41.

40. **Rao, J.S. and Carnegie, W.**, 1970. "Solution of the Equation of Motion of Coupled Bending, Bending-Torsion Vibrations of Turbine Blades by the Method Ritz-Galerkin", Int. J. of Mech. Sci., Vol. 12, pp. 875.

41. **Rao, S.S.**, 1986. "Mechanical Vibrations", Addison-Wesley Publishing Company.

42. **Rao, S.S.**, 1982. "The Finite Element Methods in Engineering", Pergamon Press.

43. **Rieger, N.F.**, 1983. "Blade Fatigue", Session Proc. Tech. Comm. on

Rotordynamics, Sixth IFToMM Congress, New Delhi, p.66.

44. **Rieger, N.F. and Nowak, W.J.**, 1977. "Analysis of Fatigue Stress in Turbine Blade Groups", EPRI Seminar on Steam Turbine Availability, Palo Alto, California.

45. **Roeder, A.**, 1984(June). "The influence of Material Properties on the Design of Large Steam Turbines", First Parsons Int. Turbine Conference, University of Dublin, June, pp. 153.

46. **Rust, T. and Swaminathan, V.P.**, 1982. "Corrosion Fatigue Testing of Steam Turbine Blading Alloys", Proc. EPRI Workshop on Steam Turbine Reliability, Boston, MA.

47. **Sato, K.**, 1980. "Transverse Vibrations of Linearly Tapered Beam with Ends Restrained Elastically Against Rotation and Subjected to Axial Force", Int. J. of Mech. Sci., Vol. 22, pp. 109.

48. **Scarborough, J.B.**, 1966. "Numerical Mathematical Analysis", Oxford & IBH Publishing Co.

49. **Segerlind, L.J.**, 1976. "Applied Finite Element Analysis", John Wiley and Sons, Inc., pp. 71-77; 212-222.

50. **Shigley, J.E.**, 1977. "Mechanical Engineering Design", McGraw-Hill.

51. **Sisto, F. and Chang, A.T.**, 1984. "A finite Element for Vibration Analysis of Twisted Blades Based on Beam Theory", AIAA Journal, Vol. 22, pp. 1646-1651.

52. **Solberg et al**, 1960. "Thermal Engineering", John Wiley & Sons, Inc.

53. **Srinivasan, A.V.**, 1983. "Vibration of Bladed Disc Assemblies - A Selected Review", Session Proc. Tech. Comm. on Rotordynamics, Sixth IFToMM Congress, New Delhi.

54. **Subrahmanuam, K.B. and Leissa, A.W.**, 1985. "An improved Finite Difference Analysis of Uncoupled Vibrations of Cantilever Beams", J. of Sound and Vibration, Vol. 98, pp. 1.

55. **Treager, I.E.**, 1970. "Aircraft Gas Turbine Engine Technology", McGraw-Hill Book Company.

56. **Thomson, W.T.**, 1988. "Theory of Vibration with Applications", Prentice Hall.

57. **Timoshenko, S.P. and Goodier, J.N.**, 1970. "Theory of Elasticity", McGraw-Hill Book Co., pp. 223-224.

58. **Vincent, E.T.**, 1950. "The Theory and Design of Gas Turbines and Jet Engines", McGraw-Hill Book Company Inc.

59. **Vyas, N.S.**, 1986. "Vibratory Stress Analysis and Fatigue Life Estimation of Turbine", Ph.D. Thesis, IIT Delhi.

60. **Wallace F.J. and Linning W.A.**, 1988. "Basic Engineering Thermodynamics", Sir Issac Pitman and Sons Limited.

61. **Warikoo, R. & Haddara, M.R.**, 1992. "Analysis of Propeller Shaft Transverse Vibrations", Marine Structures 5, pp. 255-279.

62. **Weast, R.C.**, 1975. "Handbook of Chemistry and Physics", CRC Press, Inc.

63. **Wood, D.B.**, 1969. "Applications of Thermodynamics", Addison-Wesley Publishing Company.

64. **Zienkiewicz, O.C.**, 1977. "The finite element Method", McGraw-Hill Book Company (UK) Ltd., pp. 169-171.

APPENDIX A

EXPRESSIONS FOR SHAPE FUNCTIONS OF CORNER NODES FOR THE TWENTY-NODED ELEMENT

$N1 = (1/8)*(1-\xi)*(1-\eta)*(1-\zeta)*(-\xi-\eta-\zeta-2)$
$N2 = (1/8)*(1+\xi)*(1-\eta)*(1-\zeta)*(\xi-\eta-\zeta-2)$
$N3 = (1/8)*(1+\xi)*(1+\eta)*(1-\zeta)*(\xi+\eta-\zeta-2)$
$N4 = (1/8)*(1-\xi)*(1+\eta)*(1-\zeta)*(-\xi+\eta-\zeta-2)$
$N5 = (1/8)*(1-\xi)*(1-\eta)*(1+\zeta)*(-\xi-\eta+\zeta-2)$
$N6 = (1/8)*(1+\xi)*(1-\eta)*(1+\zeta)*(\xi-\eta+\zeta-2)$
$N7 = (1/8)*(1+\xi)*(1+\eta)*(1+\zeta)*(\xi+\eta+\zeta-2)$
$N8 = (1/8)*(1-\xi)*(1+\eta)*(1+\zeta)*(-\xi+\eta+\zeta-2)$

APPENDIX B

EXPRESSIONS FOR SHAPE FUNCTIONS OF MID-SIDE NODES FOR THE TWENTY-NODED ELEMENT

N9 = (1/4)*(1-ζ**2)*(1-ξ)*(1-η)
N10 = (1/4)*(1-ζ**2)*(1+ξ)*(1-η)
N11 = (1/4)*(1-ζ**2)*(1+ξ)*(1+η)
N12 = (1/4)*(1-ζ**2)*(1-ξ)*(1+η)
N13 = (1/4)*(1-ξ**2)*(1-η)*(1-ζ)
N14 = (1/4)*(1-η**2)*(1+ξ)*(1-ζ)
N15 = (1/4)*(1-ξ**2)*(1+η)*(1-ζ)
N16 = (1/4)*(1-η**2)*(1-ξ)*(1-ζ)
N17 = (1/4)*(1-ξ**2)*(1-η)*(1+ζ)
N18 = (1/4)*(1-η**2)*(1+ξ)*(1+ζ)
N19 = (1/4)*(1-ξ**2)*(1+η)*(1+ζ)
N20 = (1/4)*(1-η**2)*(1-ξ)*(1+ζ)

APPENDIX C

EXPRESSIONS FOR ELEMENTAL MATRICES AND VECTORS FOR THE TWENTY-NODED ELEMENT

DESCRIPTION OF TERMS IN ELEMENTAL CAPACITANCE MATRIX [CP^e]

$$\int_{-1}^{+1}\int_{-1}^{+1}\int_{-1}^{+1} h^e \left[N^e(\xi,\eta,\zeta)\right]^T \left[N^e(\xi,\eta,\zeta)\right] \left| J(\xi,\eta,\zeta) \right| d\xi\ d\eta\ d\zeta$$

t1 = ζ**2

t2 = -1+t1

t3 = -1+ξ

t4 = t2*t3

t5 = 1+η

t6 = t5**2

t7 = ξ**2

t8 = -1+t7

t9 = t6*t8

t10 = -1+ζ

t12 = t4*t9*t10

t13 = t10*t2

t14 = 1+ξ

t15 = t13*t14

```
t16 = t9*t15

t17 = t14*t5

t18 = t17*t10

t19 = -ξ-η+ζ+2

t20 = η**2

t21 = -1+t20

t22 = t19*t21

t23 = 1+ζ

t24 = t3*t23

t26 = t18*t22*t24

t27 = t21*t14

t28 = t27*t23

t29 = -1+η

t31 = t8*t29*t10

t32 = t28*t31

t33 = t8**2

t34 = t29**2

t35 = t33*t34

t36 = t10**2

t38 = t36*t8

t39 = t38*t5

t40 = t27*t39
```

```
t41 = t4*t5

t42 = t41*t31

t43 = t14*t29

t44 = t43*t10

t45 = -ξ+η+ζ+2

t46 = t45*t21

t48 = t44*t46*t24

t49 = t38*t29

t50 = t27*t49

t51 = t43*t36

t52 = t45*t8

t54 = t51*t52*t5

t55 = t8*t5

t56 = t55*t23

t57 = t2*t14

t58 = t57*t29

t59 = t56*t58

t60 = t2**2

t61 = t3**2

t62 = t60*t61

t63 = t5*t29

t64 = t62*t63
```

t65 = t43*t23

t66 = ξ-η+ζ-2

t67 = t66*t2

t68 = t3*t5

t70 = t65*t67*t68

t71 = t33*t5

t72 = t23*t29

t74 = t71*t72*t10

t75 = t14**2

t76 = t75*t5

t77 = t23**2

t79 = ξ+η+ζ-2

t80 = t79*t29

t82 = t76*t77*t80*t66

t83 = t14*t34

t85 = t66*t3

t86 = -ξ-η+ζ-2

t88 = t83*t77*t85*t86

t89 = t61*t34

t90 = t86**2

t94 = t71*t77*t29

t95 = t76*t23

```
t96 = t79*t21

t98 = t95*t96*t10

t99 = t3*t29

t100 = t99*t23

t101 = t86*t2

t103 = t100*t101*t17

t104 = t17*t23

t105 = t79*t8

t106 = t29*t10

t108 = t104*t105*t106

t109 = t55*t10

t110 = t109*t58

t111 = t36*t19

t113 = t76*t111*t21

t114 = t23*t2

t115 = t114*t14

t116 = t9*t115

t117 = t21**2

t120 = t117*t3*t36*t14

t121 = t21*t3

t122 = t77*t8

t123 = t122*t29
```

t124 = t121*t123

t125 = t28*t109

t126 = t75*t34

t127 = t10*t45

t129 = t126*t127*t2

t130 = t99*t10

t131 = ξ+η+ζ+2

t132 = t131*t8

t133 = t5*t23

t135 = t130*t132*t133

t136 = t17*t36

t137 = t19*t8

t139 = t136*t137*t29

t140 = t121*t23

t141 = t140*t109

t142 = t43*t77

t143 = t66*t8

t145 = t142*t143*t5

t146 = t21*t75

t147 = t13*t29

t148 = t146*t147

t149 = t14*t6

t150 = t149*t23

t151 = t79*t2

t153 = t150*t151*t3

t154 = t61*t6

t155 = ξ-η+ζ+2

t156 = t10*t155

t158 = t154*t156*t2

t159 = t121*t49

t160 = t75*t29

t161 = t160*t23

t163 = t161*t67*t5

t164 = t10*t19

t166 = t23*t86

t168 = t17*t164*t99*t166

t169 = t3*t34

t170 = t169*t23

t172 = t170*t101*t14

t173 = t117*t61

t175 = t61*t29

t176 = t175*t10

t177 = t131*t21

t179 = t176*t177*t23

t180 = t121*t10

t182 = t180*t57*t5

t183 = t121*t39

t184 = t83*t10

t186 = t184*t52*t23

t187 = t117*t75

t188 = t23*t10

t189 = t187*t188

t191 = -ξ+η+ζ-2

t194 = t154*t23*t191*t10*t155

t195 = t68*t10

t196 = t155*t2

t198 = t195*t196*t43

t199 = t77*t79

t201 = t76*t199*t21

t202 = t61*t5

t204 = t191*t29

t206 = t202*t77*t204*t86

t207 = t77*t86

t209 = t169*t207*t8

t210 = t23*t66

t212 = t126*t210*t2

t213 = t28*t41

t214 = t99*t77

t215 = t86*t8

t217 = t214*t215*t5

t218 = t114*t5

t219 = t146*t218

t220 = t117*t14

t222 = t220*t24*t10

t223 = t8*t34

t224 = t223*t15

t225 = t169*t10

t226 = t131*t2

t228 = t225*t226*t14

t229 = t75*t6

t233 = t229*t23*t79*t10*t19

t234 = t36*t131

t236 = t169*t234*t8

t237 = t33*t6

t239 = t83*t23

t240 = t10*t131

t242 = t239*t85*t240

t243 = t17*t77

t244 = t79*t3

t247 = t243*t244*t29*t86

t249 = t149*t199*t8

t251 = t130*t226*t17

t253 = t95*t151*t29

t255 = t36*t45

t257 = t83*t255*t8

t258 = t3*t6

t259 = t36*t155

t261 = t258*t259*t8

t263 = t239*t143*t10

t265 = t225*t132*t23

t266 = t258*t23

t267 = t191*t14

t269 = t266*t267*t164

t270 = t60*t3

t272 = t270*t17*t29

t273 = t77*t66

t275 = t160*t273*t21

t278 = t68*t156*t43*t210

t280 = t149*t10

t282 = t280*t137*t23

t284 = t4*t29

t285 = t56*t284

t286 = t68*t77

t287 = t191*t8

t289 = t286*t287*t29

t290 = t122*t5

t291 = t121*t290

t292 = t60*t75

t293 = t292*t63

t295 = t202*t259*t21

t296 = t114*t29

t297 = t146*t296

t299 = t150*t105*t10

t300 = t202*t23

t302 = t300*t204*t240

t303 = t191*t21

t305 = t300*t303*t10

t306 = t66*t21

t307 = t3*t10

t309 = t65*t306*t307

t310 = t155*t21

t311 = t14*t23

```
t313 = t195*t310*t311

t314 = t77*t191

t316 = t258*t314*t8

t317 = t68*t23

t318 = t14*t10

t320 = t317*t303*t318

t322 = t175*t234*t21

t326 = t89*t23*t86*t10*t131

t327 = t45**2

t331 = t44*t52*t133

t332 = t258*t10

t334 = t332*t196*t14

t335 = t131**2

t338 = t21*t61

t339 = t338*t296

t340 = t28*t284

t342 = t266*t287*t10

t343 = t27*t290

t344 = t270*t83

t345 = t76*t10

t346 = t19*t2

t348 = t345*t346*t29
```

t350 = t243*t96*t3

t352 = t229*t164*t2

t354 = t83*t273*t8

t356 = t160*t255*t21

t357 = t338*t218

t358 = t23*t79

t361 = t17*t358*t99*t240

t363 = t142*t306*t3

t364 = t68*t36

t365 = t155*t14

t368 = t364*t365*t29*t45

t371 = t170*t86*t14*t127

t372 = t45*t2

t374 = t184*t372*t3

t375 = t86*t21

t377 = t100*t375*t318

t379 = t317*t287*t106

t380 = t202*t10

t382 = t380*t196*t29

t384 = t380*t310*t23

t388 = t136*t19*t3*t29*t131

t390 = t155*t29

```
t392 = t202*t36*t390*t131

t394 = t89*t166*t2

t395 = t155*t8

t397 = t364*t395*t29

t398 = t160*t10

t400 = t398*t46*t23

t402 = t18*t137*t72

t404 = t44*t372*t68

t406 = t338*t147

t407 = t19*t29

t409 = t345*t407*t210

t410 = t13*t5

t411 = t338*t410

t412 = t237*t188

t414 = t18*t346*t99

t416 = t214*t375*t14

t417 = t5*t10

t419 = t100*t215*t417

t421 = t364*t310*t14

t423 = t195*t395*t72

t424 = t19**2

t429 = t286*t267*t29*t66
```

```
t431 = t229*t358*t2

t432 = t114*t3

t433 = t223*t432

t435 = t95*t80*t127

t436 = t140*t31

t437 = t191*t2

t439 = t300*t437*t29

t440 = t191**2

t444 = t345*t22*t23

t447 = t76*t36*t407*t45

t450 = t71*t36*t29

t452 = t104*t96*t307

t453 = t175*t23

t455 = t453*t101*t5

t457 = t202*t314*t21

t459 = t130*t177*t311

t460 = t270*t149

t462 = t4*t223*t10

t464 = t176*t226*t5

t465 = t180*t58

t466 = t146*t410

t468 = t266*t437*t14
```

```
t470 = t280*t346*t3

t471 = t35*t188

t472 = t27*t123

t474 = t332*t395*t23

t475 = t79**2

t479 = t170*t215*t10

t480 = t23*t191

t482 = t154*t480*t2

t484 = t380*t390*t166

t487 = t149*t77*t244*t191

t489 = t286*t303*t14

t491 = t220*t77*t3

t493 = t65*t143*t417

t495 = t243*t105*t29

t497 = t89*t240*t2

t499 = t51*t46*t3

t501 = t398*t372*t5

t503 = t149*t111*t8

t505 = t173*t188

t506 = t155**2

t510 = t175*t207*t21

t514 = t169*t36*t131*t14*t45
```

```
t516 = t136*t22*t3

t517 = t99*t36

t519 = t517*t132*t5

t521 = t150*t244*t156

t522 = t9*t432

t524 = t161*t306*t10

t525 = t223*t115

t527 = t317*t437*t43

t529 = t453*t375*t10

t533 = t126*t23*t66*t10*t45

t535 = t104*t151*t99

t537 = t517*t177*t14

t540 = t68*t480*t43*t127

t542 = t66**2

t546 = t239*t67*t3

t551 = t258*t36*t365*t19
```

ELEMENTAL CAPACITANCE MATRIX [CP°]

[20 x 20]

t229*t77*t475/64	-t487/64	-t521/64	t233/64	-t82/64	t247/64	t361/64	-t435/64	-t201/32	t350/32	-t452/32	t98/32	-t249/32	t153/32	t299/32	t431/32	t495/32	-t535/32	t108/32	t253/32
-t487/64	t154*t77*t440/64	t194/64	-t269/64	t429/64	-t206/64	-t302/64	t540/64	t489/32	-t457/32	t305/32	-t320/32	t316/32	-t482/32	-t342/32	t468/32	-t289/32	t439/32	t379/32	t527/32
-t521/64	t194/64	t154*t36*t506/64	-t551/64	t278/64	-t484/64	-t392/64	t368/64	t313/32	-t384/32	t295/32	-t421/32	t474/32	-t158/32	-t261/32	t334/32	-t423/32	t382/32	t397/32	t198/32
t233/64	-t269/64	-t551/64	t229*t36*t424/64	-t409/64	t168/64	t388/64	-t447/64	-t444/32	t26/32	-t516/32	t113/32	-t282/32	t470/32	t503/32	-t352/32	t402/32	-t414/32	-t139/32	t348/32
-t82/64	t429/64	t278/64	-t409/64	t126*t77*t542/64	-t88/64	-t242/64	t533/64	t275/32	-t363/32	t309/32	-t524/32	t145/32	-t70/32	-t493/32	t163/32	-t354/32	t546/32	t263/32	t212/32
t247/64	-t206/64	-t484/64	t168/64	-t88/64	t89*t77*t90/64	t326/64	-t371/64	-t416/32	t510/32	-t529/32	t377/32	-t217/32	t455/32	t419/32	-t103/32	t209/32	-t394/32	-t479/32	t172/32
t361/64	-t302/64	-t392/64	t388/64	-t242/64	t326/64	t89*t36*t335/64	-t514/64	-t459/32	t179/32	-t322/32	t537/32	-t135/32	t464/32	t519/32	-t251/32	t265/32	-t497/32	-t236/32	t228/32
-t435/64	t540/64	t368/64	-t447/64	t533/64	-t371/64	-t514/64	t126*t36*t327/64	t400/32	-t48/32	t499/32	-t356/32	t331/32	-t404/32	-t54/32	t501/32	-t186/32	t374/32	t257/32	t129/32
-t201/32	t489/32	t313/32	-t444/32	t275/32	-t416/32	-t459/32	t400/32	t187*t77/16	-t491/16	t222/16	-t189/16	t343/16	-t213/16	-t125/16	t219/16	-t472/16	t340/16	t32/16	-t297/16
t350/32	-t457/32	-t384/32	t26/32	-t363/32	t510/32	t179/32	-t48/32	-t491/16	t173*t77/16	-t505/16	t222/16	-t291/16	t357/16	t141/16	-t213/16	t124/16	-t339/16	-t436/16	t340/16
-t452/32	t305/32	t295/32	-t516/32	t309/32	-t529/32	-t322/32	t499/32	t222/16	-t505/16	t173*t36/16	-t120/16	t141/16	-t411/16	-t183/16	t182/16	t436/16	t406/16	t159/16	t465/16
t98/32	-t320/32	-t421/32	t113/32	-t524/32	t377/32	t537/32	-t356/32	-t189/16	t222/16	-t120/16	t187*t36/16	-t125/16	t182/16	t40/16	-t466/16	t32/16	-t465/16	-t50/16	t148/16
-t249/32	t316/32	t474/32	-t282/32	t145/32	-t217/32	-t135/32	t331/32	t343/16	-t291/16	t141/16	-t125/16	t237*t77/16	-t522/16	-t412/16	t116/16	-t94/16	t285/16	t74/16	-t59/16
t153/32	-t482/32	-t158/32	t470/32	-t70/32	t455/32	t464/32	-t104/32	-t213/16	t357/16	-t411/16	t182/16	-t522/16	t62*t6/16	t12/16	-t460/16	t285/16	-t64/16	-t42/16	t272/16
t299/32	-t342/32	-t261/32	t503/32	-t493/32	t419/32	t519/32	-t54/32	-t125/16	t141/16	-t183/16	t40/16	-t412/16	t12/16	t237*t36/1	-t16/16	t74/16	-t42/16	t450/16	t110/16
-t431/32	t468/32	t334/32	-t352/32	t163/32	-t103/32	-t251/32	t501/32	t219/16	-t213/16	t182/16	-t466/16	t116/16	-t460/16	-t16/16	t292*t6/16	-t59/16	t272/16	t110/16	-t293/16
t495/32	-t289/32	-t423/32	t402/32	-t354/32	t209/32	t265/32	-t186/32	-t472/16	t124/16	-t436/16	t32/16	-t94/16	t285/16	t74/16	-t59/16	t35*t77/16	-t433/16	-t471/16	t525/16
-t535/32	t439/32	t382/32	-t414/32	t546/32	-t394/32	-t497/32	t374/32	t340/16	-t339/16	t406/16	-t465/16	t285/16	-t64/16	-t42/16	t272/16	-t433/16	t62*t34/16	t462/16	t344/16
-t108/32	t379/32	t397/32	-t139/32	t263/32	-t479/32	-t236/32	t257/32	t32/16	-t436/16	t159/16	-t50/16	t74/16	-t42/16	-t450/16	t110/16	-t471/16	t462/16	t35*t36/1	t224/16
t253/32	-t527/32	-t198/32	t348/32	-t212/32	t172/32	t228/32	-t129/32	-t297/16	t340/16	-t465/16	t148/16	-t59/16	t272/16	t110/16	-t293/16	t525/16	-t344/16	-t224/16	t292*t34/16

DESCRIPTION OF TERMS IN ELEMENTAL TEMPERATURE-GRADIENT

INTERPOLATION MATRIX [B^e]

$$[J(\xi,\eta,\zeta)]^{-1}\begin{bmatrix} \frac{\partial N_1}{\partial \xi} & \frac{\partial N_2}{\partial \xi} & \cdots & \frac{\partial N_r}{\partial \xi} \\ \frac{\partial N_1}{\partial \eta} & \frac{\partial N_2}{\partial \eta} & \cdots & \frac{\partial N_r}{\partial \eta} \\ \frac{\partial N_1}{\partial \zeta} & \frac{\partial N_2}{\partial \zeta} & \cdots & \frac{\partial N_r}{\partial \eta} \end{bmatrix}$$

t1 = ζ**2

t2 = 1-t1

t3 = 1-η

t4 = t2*t3

t5 = 1-ξ

t6 = 1+η

t7 = t5*t6

t8 = -ξ+η-ζ-2

t10 = 1-ζ

t11 = t7*t10

t13 = ξ*t6

t14 = 1+ζ

t16 = t2*t5

t17 = ζ*t5

t19 = t3*t10

t20 = ξ-η-ζ-2

t22 = 1+ξ

t23 = t22*t3

t24 = t23*t10

t26 = t2*t22

t27 = η*t22

t29 = ξ**2

t30 = 1-t29

t31 = t30*t6

t32 = t6*t10

t35 = t22*t10

t36 = ξ+η-ζ-2

t38 = t22*t6

t39 = t38*t10

t43 = ξ*t3

t47 = t2*t6

t48 = t30*t10

t49 = t30*t3

t50 = ζ*t22

t52 = η**2

t53 = 1-t52

t54 = t53*t14

t55 = η*t5

t60 = t22*t14

t61 = ξ-η+ζ-2

t63 = t23*t14

t65 = t53*t22

t68 = t3*t14

t71 = t5*t14

t72 = -ξ-η+ζ-2

t74 = t5*t3

t75 = t74*t14

t77 = t53*t5

t78 = t6*t14

t79 = ξ+η+ζ-2

t81 = t38*t14

t89 = t53*t10

t94 = t5*t10

t95 = -ξ-η-ζ-2

t97 = t74*t10

t99 = -ξ+η+ζ-2

t101 = t7*t14

t110 = t30*t14

ELEMENTAL TEMPERATURE-GRADIENT INTERPOLATION MATRIX $[B^e]$

[3 x 20]

t78*t79/8+t81/8	-t78*t95/8-t101/8	-t32*t8/8-t11/8	t32*t36/8+t39/8	t68*t61/8+t63/8	-t68*t72/8-t75/8	-t19*t95/8-t97/8	t19*t20/8+t24/8	t54/4	-t54/4	-t89/4	t89/4	-t13*t14/2	-t47/4	-t13*t10/2	t47/4	t43*t14/2	-t4/4	-t43*t10/2	t4/4
t60*t79/8+t81/8	t71*t95/8+t101/8	t94*t8/8+t11/8	t35*t36/8+t39/8	-t60*t61/8-t63/8	-t71*t72/8-t75/8	-t94*t95/8-t97/8	-t35*t20/8-t24/8	-t27*t14/2	-t55*t14/2	-t55*t10/2	-t27*t10/2	t110/4	t16/4	t48/4	t26/4	-t110/4	-t16/4	-t48/4	-t26/4
t38*t79/8+t81/8	t7*t99/8+t101/8	-t7*t8/8-t11/8	-t38*t36/8-t39/8	t23*t61/J+t63/8	t74*t72/8+t75/8	-t74*t95/8-t97/8	-t23*t20/8-t24/8	t65/4	t77/4	-t77/4	-t65/4	t31/4	-t17*t6/2	-t31/4	-t50*t6/2	t49/4	t17*t3/2	-t49/4	-t50*t3/2

DESCRIPTION OF TERMS IN SECOND PART OF ELEMENTAL CONDUCTION

MATRIX FOR $\xi = 1$

$$\int_{-1}^{+1}\int_{-1}^{+1} \left[N^e(\eta,\zeta)\right]^T \left[N^e(\eta,\zeta)\right] \left| J(\eta,\zeta) \right| d\eta \; d\zeta$$

t1 = 1+η

t2 = t1**2

t3 = 1+ζ

t4 = t3**2

t6 = -1+η+ζ

t7 = t6**2

t9 = t2*t3

t10 = -1+ζ

t12 = 1-η+ζ

t14 = t9*t6*t10*t12

t15 = t1*t4

t16 = -1+η

t18 = -1-η+ζ

t20 = t15*t6*t16*t18

t21 = t1*t3

t23 = t16*t10

t24 = 1+η+ζ

```
t26 = t21*t6*t23*t24

t27 = η**2

t28 = -1+t27

t29 = t6*t28

t30 = t15*t29

t32 = t21*t29*t10

t33 = ζ**2

t34 = -1+t33

t35 = t6*t34

t36 = t9*t35

t38 = t21*t35*t16

t39 = t10**2

t41 = t12**2

t43 = t1*t10

t45 = t16*t3

t47 = t43*t12*t45*t18

t48 = t1*t39

t51 = t48*t12*t16*t24

t52 = t12*t28

t54 = t43*t52*t3

t55 = t48*t52

t57 = t12*t34
```

```
t58 = t2*t10*t57

t60 = t43*t57*t16

t61 = t16**2

t63 = t18**2

t65 = t61*t3

t68 = t65*t18*t10*t24

t70 = t18*t28

t71 = t16*t4*t70

t73 = t45*t70*t10

t74 = t18*t34

t76 = t45*t74*t1

t77 = t65*t74

t79 = t24**2

t81 = t24*t28

t83 = t23*t81*t3

t85 = t16*t39*t81

t86 = t24*t34

t88 = t23*t86*t1

t90 = t61*t10*t86

t91 = t28**2

t94 = t91*t3*t10

t95 = t28*t3
```

```
t96 = t34*t1

t97 = t95*t96

t98 = t34*t16

t99 = t95*t98

t101 = t28*t10

t102 = t101*t96

t103 = t101*t98

t104 = t34**2

t107 = t104*t1*t16
```

SECOND PART OF ELEMENTAL CONDUCTION MATRIX FOR $\xi = 1$

[20 x 20]

t2*t4*t7/16	0	0	t14/16	-t20/16	0	0	-t26/16	0	0	0	t32/8	0	0	0	-t36/8	-t30/8	0	0	t38/8
0	0	0	0	0	0	0	0	0	0	0	0	0	0	0	0	0	0	0	0
0	0	0	0	0	0	0	0	0	0	0	0	0	0	0	0	0	0	0	0
t14'16	0	0	t2*t39*t41/16	-t47/16	0	0	-t51/16	0	0	0	t55/8	0	0	0	-t58/8	-t54/8	0	0	t60/8
-t20/16	0	0	-t47/16	t61*t4*t63/16	0	0	t68/16	0	0	0	-t73/8	0	0	0	t76/8	t71/8	0	0	-t77/8
0	0	0	0	0	0	0	0	0	0	0	0	0	0	0	0	0	0	0	0
0	0	0	0	0	0	0	0	0	0	0	0	0	0	0	0	0	0	0	0
-t26/16	0	0	-t51/16	t68/16	0	0	t61*t39*t79/16	0	0	0	-t85/8	0	0	0	t88/8	t83/8	0	0	-t90/8
0	0	0	0	0	0	0	0	0	0	0	0	0	0	0	0	0	0	0	0
0	0	0	0	0	0	0	0	0	0	0	0	0	0	0	0	0	0	0	0
0	0	0	0	0	0	0	0	0	0	0	0	0	0	0	0	0	0	0	0
t32/8	0	0	t55/8	-t73/8	0	0	-t85/8	0	0	0	t91*t39/4	0	0	0	-t102/4	-t94/4	0	0	t103/4
0	0	0	0	0	0	0	0	0	0	0	0	0	0	0	0	0	0	0	0
0	0	0	0	0	0	0	0	0	0	0	0	0	0	0	0	0	0	0	0
0	0	0	0	0	0	0	0	0	0	0	0	0	0	0	0	0	0	0	0
-t36/8	0	0	-t58/8	t76/8	0	0	t88/8	0	0	0	-t102/4	0	0	0	t104*t2/4	t97/4	0	0	-t107/4
-t30/8	0	0	-t54/8	t71/8	0	0	t83/8	0	0	0	-t94/4	0	0	0	t97/4	t91*t4/4	0	0	-t99/4
0	0	0	0	0	0	0	0	0	0	0	0	0	0	0	0	0	0	0	0
0	0	0	0	0	0	0	0	0	0	0	0	0	0	0	0	0	0	0	0
t38/8	0	0	t60/8	-t77/8	0	0	-t90/8	0	0	0	t103/4	0	0	0	-t107/4	-t99/4	0	0	t104*t61/4

DESCRIPTION OF TERMS IN SECOND PART OF ELEMENTAL CONDUCTION

MATRIX FOR $\xi = -1$

$$\int_{-1}^{1}\int_{-1}^{1} \left[N^e(\eta,\zeta)\right]^T \left[N^e(\eta,\zeta)\right] \left| J(\eta,\zeta) \right| d\eta \; d\zeta$$

t1 = 1+η

t2 = t1**2

t3 = 1+ζ

t4 = t3**2

t6 = -1+η+ζ

t7 = t6**2

t9 = t2*t3

t10 = -1+ζ

t12 = 1-η+ζ

t14 = t9*t6*t10*t12

t15 = t1*t4

t16 = -1+η

t18 = -1-η+ζ

t20 = t15*t6*t16*t18

t21 = t1*t3

t23 = t13*t10

t24 = 1+η+ζ

```
t26 = t21*t6*t23*t24

t27 = η**2

t28 = -1+t27

t29 = t6*t28

t30 = t15*t29

t32 = t21*t29*t10

t33 = ζ**2

t34 = -1+t33

t35 = t6*t34

t36 = t9*t35

t38 = t21*t35*t16

t39 = t10**2

t41 = t12**2

t43 = t1*t10

t45 = t16*t3

t47 = t43*t12*t45*t18

t48 = t1*t39

t51 = t48*t12*t16*t24

t52 = t12*t28

t54 = t43*t52*t3

t55 = t48*t52

t57 = t12*t34
```

```
t58 = t2*t10*t57

t60 = t43*t57*t16

t61 = t16**2

t63 = t18**2

t65 = t61*t3

t68 = t65*t18*t10*t24

t70 = t18*t28

t71 = t16*t4*t70

t73 = t45*t70*t10

t74 = t18*t34

t76 = t45*t74*t1

t77 = t65*t74

t79 = t24**2

t81 = t24*t28

t83 = t23*t81*t3

t85 = t16*t39*t81

t86 = t24*t34

t88 = t23*t86*t1

t90 = t61*t10*t86

t91 = t28**2

t94 = t91*t3*t10

t95 = t28*t3
```

```
t96 = t34*t1

t97 = t95*t96

t98 = t34*t16

t99 = t95*t98

t101 = t28*t10

t102 = t101*t96

t103 = t101*t98

t104 = t34**2

t107 = t104*t1*t16
```

SECOND PART OF ELEMENTAL CONDUCTION MATRIX FOR $\xi = -1$

[20 x 20]

0	0	0	0	0	0	0	0	0	0	0	0	0	0	0	0	0	0	0	0
0	t2*t4*t7/16	t14/16	0	0	-t20/16	-t26/16	0	0	-t30/8	0	0	0	-t36/8	0	0	0	t38/8	t32/8	0
0	t14/16	t2*t39*t41/16	0	0	-t47/16	-t51/16	0	0	-t54/8	0	0	0	-t58/8	0	0	0	t60/8	t55/8	0
0	0	0	0	0	0	0	0	0	0	0	0	0	0	0	0	0	0	0	0
0	0	0	0	0	0	0	0	0	0	0	0	0	0	0	0	0	0	0	0
0	-t20/16	-t47/16	0	0	t61*t4*t63/16	t68/16	0	0	t71/8	0	0	0	t76/8	0	0	0	-t77/8	-t73/8	0
0	-t26/16	-t51/16	0	0	t68/16	t61*t39*t79/16	0	0	t83/8	0	0	0	t88/8	0	0	0	-t90/8	-t85/8	0
0	0	0	0	0	0	0	0	0	0	0	0	0	0	0	0	0	0	0	0
0	0	0	0	0	0	0	0	0	0	0	0	0	0	0	0	0	0	0	0
0	-t30/8	-t54/8	0	0	t71/8	t83/8	0	0	t91*t4/4	0	0	0	t97/4	0	0	0	-t99/4	-t94/4	0
0	0	0	0	0	0	0	0	0	0	0	0	0	0	0	0	0	0	0	0
0	0	0	0	0	0	0	0	0	0	0	0	0	0	0	0	0	0	0	0
0	0	0	0	0	0	0	0	0	0	0	0	0	0	0	0	0	0	0	0
0	-t36/8	-t58/8	0	0	t76/8	t88/8	0	0	t97/4	0	0	0	t104*t2/4	0	0	0	-t107/4	-t102/4	0
0	0	0	0	0	0	0	0	0	0	0	0	0	0	0	0	0	0	0	0
0	0	0	0	0	0	0	0	0	0	0	0	0	0	0	0	0	0	0	0
0	0	0	0	0	0	0	0	0	0	0	0	0	0	0	0	0	0	0	0
0	t38/8	t60/8	0	0	-t77/8	-t90/8	0	0	-t99/4	0	0	0	-t107/4	0	0	0	t104*t61/4	t103/4	0
0	t32/8	t55/8	0	0	-t73/8	-t85/8	0	0	-t94/4	0	0	0	-t102/4	0	0	0	t103/4	t91*t39/4	0
0	0	0	0	0	0	0	0	0	0	0	0	0	0	0	0	0	0	0	0

DESCRIPTION OF TERMS IN SECOND PART OF ELEMENTAL CONDUCTION

MATRIX FOR $\eta = 1$

$$\int_{-1}^{+1} \int_{-1}^{+1} \left[N^e(\xi,\zeta)\right]^T \left[N^e(\xi,\zeta)\right] \left| J(\xi,\zeta) \right| d\xi \, d\zeta$$

t1 = 1+ξ

t2 = t1**2

t3 = 1+ζ

t4 = t3**2

t6 = ξ-1+ζ

t7 = t6**2

t9 = t1*t4

t10 = -1+ξ

t12 = -ξ-1+ζ

t14 = t9*t6*t10*t12

t15 = t1*t3

t17 = -1+ζ

t18 = t10*t17

t19 = ξ+1+ζ

t21 = t15*t6*t18*t19

t22 = t2*t3

t24 = -ξ+1+ζ

```
t26 = t22*t6*t17*t24

t27 = ξ**2

t28 = -1+t27

t29 = t6*t28

t30 = t9*t29

t31 = ζ**2

t32 = -1+t31

t33 = t6*t32

t35 = t15*t33*t10

t37 = t15*t29*t17

t38 = t22*t33

t39 = t10**2

t41 = t12**2

t43 = t39*t3

t46 = t43*t12*t17*t19

t47 = t10*t3

t49 = t1*t17

t51 = t47*t12*t49*t24

t53 = t12*t28

t54 = t10*t4*t53

t55 = t12*t32

t56 = t43*t55
```

```
t58 = t47*t53*t17

t60 = t47*t55*t1

t61 = t17**2

t63 = t19**2

t65 = t10*t61

t68 = t65*t19*t1*t24

t69 = t19*t28

t71 = t18*t69*t3

t73 = t19*t32

t74 = t39*t17*t73

t75 = t65*t69

t77 = t18*t73*t1

t79 = t24**2

t81 = t24*t28

t83 = t49*t81*t3

t84 = t24*t32

t86 = t49*t84*t10

t88 = t1*t61*t81

t90 = t2*t17*t84

t91 = t28**2

t93 = t28*t3

t94 = t32*t10
```

```
t95 = t93*t94

t97 = t91*t3*t17

t98 = t32*t1

t99 = t93*t98

t100 = t32**2

t102 = t28*t17

t103 = t94*t102

t105 = t100*t10*t1

t107 = t102*t98
```

SECOND PART OF ELEMENTAL CONDUCTION MATRIX FOR $\eta = 1$

[20 x 20]

t2*t4*t7/16	-t14/16	-t21/16	t26/16	0	0	0	0	-t30/8	t35/8	t37/8	-t38/8	0	0	0	0	0	0	0	0
-t14/16	t39*t4*t41/16	t46/16	-t51/16	0	0	0	0	t54/8	-t56/8	-t58/8	t60/8	0	0	0	0	0	0	0	0
-t21/16	t46/16	t39*t61*t63/16	-t68/16	0	0	0	0	t71/8	-t74/8	-t75/8	t77/8	0	0	0	0	0	0	0	0
t26/16	-t51/16	-t68/16	t2*t61*t79/16	0	0	0	0	-t83/8	t86/8	t88/8	-t90/8	0	0	0	0	0	0	0	0
0	0	0	0	0	0	0	0	0	0	0	0	0	0	0	0	0	0	0	0
0	0	0	0	0	0	0	0	0	0	0	0	0	0	0	0	0	0	0	0
0	0	0	0	0	0	0	0	0	0	0	0	0	0	0	0	0	0	0	0
0	0	0	0	0	0	0	0	0	0	0	0	0	0	0	0	0	0	0	0
-t30/8	t54/8	t71/8	-t83/8	0	0	0	0	t91*t4/4	-t95/4	-t97/4	t99/4	0	0	0	0	0	0	0	0
t35/8	-t56/8	-t74/8	t86/8	0	0	0	0	-t95/4	t100*t39/4	t103/4	-t105/4	0	0	0	0	0	0	0	0
t37/8	-t58/8	-t75/8	t88/8	0	0	0	0	-t97/4	t103/4	t91*t61/4	-t107/4	0	0	0	0	0	0	0	0
-t38/8	t60/8	t77/8	-t90/8	0	0	0	0	t99/4	-t105/4	-t107/4	t100*t2/4	0	0	0	0	0	0	0	0
0	0	0	0	0	0	0	0	0	0	0	0	0	0	0	0	0	0	0	0
0	0	0	0	0	0	0	0	0	0	0	0	0	0	0	0	0	0	0	0
0	0	0	0	0	0	0	0	0	0	0	0	0	0	0	0	0	0	0	0
0	0	0	0	0	0	0	0	0	0	0	0	0	0	0	0	0	0	0	0
0	0	0	0	0	0	0	0	0	0	0	0	0	0	0	0	0	0	0	0
0	0	0	0	0	0	0	0	0	0	0	0	0	0	0	0	0	0	0	0
0	0	0	0	0	0	0	0	0	0	0	0	0	0	0	0	0	0	0	0
0	0	0	0	0	0	0	0	0	0	0	0	0	0	0	0	0	0	0	0

DESCRIPTION OF TERMS IN SECOND PART OF ELEMENTAL CONDUCTION

MATRIX FOR $\eta = -1$

$$\int_{-1}^{+1} \int_{-1}^{+1} \left[N^e(\xi,\zeta)\right]^T \left[N^e(\xi,\zeta)\right] \left| J(\xi,\zeta) \right| d\xi \; d\zeta$$

t1 = 1+ξ

t2 = t1**2

t3 = 1+ζ

t4 = t3**2

t6 = ξ-1+ζ

t7 = t6**2

t9 = t1*t4

t10 = -1+ξ

t12 = -ξ-1+ζ

t14 = t9*t6*t10*t12

t15 = t1*t3

t17 = -1+ζ

t18 = t10*t17

t19 = ξ+1+ζ

t21 = t15*t6*t18*t19

t22 = t2*t3

t24 = -ξ+1+ζ

```
t26 = t22*t6*t17*t24

t27 = ξ**2

t28 = -1+t27

t29 = t6*t28

t30 = t9*t29

t31 = ζ**2

t32 = -1+t31

t33 = t6*t32

t35 = t15*t33*t10

t37 = t15*t29*t17

t38 = t22*t33

t39 = t10**2

t41 = t12**2

t43 = t39*t3

t46 = t43*t12*t17*t19

t47 = t10*t3

t49 = t1*t17

t51 = t47*t12*t49*t24

t53 = t12*t28

t54 = t10*t4*t53

t55 = t12*t32

t56 = t43*t55
```

```
t58 = t47*t53*t17

t60 = t47*t55*t1

t61 = t17**2

t63 = t19**2

t65 = t10*t61

t68 = t65*t19*t1*t24

t69 = t19*t28

t71 = t18*t69*t3

t73 = t19*t32

t74 = t39*t17*t73

t75 = t65*t69

t77 = t18*t73*t1

t79 = t24**2

t81 = t24*t28

t83 = t49*t81*t3

t84 = t24*t32

t86 = t49*t84*t10

t88 = t1*t61*t61

t90 = t2*t17*t84

t91 = t28**2

t93 = t28*t3

t94 = t32*t10
```

```
t95 = t93*t94

t97 = t91*t3*t17

t98 = t32*t1

t99 = t93*t98

t100 = t32**2

t102 = t28*t17

t103 = t94*t102

t105 = t100*t10*t1

t107 = t102*t98
```

SECOND PART OF ELEMENTAL CONDUCTION MATRIX FOR $\eta = -1$

[20 x 20]

0	0	0	0	0	0	0	0	0	0	0	0	0	0	0	0	0	0	0	0
0	0	0	0	0	0	0	0	0	0	0	0	0	0	0	0	0	0	0	0
0	0	0	0	0	0	0	0	0	0	0	0	0	0	0	0	0	0	0	0
0	0	0	0	0	0	0	0	0	0	0	0	0	0	0	0	0	0	0	0
0	0	0	0	t2*t4*t7/16	-t14/16	-t21/16	t26/16	0	0	0	0	-t30/8	t35/8	t37/8	-t38/8	0	0	0	0
0	0	0	0	-t14/16	t39*t4*t41/16	t46/16	-t51/16	0	0	0	0	t54/8	-t56/8	-t58/8	t60/8	0	0	0	0
0	0	0	0	-t21/16	t46/16	t39*t61*t63/16	-t68/16	0	0	0	0	t71/8	-t74/8	-t75/8	t77/8	0	0	0	0
0	0	0	0	t26/16	-t51/16	-t68/16	t2*t61*t79/16	0	0	0	0	-t83/8	t86/8	t88/8	-t90/8	0	0	0	0
0	0	0	0	0	0	0	0	0	0	0	0	0	0	0	0	0	0	0	0
0	0	0	0	0	0	0	0	0	0	0	0	0	0	0	0	0	0	0	0
0	0	0	0	0	0	0	0	0	0	0	0	0	0	0	0	0	0	0	0
0	0	0	0	0	0	0	0	0	0	0	0	0	0	0	0	0	0	0	0
0	0	0	0	-t30/8	t54/8	t71/8	-t83/8	0	0	0	0	t91*t4/4	-t95/4	-t97/4	t99/4	0	0	0	0
0	0	0	0	t35/8	-t56/8	-t74/8	t86/8	0	0	0	0	-t95/4	t100*t39/4	t103/4	-t105/4	0	0	0	0
0	0	0	0	t37/8	-t58/8	-t75/8	t88/8	0	0	0	0	-t97/4	t103/4	t91*t61/4	-t107/4	0	0	0	0
0	0	0	0	-t38/8	t60/8	t77/8	-t90/8	0	0	0	0	t99/4	-t105/4	-t107/4	t100*t2/4	0	0	0	0
0	0	0	0	0	0	0	0	0	0	0	0	0	0	0	0	0	0	0	0
0	0	0	0	0	0	0	0	0	0	0	0	0	0	0	0	0	0	0	0
0	0	0	0	0	0	0	0	0	0	0	0	0	0	0	0	0	0	0	0
0	0	0	0	0	0	0	0	0	0	0	0	0	0	0	0	0	0	0	0

DESCRIPTION OF TERMS IN SECOND PART OF ELEMENTAL CONDUCTION

MATRIX FOR $\zeta = 1$

$$\int_{-1}^{+1}\int_{-1}^{+1} \left[N^e(\xi,\eta)\right]^T \left[N^e(\xi,\eta)\right] \left| J(\xi,\eta) \right| d\xi \; d\eta$$

t1 = 1+ξ

t2 = t1**2

t3 = 1+η

t4 = t3**2

t6 = ξ+η-1

t7 = t6**2

t9 = t1*t4

t10 = -1+ξ

t12 = ξ-η+1

t14 = t9*t6*t10*t12

t15 = t2*t3

t16 = -1+η

t18 = ξ-η-1

t20 = t15*t6*t16*t18

t21 = t1*t3

t23 = t10*t16

t24 = ξ+η+1

```
t26 = t21*t6*t23*t24

t27 = η**2

t28 = -1+t27

t29 = t6*t28

t30 = t15*t29

t32 = t21*t29*t10

t33 = ξ**2

t34 = -1+t33

t35 = t6*t34

t36 = t9*t35

t38 = t21*t35*t16

t39 = t10**2

t41 = t12**2

t43 = t10*t3

t45 = t1*t16

t47 = t43*t12*t45*t18

t48 = t39*t3

t51 = t48*t12*t16*t24

t52 = t12*t28

t54 = t43*t52*t1

t55 = t48*t52

t57 = t12*t34
```

```
t58 = t10*t4*t57

t60 = t43*t57*t16

t61 = t16**2

t63 = t18**2

t65 = t1*t61

t68 = t65*t18*t10*t24

t70 = t18*t28

t71 = t2*t16*t70

t73 = t45*t70*t10

t74 = t18*t34

t76 = t45*t74*t3

t77 = t65*t74

t79 = t24**2

t81 = t24*t28

t83 = t23*t81*t1

t85 = t39*t16*t81

t86 = t24*t34

t88 = t23*t86*t3

t90 = t10*t61*t86

t91 = t28**2

t94 = t91*t1*t10

t95 = t28*t1
```

```
t96 = t34*t3

t97 = t95*t96

t98 = t34*t16

t99 = t95*t98

t101 = t28*t10

t102 = t101*t96

t103 = t101*t98

t104 = t34**2

t107 = t104*t3*t16
```

SECOND PART OF ELEMENTAL CONDUCTION MATRIX FOR $\zeta = 1$

[20 x 20]

t2*t4*t7/16	t14/16	0	0	-t20/16	-t26/16	0	0	-t36/8	0	0	0	t38/8	0	0	0	-t30/8	t32/8	0	0
t14/16	t39*t4*t41/16	0	0	-t47/16	-t51/16	0	0	-t58/8	0	0	0	t60/8	0	0	0	-t54/8	t55/8	0	0
0	0	0	0	0	0	0	0	0	0	0	0	0	0	0	0	0	0	0	0
0	0	0	0	0	0	0	0	0	0	0	0	0	0	0	0	0	0	0	0
-t20/16	-t47/16	0	0	t2*t61*t63/16	t68/16	0	0	t76/8	0	0	0	-t77/8	0	0	0	t71/8	-t73/8	0	0
-t26/16	-t51/16	0	0	t68/16	t39*t61*t79/16	0	0	t88/8	0	0	0	-t90/8	0	0	0	t83/8	-t85/8	0	0
0	0	0	0	0	0	0	0	0	0	0	0	0	0	0	0	0	0	0	0
0	0	0	0	0	0	0	0	0	0	0	0	0	0	0	0	0	0	0	0
-t36/8	-t58/8	0	0	t76/8	t88/8	0	0	t104*t4/4	0	0	0	-t107/4	0	0	0	t97/4	-t102/4	0	0
0	0	0	0	0	0	0	0	0	0	0	0	0	0	0	0	0	0	0	0
0	0	0	0	0	0	0	0	0	0	0	0	0	0	0	0	0	0	0	0
0	0	0	0	0	0	0	0	0	0	0	0	0	0	0	0	0	0	0	0
t38/8	t60/8	0	0	-t77/8	-t90/8	0	0	-t107/4	0	0	0	t104*t61/4	0	0	0	-t99/4	t103/4	0	0
0	0	0	0	0	0	0	0	0	0	0	0	0	0	0	0	0	0	0	0
0	0	0	0	0	0	0	0	0	0	0	0	0	0	0	0	0	0	0	0
0	0	0	0	0	0	0	0	0	0	0	0	0	0	0	0	0	0	0	0
-t30/8	-t54/8	0	0	t71/8	t83/8	0	0	t97/4	0	0	0	-t99/4	0	0	0	t91*t2/4	-t94/4	0	0
t32/8	t55/8	0	0	-t73/8	-t85/8	0	0	-t102/4	0	0	0	t103/4	0	0	0	-t94/4	t91*t39/4	0	0
0	0	0	0	0	0	0	0	0	0	0	0	0	0	0	0	0	0	0	0
0	0	0	0	0	0	0	0	0	0	0	0	0	0	0	0	0	0	0	0

DESCRIPTION OF TERMS IN SECOND PART OF ELEMENTAL CONDUCTION

MATRIX FOR $\zeta = -1$

$$\int_{-1}^{+1}\int_{-1}^{+1} \left[N^e(\xi,\eta)\right]^T \left[N^e(\xi,\eta)\right] \left| J(\xi,\eta) \right| d\xi \; d\eta$$

t1 = -1+ξ

t2 = t1**2

t3 = 1+η

t4 = t3**2

t6 = ξ-η+1

t7 = t6**2

t9 = t1*t4

t10 = 1+ξ

t12 = ξ+η-1

t14 = t9*t6*t10*t12

t15 = t2*t3

t16 = -1+η

t18 = ξ+η+1

t20 = t15*t6*t16*t18

t21 = t1*t3

t23 = t10*t16

t24 = ξ-η-1

```
t26 = t21*t6*t23*t24

t27 = η**2

t28 = -1+t27

t29 = t6*t28

t30 = t15*t29

t32 = t21*t29*t10

t33 = ξ**2

t34 = -1+t33

t35 = t6*t34

t36 = t9*t35

t38 = t21*t35*t16

t39 = t10**2

t41 = t12**2

t43 = t10*t3

t45 = t1*t16

t47 = t43*t12*t45*t18

t48 = t39*t3

t51 = t48*t12*t16*t24

t52 = t12*t28

t54 = t43*t52*t1

t55 = t48*t52

t57 = t12*t34
```

```
t58 = t10*t4*t57

t60 = t43*t57*t16

t61 = t16**2

t63 = t18**2

t65 = t1*t61

t68 = t65*t18*t10*t24

t70 = t18*t28

t71 = t2*t16*t70

t73 = t45*t70*t10

t74 = t18*t34

t76 = t45*t74*t3

t77 = t65*t74

t79 = t24**2

t81 = t24*t28

t83 = t23*t81*t1

t85 = t39*t16*t81

t86 = t24*t34

t88 = t23*t86*t3

t90 = t10*t61*t86

t91 = t28**2

t94 = t91*t1*t10

t95 = t28*t1
```

```
t96 = t34*t3

t97 = t95*t96

t98 = t34*t16

t99 = t95*t98

t101 = t28*t10

t102 = t101*t96

t103 = t101*t98

t104 = t34**2

t107 = t104*t3*t16
```

SECOND PART OF ELEMENTAL CONDUCTION MATRIX FOR $\zeta = -1$

[20 x 20]

0	0	0	0	0	0	0	0	0	0	0	0	0	0	0	0	0	0	0	0
0	0	0	0	0	0	0	0	0	0	0	0	0	0	0	0	0	0	0	0
0	0	t2*t4*t7/16	t14/16	0	0	-t20/16	-t26/16	0	0	-t36/8	0	0	0	t38/8	0	0	0	t30/8	-t32/8
0	0	t14/16	t39*t4*t41/16	0	0	-t47/16	-t51/16	0	0	-t58/8	0	0	0	t60/8	0	0	0	t54/8	-t55/8
0	0	0	0	0	0	0	0	0	0	0	0	0	0	0	0	0	0	0	0
0	0	0	0	0	0	0	0	0	0	0	0	0	0	0	0	0	0	0	0
0	0	-t20/16	-t47/16	0	0	t2*t61*t63/16	t68/16	0	0	t76/8	0	0	0	-t77/8	0	0	0	-t71/8	t73/8
0	0	-t26/16	-t51/16	0	0	t68/16	t39*t61*t79/16	0	0	t88/8	0	0	0	-t90/8	0	0	0	-t83/8	t85/8
0	0	0	0	0	0	0	0	0	0	0	0	0	0	0	0	0	0	0	0
0	0	0	0	0	0	0	0	0	0	0	0	0	0	0	0	0	0	0	0
0	0	-t36/8	-t58/8	0	0	t76/8	t88/8	0	0	t104*t4/4	0	0	0	-t107/4	0	0	0	-t97/4	t102/4
0	0	0	0	0	0	0	0	0	0	0	0	0	0	0	0	0	0	0	0
0	0	0	0	0	0	0	0	0	0	0	0	0	0	0	0	0	0	0	0
0	0	0	0	0	0	0	0	0	0	0	0	0	0	0	0	0	0	0	0
0	0	t38/8	t60/8	0	0	-t77/8	-t90/8	0	0	-t107/4	0	0	0	t104*t61/4	0	0	0	t99/4	-t103/4
0	0	0	0	0	0	0	0	0	0	0	0	0	0	0	0	0	0	0	0
0	0	0	0	0	0	0	0	0	0	0	0	0	0	0	0	0	0	0	0
0	0	0	0	0	0	0	0	0	0	0	0	0	0	0	0	0	0	0	0
0	0	t30/8	t54/8	0	0	-t71/8	-t83/8	0	0	-t97/4	0	0	0	t99/4	0	0	0	t91*t2/4	-t94/4
0	0	-t32/8	-t55/8	0	0	t73/8	t85/8	0	0	t102/4	0	0	0	-t103/4	0	0	0	-t94/4	t91*t39/4

DESCRIPTION OF TERMS IN ELEMENTAL CONVECTION VECTOR $[F_c^e]$ FOR $\xi = 1$

$$\int_{-1}^{+1} \int_{-1}^{+1} \left[N^e(\eta,\zeta)\right]^T \left| J(\eta,\zeta) \right| d\eta \; d\zeta$$

t1 = 1+η

t2 = 1+ζ

t6 = 1-ζ

t10 = 1-η

t17 = η**2

t18 = 1-t17

t21 = ζ**2

t22 = 1-t21

ELEMENTAL CONVECTION VECTOR {FC1} FOR $\xi = 1$

FC1(1,1) = t1*t2*(-1+η+ζ)/4
FC1(2,1) = 0
FC1(3,1) = 0
FC1(4,1) = t1*t6*(-1+η-ζ)/4
FC1(5,1) = t10*t2*(-1-η+ζ)/4
FC1(6,1) = 0
FC1(7,1) = 0
FC1(8,1) = t10*t6*(-1-η-ζ)/4
FC1(9,1) = 0
FC1(10,1) = 0
FC1(11,1) = 0
FC1(12,1) = t22*t1/2
FC1(13,1) = 0
FC1(14,1) = 0
FC1(15,1) = 0
FC1(16,1) = t22*t10/2
FC1(17,1) = t18*t2/2
FC1(18,1) = 0
FC1(19,1) = 0
FC1(20,1) = t18*t6/2

DESCRIPTION OF TERMS IN ELEMENTAL CONVECTION VECTOR $[F_c^e]$ FOR ξ =-1

$$\int_{-1}^{+1}\int_{-1}^{+1} \left[N^e(\eta,\zeta)\right]^T \left| J(\eta,\zeta) \right| d\eta \; d\zeta$$

t1 = 1+η

t2 = 1+ζ

t6 = 1-ζ

t10 = 1-η

t17 = η**2

t18 = 1-t17

t21 = ζ**2

t22 = 1-t21

ELEMENTAL CONVECTION VECTOR {FC2} FOR $\xi = -1$

FC2(1,1) = 0
FC2(2,1) = t1*t2*(-1+η+ζ)/4
FC2(3,1) = t1*t6*(-1+η-ζ)/4
FC2(4,1) = 0
FC2(5,1) = 0
FC2(6,1) = t10*t2*(-1-η+ζ)/4
FC2(7,1) = t10*t6*(-1-η-ζ)/4
FC2(8,1) = 0
FC2(9,1) = 0
FC2(10,1) = t22*t1/2
FC2(11,1) = 0
FC2(12,1) = 0
FC2(13,1) = 0
FC2(14,1) = t22*t10/2
FC2(15,1) = 0
FC2(16,1) = 0
FC2(17,1) = 0
FC2(18,1) = t18*t2/2
FC2(19,1) = t18*t6/2
FC2(20,1) = 0

DESCRIPTION OF TERMS IN ELEMENTAL CONVECTION VECTOR $[F_c^e]$ FOR $\eta = 1$

$$\int_{-1}^{+1} \int_{-1}^{+1} \left[N^e(\xi,\zeta)\right]^T \left| J(\xi,\zeta) \right| d\xi \, d\zeta$$

t1 = 1+ξ

t2 = 1+ζ

t6 = 1-ξ

t10 = 1-ζ

t17 = ξ**2

t18 = 1-t17

t20 = ζ**2

t21 = 1-t20

ELEMENTAL CONVECTION VECTOR {FC3} FOR $\eta = 1$

FC3(1,1) = t1*t2*(ξ-1+ζ)/4
FC3(2,1) = t6*t2*(-ξ-1+ζ)/4
FC3(3,1) = t6*t10*(-ξ-1-ζ)/4
FC3(4,1) = t1*t10*(ξ-1-ζ)/4
FC3(5,1) = 0
FC3(6,1) = 0
FC3(7,1) = 0
FC3(8,1) = 0
FC3(9,1) = t18*t2/2
FC3(10,1) = t21*t6/2
FC3(11,1) = t18*t10/2
FC3(12,1) = t21*t1/2
FC3(13,1) = 0
FC3(14,1) = 0
FC3(15,1) = 0
FC3(16,1) = 0
FC3(17,1) = 0
FC3(18,1) = 0
FC3(19,1) = 0
FC3(20,1) = 0

DESCRIPTION OF TERMS IN ELEMENTAL CONVECTION VECTOR $[F_c^e]$ FOR $\eta = -1$

$$\int_{-1}^{+1} \int_{-1}^{+1} \left[N^e(\xi,\zeta)\right]^T \left| J(\xi,\zeta) \right| d\xi \; d\zeta$$

t1 = 1+ξ

t2 = 1+ζ

t6 = 1-ξ

t10 = 1-ζ

t17 = ξ**2

t18 = 1-t17

t20 = ζ**2

t21 = 1-t20

ELEMENTAL CONVECTION VECTOR {FC4} FOR $\eta = -1$

FC4(1,1) = 0
FC4(2,1) = 0
FC4(3,1) = 0
FC4(4,1) = 0
FC4(5,1) = t1*t2*(ξ-1+ζ)/4
FC4(6,1) = t6*t2*(-ξ-1+ζ)/4
FC4(7,1) = t6*t10*(-ξ-1-ζ)/4
FC4(8,1) = t1*t10*(ξ-1-ζ)/4
FC4(9,1) = 0
FC4(10,1) = 0
FC4(11,1) = 0
FC4(12,1) = 0
FC4(13,1) = t18*t2/2
FC4(14,1) = t21*t6/2
FC4(15,1) = t18*t10/2
FC4(16,1) = t21*t1/2
FC4(17,1) = 0
FC4(18,1) = 0
FC4(19,1) = 0
FC4(20,1) = 0

DESCRIPTION OF TERMS IN ELEMENTAL CONVECTION VECTOR $[F_c^e]$ FOR $\zeta = 1$

$$\int_{-1}^{+1}\int_{-1}^{+1} \left[N^e(\xi,\eta)\right]^T \left| J(\xi,\eta) \right| d\xi \, d\eta$$

t1 = 1+ξ

t2 = 1+η

t6 = 1-ξ

t10 = 1-η

t17 = η**2

t18 = 1-t17

t21 = ξ**2

t22 = 1-t21

ELEMENTAL CONVECTION VECTOR {FC5} FOR $\zeta = 1$

FC5(1,1) = t1*t2*(ξ+η-1)/4
FC5(2,1) = t6*t2*(-ξ+η-1)/4
FC5(3,1) = 0
FC5(4,1) = 0
FC5(5,1) = t1*t10*(ξ-η-1)/4
FC5(6,1) = t6*t10*(-ξ-η-1)/4
FC5(7,1) = 0
FC5(8,1) = 0
FC5(9,1) = t22*t2/2
FC5(10,1) = 0
FC5(11,1) = 0
FC5(12,1) = 0
FC5(13,1) = t22*t10/2
FC5(14,1) = 0
FC5(15,1) = 0
FC5(16,1) = 0
FC5(17,1) = t18*t1/2
FC5(18,1) = t18*t6/2
FC5(19,1) = 0
FC5(20,1) = 0

DESCRIPTION OF TERMS IN ELEMENTAL CONVECTION VECTOR $[F_c^e]$ FOR $\zeta = -1$

$$\int_{-1}^{+1} \int_{-1}^{+1} \left[N^e(\xi,\eta)\right]^T \left| J(\xi,\eta) \right| d\xi \; d\eta$$

t1 = 1-ξ

t2 = 1+η

t6 = 1+ξ

t10 = 1-η

t17 = η**2

t18 = 1-t17

t21 = ξ**2

t22 = 1-t21

ELEMENTAL CONVECTION VECTOR {FC6} FOR $\zeta = -1$

FC6(1,1) = 0
FC6(2,1) = 0
FC6(3,1) = t1*t2*(-ξ+η-1)/4
FC6(4,1) = t6*t2*(ξ+η-1)/4
FC6(5,1) = 0
FC6(6,1) = 0
FC6(7,1) = t1*t10*(-ξ-η-1)/4
FC6(8,1) = t6*t10*(ξ-η-1)/4
FC6(9,1) = 0
FC6(10,1) = 0
FC6(11,1) = t22*t2/2
FC6(12,1) = 0
FC6(13,1) = 0
FC6(14,1) = 0
FC6(15,1) = t22*t10/2
FC6(16,1) = 0
FC6(17,1) = 0
FC6(18,1) = 0
FC6(19,1) = t18*t1/2
FC6(20,1) = t18*t6/2

DESCRIPTION OF TERMS IN FIRST PART OF ELEMENTAL RADIATION VECTOR

$[F_r^e]$ FOR $\xi = 1$

$$\int_{-1}^{+1}\int_{-1}^{+1} \left[N^e(\eta,\zeta)\right]^T \left| J(\eta,\zeta) \right| d\eta \; d\zeta$$

t1 = 1+η

t2 = 1+ζ

t6 = 1-ζ

t10 = 1-η

t17 = η**2

t18 = 1-t17

t21 = ζ**2

t22 = 1-t21

FIRST PART OF ELEMENTAL RADIATION VECTOR {FR1} FOR $\xi = 1$

FR1(1,1) = t1*t2*(-1+η+ζ)/4
FR1(2,1) = 0
FR1(3,1) = 0
FR1(4,1) = t1*t6*(-1+η-ζ)/4
FR1(5,1) = t10*t2*(-1-η+ζ)/4
FR1(6,1) = 0
FR1(7,1) = 0
FR1(8,1) = t10*t6*(-1-η-ζ)/4
FR1(9,1) = 0
FR1(10,1) = 0
FR1(11,1) = 0
FR1(12,1) = t22*t1/2
FR1(13,1) = 0
FR1(14,1) = 0
FR1(15,1) = 0
FR1(16,1) = t22*t10/2
FR1(17,1) = t18*t2/2
FR1(18,1) = 0
FR1(19,1) = 0
FR1(20,1) = t18*t6/2

DESCRIPTION OF TERMS IN FIRST PART OF ELEMENTAL RADIATION VECTOR

$[F_r^e]$ FOR $\xi = -1$

$$\int_{-1}^{+1} \int_{-1}^{+1} \left[N^e(\eta,\zeta)\right]^T \left| J(\eta,\zeta) \right| d\eta \; d\zeta$$

t1 = 1+η

t2 = 1+ζ

t6 = 1-ζ

t10 = 1-η

t17 = η**2

t18 = 1-t17

t21 = ζ**2

t22 = 1-t21

FIRST PART OF ELEMENTAL RADIATION VECTOR {FR2} FOR $\xi = -1$

FR2(1,1) = 0
FR2(2,1) = t1*t2*(-1+η+ζ)/4
FR2(3,1) = t1*t6*(-1+η-ζ)/4
FR2(4,1) = 0
FR2(5,1) = 0
FR2(6,1) = t10*t2*(-1-η+ζ)/4
FR2(7,1) = t10*t6*(-1-η-ζ)/4
FR2(8,1) = 0
FR2(9,1) = 0
FR2(10,1) = t22*t1/2
FR2(11,1) = 0
FR2(12,1) = 0
FR2(13,1) = 0
FR2(14,1) = t22*t10/2
FR2(15,1) = 0
FR2(16,1) = 0
FR2(17,1) = 0
FR2(18,1) = t18*t2/2
FR2(19,1) = t18*t6/2
FR2(20,1) = 0

DESCRIPTION OF TERMS IN FIRST PART OF ELEMENTAL RADIATION VECTOR

$[F_r^e]$ FOR $\eta = 1$

$$\int_{-1}^{+1} \int_{-1}^{+1} \left[N^e(\xi,\zeta)\right]^T \left| J(\xi,\zeta) \right| d\xi \, d\zeta$$

t1 = 1+ξ

t2 = 1+ζ

t6 = 1-ξ

t10 = 1-ζ

t17 = ξ**2

t18 = 1-t17

t20 = ζ**2

t21 = 1-t20

FIRST PART OF ELEMENTAL RADIATION VECTOR {FR3} FOR $\eta = 1$

FR3(1,1) = t1*t2*(ξ-1+ζ)/4
FR3(2,1) = t6*t2*(-ξ-1+ζ)/4
FR3(3,1) = t6*t10*(-ξ-1-ζ)/4
FR3(4,1) = t1*t10*(ξ-1-ζ)/4
FR3(5,1) = 0
FR3(6,1) = 0
FR3(7,1) = 0
FR3(8,1) = 0
FR3(9,1) = t18*t2/2
FR3(10,1) = t21*t6/2
FR3(11,1) = t18*t10/2
FR3(12,1) = t21*t1/2
FR3(13,1) = 0
FR3(14,1) = 0
FR3(15,1) = 0
FR3(16,1) = 0
FR3(17,1) = 0
FR3(18,1) = 0
FR3(19,1) = 0
FR3(20,1) = 0

DESCRIPTION OF TERMS IN FIRST PART OF ELEMENTAL RADIATION VECTOR

$[F_r^e]$ FOR $\eta = -1$

$$\int_{-1}^{+1}\int_{-1}^{+1} \left[N^e(\xi,\zeta)\right]^T \left| J(\xi,\zeta) \right| d\xi \; d\zeta$$

t1 = 1+ξ

t2 = 1+ζ

t6 = 1-ξ

t10 = 1-ζ

t17 = ξ**2

t18 = 1-t17

t20 = ζ**2

t21 = 1-t20

FIRST PART OF ELEMENTAL RADIATION VECTOR {FR4} FOR $\eta = -1$

FR4(1,1) = 0
FR4(2,1) = 0
FR4(3,1) = 0
FR4(4,1) = 0
FR4(5,1) = t1*t2*(ξ-1+ζ)/4
FR4(6,1) = t6*t2*(-ξ-1+ζ)/4
FR4(7,1) = t6*t10*(-ξ-1-ζ)/4
FR4(8,1) = t1*t10*(ξ-1-ζ)/4
FR4(9,1) = 0
FR4(10,1) = 0
FR4(11,1) = 0
FR4(12,1) = 0
FR4(13,1) = t18*t2/2
FR4(14,1) = t21*t6/2
FR4(15,1) = t18*t10/2
FR4(16,1) = t21*t1/2
FR4(17,1) = 0
FR4(18,1) = 0
FR4(19,1) = 0
FR4(20,1) = 0

DESCRIPTION OF TERMS IN FIRST PART OF ELEMENTAL RADIATION VECTOR

$[F_r^e]$ FOR $\zeta = 1$

$$\int_{-1}^{+1}\int_{-1}^{+1} \left[N^e(\xi,\eta)\right]^T \left| J(\xi,\eta) \right| d\xi \, d\eta$$

t1 = 1+ξ

t2 = 1+η

t6 = 1-ξ

t10 = 1-η

t17 = η**2

t18 = 1-t17

t21 = ξ**2

t22 = 1-t21

FIRST PART OF ELEMENTAL RADIATION VECTOR {FR5} FOR $\zeta = 1$

FR5(1,1) = t1*t2*(ξ+η-1)/4
FR5(2,1) = t6*t2*(-ξ+η-1)/4
FR5(3,1) = 0
FR5(4,1) = 0
FR5(5,1) = t1*t10*(ξ-η-1)/4
FR5(6,1) = t6*t10*(-ξ-η-1)/4
FR5(7,1) = 0
FR5(8,1) = 0
FR5(9,1) = t22*t2/2
FR5(10,1) = 0
FR5(11,1) = 0
FR5(12,1) = 0
FR5(13,1) = t22*t10/2
FR5(14,1) = 0
FR5(15,1) = 0
FR5(16,1) = 0
FR5(17,1) = t18*t1/2
FR5(18,1) = t18*t6/2
FR5(19,1) = 0
FR5(20,1) = 0

DESCRIPTION OF TERMS IN FIRST PART OF ELEMENTAL RADIATION VECTOR

$[F_r^e]$ FOR $\zeta = -1$

$$\int_{-1}^{+1}\int_{-1}^{+1} \left[N^e(\xi,\eta)\right]^T \left| J(\xi,\eta) \right| d\xi \, d\eta$$

t1 = 1-ξ

t2 = 1+η

t6 = 1+ξ

t10 = 1-η

t17 = η**2

t18 = 1-t17

t21 = ξ**2

t22 = 1-t21

FIRST PART OF ELEMENTAL RADIATION VECTOR {FR6} FOR $\zeta = -1$

FR6(1,1) = 0
FR6(2,1) = 0
FR6(3,1) = t1*t2*(-ξ+η-1)/4
FR6(4,1) = t6*t2*(ξ+η-1)/4
FR6(5,1) = 0
FR6(6,1) = 0
FR6(7,1) = t1*t10*(-ξ-η-1)/4
FR6(8,1) = t6*t10*(ξ-η-1)/4
FR6(9,1) = 0
FR6(10,1) = 0
FR6(11,1) = t22*t2/2
FR6(12,1) = 0
FR6(13,1) = 0
FR6(14,1) = 0
FR6(15,1) = t22*t10/2
FR6(16,1) = 0
FR6(17,1) = 0
FR6(18,1) = 0
FR6(19,1) = t18*t1/2
FR6(20,1) = t18*t6/2

DESCRIPTION OF TERMS IN SECOND PART OF ELEMENTAL RADIATION VECTOR $[F_r^e]$ FOR $\xi = 1$(C1, C4, C5, C8, C12, C16, C17, C20 are the nodal temperatures)

$$\int_{-1}^{+1}\int_{-1}^{+1} \left[N^e(\eta,\zeta)\right]^T \left(\left[N^e(\eta,\zeta)\right]\left\{T^e(\eta,\zeta)\right\}\right)^4 d\eta\ d\zeta$$

t1 = 1+η

t2 = 1+ζ

t5 = C4*η

t7 = C16*η

t8 = ζ**2

t10 = η**2

t11 = C1*t10

t13 = C8*t10

t15 = C4*t10

t17 = C5*η

t19 = C5*t10

t21 = C1*η

t29 = C17*t10

t31 = -t5*ζ-2*t7*t8+t11*ζ-t13*ζ-t15*ζ-t17*t8+t19*ζ+

#t21*t8+C5*t8-2*C16*t8+2*t7+C1*t8+t11+C4*t8+t15+C8*t8+t13+2*C17*ζ

#-2*t29-2*C12*ζ

```
t32 = C12*t10

t33 = C20*η

t39 = C8*η

t44 = -2*t32-2*t33-2*C20*t8-2*t29*ζ+t5*t8+2*C17+t19-C8+2*t32*zet

#a-t17*ζ+t39*ζ-t39*t8-C4+2*C12+2*C16-C1-C5+t21*ζ+2*t33*t8+

#2*C20

t46 = (t31+t44)**2

t47 = t46**2

t50 = -1+ζ

t55 = -1+η

t64 = -1+t10

t69 = -1+t8
```

SECOND PART OF ELEMENTAL RADIATION VECTOR {FR11} FOR $\xi = 1$

FR11(1,1) = t1*t2*(-1+η+ζ)*t47/1024
FR11(2,1) = 0
FR11(3,1) = 0
FR11(4,1) = t1*t50*(1-η+ζ)*t47/1024
FR11(5,1) = -t55*t2*(-1-η+ζ)*t47/1024
FR11(6,1) = 0
FR11(7,1) = 0
FR11(8,1) = -t55*t50*(1+η+ζ)*t47/1024
FR11(9,1) = 0
FR11(10,1) = 0
FR11(11,1) = 0
FR11(12,1) = t64*t50*t47/512
FR11(13,1) = 0
FR11(14,1) = 0
FR11(15,1) = 0
FR11(16,1) = -t69*t1*t47/512
FR11(17,1) = -t64*t2*t47/512
FR11(18,1) = 0
FR11(19,1) = 0
FR11(20,1) = t69*t55*t47/512

DESCRIPTION OF TERMS IN SECOND PART OF ELEMENTAL RADIATION VECTOR $[F_r^e]$ FOR $\xi = -1$(C2, C3, C6, C7, C10, C14, C18, C19 are the nodal temperatures)

$$\int_{-1}^{+1}\int_{-1}^{+1} \left[N^e(\eta,\zeta)\right]^T \left(\left[N^e(\eta,\zeta)\right]\left\{T^e(\eta,\zeta)\right\}\right)^4 d\eta\, d\zeta$$

t1 = 1+η

t2 = 1+ζ

t5 = C3*η

t7 = C2*η

t9 = η**2

t10 = C2*t9

t12 = ζ**2

t14 = C3*t9

t17 = C14*η

t19 = C10*t9

t21 = C6*t9

t24 = C6*η

t26 = C7*η

t29 = -t5*ζ+t7*ζ+t10*ζ+t5*t12-t14*ζ+t7*t12-2*t17*t12-2

#*t19*ζ+t21*ζ+2*C14-C3-C6+2*C18+2*C19-C2-2*C18*t12-t24*ζ-t

#26*t12+t26*ζ-C7

```
t30 = C19*t9

t35 = C7*t9

t39 = C18*η

t44 = -2*t30+C2*t12+t10+C3*t12+t14+C6*t12+t21+C7*t12+t35+2*C10*zet

#a-2*t19-2*C19*ζ+2*t17-2*C14*t12-2*t39+2*C10+2*t39*t12-t24*t12-t

#35*ζ+2*t30*ζ

t46 = (t29+t44)**2

t47 = t46**2

t50 = -1+ζ

t55 = -1+η

t64 = -1+t9

t69 = -1+t12
```

SECOND PART OF ELEMENTAL RADIATION VECTOR {FR22} FOR $\xi = -1$

FR22(1,1) = 0
FR22(2,1) = t1*t2*(-1+η+ζ)*t47/1024
FR22(3,1) = t1*t50*(1-η+ζ)*t47/1024
FR22(4,1) = 0
FR22(5,1) = 0
FR22(6,1) = -t55*t2*(-1-η+ζ)*t47/1024
FR22(7,1) = -t55*t50*(1+η+ζ)*t47/1024
FR22(8,1) = 0
FR22(9,1) = 0
FR22(10,1) = -t64*t2*t47/512
FR22(11,1) = 0
FR22(12,1) = 0
FR22(13,1) = 0
FR22(14,1) = -t69*t1*t47/512
FR22(15,1) = 0
FR22(16,1) = 0
FR22(17,1) = 0
FR22(18,1) = t69*t55*t47/512
FR22(19,1) = t64*t50*t47/512
FR22(20,1) = 0

DESCRIPTION OF TERMS IN SECOND PART OF ELEMENTAL RADIATION VECTOR $[F_i^e]$ FOR $\eta = 1$(C1, C2, C3, C4, C9, C10, C11, C12 are the nodal temperatures)

$$\int_{-1}^{+1}\int_{-1}^{+1} \left[N^e(\xi,\zeta)\right]^T \left(\left[N^e(\xi,\zeta)\right] \left\{T^e(\xi,\zeta)\right\}\right)^4 d\xi\, d\zeta$$

t1 = 1+ξ

t2 = 1+ζ

t5 = ξ**2

t6 = C4*t5

t8 = C1*ξ

t9 = ζ**2

t11 = C4*ξ

t14 = C9*t5

t16 = C12*ξ

t18 = C2*t5

t20 = C2*ξ

t22 = C11*t5

t24 = C1*t5

t27 = C10*ξ

t30 = -t6*ζ+t8*t9-t11*ζ+t8*ζ-2*t14*ζ-2*t16*t9+t18*ζ

#-t20*t9+2*t22*ζ+t24*ζ-t20*ζ+2*C10-C2-C3-C4+2*t27*t9-C1+2*

```
#C11+2*C12+t11*t9

 t35 = C3*t5

 t40 = C3*ξ

 t44 = -2*C12*t9+C1*t9+t24+C2*t9-t18+C3*t9+t35+C4*t9+t6+2*C9*ζ-

#2*t14-2*t27-2*C10*t9-2*C11*ζ-2*t22+2*t16+2*C9+t40*ζ-t35*zet

#a-t40*t9

 t46 = (t30+t44)**2

 t47 = t46**2

 t50 = -1+ξ

 t55 = -1+ζ

 t64 = -1+t5

 t67 = -1+t9
```

SECOND PART OF ELEMENTAL RADIATION VECTOR {FR33} FOR $\eta = 1$

FR33(1,1) = t1*t2*(ξ-1+ζ)*t47/1024
FR33(2,1) = -t50*t2*(-ξ-1+ζ)*t47/1024
FR33(3,1) = -t50*t55*(ξ+1+ζ)*t47/1024
FR33(4,1) = t1*t55*(-ξ+1+ζ)*t47/1024
FR33(5,1) = 0
FR33(6,1) = 0
FR33(7,1) = 0
FR33(8,1) = 0
FR33(9,1) = -t64*t2*t47/512
FR33(10,1) = t67*t50*t47/512
FR33(11,1) = t64*t55*t47/512
FR33(12,1) = -t67*t1*t47/512
FR33(13,1) = 0
FR33(14,1) = 0
FR33(15,1) = 0
FR33(16,1) = 0
FR33(17,1) = 0
FR33(18,1) = 0
FR33(19,1) = 0
FR33(20,1) = 0

DESCRIPTION OF TERMS IN SECOND PART OF ELEMENTAL RADIATION VECTOR $[F_r^e]$ FOR $\eta = -1$(C5, C6, C7, C8, C13, C14, C15, C16 are the nodal temperatures)

$$\int_{-1}^{+1}\int_{-1}^{+1} \left[N^e(\eta,\zeta)\right]^T \left(\left[N^e(\eta,\zeta)\right] \left\{T^e(\eta,\zeta)\right\}\right)^4 d\eta \; d\zeta$$

t1 = 1+ξ

t2 = 1+ζ

t5 = C7*ξ

t6 = ζ**2

t8 = C8*ξ

t10 = C16*ξ

t12 = C6*ξ

t14 = ξ**2

t15 = C5*t14

t18 = C6*t14

t20 = C7*t14

t22 = C8*t14

t24 = C13*t14

t26 = C15*t14

t27 = -t5*t6-t8*ζ-C7-2*t10*t6-t12*t6+2*C16-C6+t15+C5*t6+C6*t6+t

#18+C7*t6+t20+C8*t6+t22+2*C13*ζ-2*t24-2*C14*t6-2*t26+2*t10

```
 t31 = C5*ξ

 t38 = C14*ξ

 t44 = -2*C16*t6+t5*ζ-t12*ζ+t31*ζ+t15*ζ+t18*ζ-t20*ze

#ta-t22*ζ-2*t24*ζ+2*t38*t6+2*t26*ζ+t8*t6-2*C15*ζ+2*C14+

#2*C15-2*t38-C8+2*C13+t31*t6-C5

 t46 = (t27+t44)**2

 t47 = t46**2

 t50 = -1+ξ

 t55 = -1+ζ

 t64 = -1+t14

 t67 = -1+t6
```

SECOND PART OF ELEMENTAL RADIATION VECTOR {FR44} FOR $\eta = -1$

FR44(1,1) = 0
FR44(2,1) = 0
FR44(3,1) = 0
FR44(4,1) = 0
FR44(5,1) = t1*t2*(ξ-1+ζ)*t47/1024
FR44(6,1) = -t50*t2*(-ξ-1+ζ)*t47/1024
FR44(7,1) = -t50*t55*(ξ+1+ζ)*t47/1024
FR44(8,1) = t1*t55*(-ξ+1+ζ)*t47/1024
FR44(9,1) = 0
FR44(10,1) = 0
FR44(11,1) = 0
FR44(12,1) = 0
FR44(13,1) = -t64*t2*t47/512
FR44(14,1) = t67*t50*t47/512
FR44(15,1) = t64*t55*t47/512
FR44(16,1) = -t67*t1*t47/512
FR44(17,1) = 0
FR44(18,1) = 0
FR44(19,1) = 0
FR44(20,1) = 0

DESCRIPTION OF TERMS IN SECOND PART OF ELEMENTAL RADIATION VECTOR $[F_r^e]$ FOR $\zeta = 1$(C1, C2, C5, C6, C9, C13, C17, C18 are the nodal temperatures)

$$\int_{-1}^{+1}\int_{-1}^{+1} \left[N^e(\xi,\eta)\right]^T \left(\left[N^e(\xi,\eta)\right] \left\{T^e(\xi,\eta)\right\}\right)^4 d\xi\, d\eta$$

```
t1 = 1+ξ

t2 = 1+η

t5 = ξ**2

t6 = C9*t5

t8 = C17*ξ

t9 = η**2

t11 = C2*ξ

t14 = C5*t5

t16 = C1*ξ

t19 = C5*ξ

t21 = C6*t5

t25 = C1*t5

t27 = C2*t5

t30 = -2*t6*η-2*t8*t9-t11*t9-t11*η-t14*η+t16*η+t16*t9-t19*
#η-t21*η-2*C17*t9+2*C17+C1*t9+t25+C2*t9+t27+C5*t9+t14+C6*t9+t21+2
#*t8
```

```
t34 = C13*t5

t36 = C6*ξ

t40 = C18*ξ

t44 = -2*C18*t9+2*C9*η-2*t6-2*C13*η-2*t34+t25*η+t36*η+2*t

#34*η-C1-t36*t9-2*t40-C6+2*C18+2*C13+2*C13-C2-C5+2*t40*t9+t27*η

#+t19*t9

t46 = (t30+t44)**2

t47 = t46**2

t50 = -1+ξ

t55 = -1+η

t64 = -1+t9

t69 = -1+t5
```

SECOND PART OF ELEMENTAL RADIATION VECTOR {FR55} FOR $\zeta = 1$

FR55(1,1) = t1*t2*(ξ+η-1)*t47/1024
FR55(2,1) = t50*t2*(ξ-η+1)*t47/1024
FR55(3,1) = 0
FR55(4,1) = 0
FR55(5,1) = -t1*t55*(ξ-η-1)*t47/1024
FR55(6,1) = -t50*t55*(ξ+η+1)*t47/1024
FR55(7,1) = 0
FR55(8,1) = 0
FR55(9,1) = -t69*t2*t47/512
FR55(10,1) = 0
FR55(11,1) = 0
FR55(12,1) = 0
FR55(13,1) = t69*t55*t47/512
FR55(14,1) = 0
FR55(15,1) = 0
FR55(16,1) = 0
FR55(17,1) = -t64*t1*t47/512
FR55(18,1) = t64*t50*t47/512
FR55(19,1) = 0
FR55(20,1) = 0

DESCRIPTION OF TERMS IN SECOND PART OF ELEMENTAL RADIATION VECTOR $[F_r^e]$ FOR ζ = -1(C3, C4, C7, C8, C11, C15, C19, C20 are the nodal temperatures)

$$\int_{-1}^{+1}\int_{-1}^{+1} \left[N^e(\xi,\eta)\right]^T \left(\left[N^e(\xi,\eta)\right]\left\{T^e(\xi,\eta)\right\}\right)^4 d\xi\, d\eta$$

t1 = -1+ξ

t2 = 1+η

t5 = C8*ξ

t7 = ξ**2

t8 = C3*t7

t10 = C4*ξ

t12 = η**2

t15 = C11*t7

t18 = C4*t7

t19 = C7*t7

t21 = t5*η-t8*η-t10*η-C7*t12-C4*t12+C8-2*C19+2*t15-2*C20-2*C

#11-2*C15+C3+C7+C4+2*t15*η-C3*t12-t8-t18-t19-C8*t12

t22 = C8*t7

t23 = C19*ξ

t25 = C20*ξ

t29 = C15*t7

```
t30 = C7*ξ

t34 = C3*ξ

t44 = -t22+2*t23+2*C19*t12-2*t25+2*C20*t12-2*C11*η+2*C15*η+2*t

#29-t30*η-t18*η-t10*t12+t34*η-2*t23*t12+2*t25*t12-2*t29*η+t

#19*η+t30*t12+t22*η-t5*t12+t34*t12

t46 = (t21+t44)**2

t47 = t46**2

t50 = 1+ξ

t55 = -1+η

t64 = -1+t12

t69 = -1+t7
```

SECOND PART OF ELEMENTAL RADIATION VECTOR {FR66} FOR $\zeta = -1$

FR66(1,1) = 0
FR66(2,1) = 0
FR66(3,1) = t1*t2*(ξ-η+1)*t47/1024
FR66(4,1) = t50*t2*(ξ+η-1)*t47/1024
FR66(5,1) = 0
FR66(6,1) = 0
FR66(7,1) = -t1*t55*(ξ+η+1)*t47/1024
FR66(8,1) = -t50*t55*(ξ-η-1)*t47/1024
FR66(9,1) = 0
FR66(10,1) = 0
FR66(11,1) = -t69*t2*t47/512
FR66(12,1) = 0
FR66(13,1) = 0
FR66(14,1) = 0
FR66(15,1) = t69*t55*t47/512
FR66(16,1) = 0
FR66(17,1) = 0
FR66(18,1) = 0
FR66(19,1) = t64*t1*t47/512
FR66(20,1) = -t64*t50*t47/512

DESCRIPTION OF TERMS IN MATRIX [JJ1] [3 × 20] WHICH WHEN MULTIPLIED BY COORDINATE MATRIX [20 × 3] GIVES JACOBIAN MATRIX [J]

$t1 = 1+\eta$

$t2 = 1+\zeta$

$t3 = t1*t2$

$t4 = \xi+\eta+\zeta-2$

$t6 = 1+\xi$

$t7 = t6*t1$

$t8 = t7*t2$

$t10 = -\xi+\eta+\zeta-2$

$t12 = 1-\xi$

$t13 = t12*t1$

$t14 = t13*t2$

$t16 = 1-\zeta$

$t17 = t1*t16$

$t18 = -\xi+\eta-\zeta-2$

$t20 = t13*t16$

$t22 = \xi+\eta-\zeta-2$

$t24 = t7*t16$

$t26 = 1-\eta$

$t27 = t26*t2$

t28 = ξ-η+ζ-2

t30 = t6*t26

t31 = t30*t2

t33 = -ξ-η+ζ-2

t35 = t12*t26

t36 = t35*t2

t38 = t26*t16

t39 = -ξ-η-ζ-2

t41 = t35*t16

t43 = ξ-η-ζ-2

t45 = t30*t16

t47 = η**2

t48 = 1-t47

t49 = t48*t2

t50 = t48*t16

t51 = ξ*t1

t53 = ζ**2

t54 = 1-t53

t55 = t54*t1

t57 = ξ*t26

t59 = t54*t26

t61 = t6*t2

t64 = t12*t2

t67 = t12*t16

t70 = t6*t16

t81 = η*t6

t83 = η*t12

t87 = ξ**2

t88 = 1-t87

t89 = t88*t2

t90 = t54*t12

t91 = t88*t16

t92 = t54*t6

t109 = t48*t6

t110 = t48*t12

t111 = t88*t1

t112 = ζ*t12

t114 = ζ*t6

t116 = t88*t26

MATRIX [JJ1] [3 × 20] WHICH WHEN MULTIPLIED BY COORDINATE

MATRIX [20 × 3] GIVES JACOBIAN MATRIX [J]

t3*t4/8+t6/8	-t3*t10/8-t14/8	-t17*t18/8-t20/0	t17*t22/8+t24/8	t27*t28/8+t31/8	-t27*t33/8-t36/8	-t38*t33/8-t41/8	t38*t43/8+t45/8	t49/4	-t49/4	-t50/4	t50/4	-t51*t2/2	-t55/4	-t51*t16/2	t55/4	-t57*t2/2	-t59/4	-t57*t16/2	t59/4
t61*t4/8+t8/8	t64*t10/8+t14/8	t57*t18/8+t20/8	t70*t22/8+t24/8	-t61*t28/8-t31/8	-t64*t33/8-t36/8	-t67*t39/8-t41/8	-t70*t43/8-t45/8	-t81*t2/2	-t83*t2/2	-t83*t16/2	-t81*t16/2	t89/4	t90/4	t91/4	t92/4	-t89/4	-t90/4	-t91/4	-t92/4
t7*t4/8+t9/8	t13*t10/8+t14/8	-t13*t18/8-t20/8	-t7*t22/8-t24/8	t30*t28/8+t31/8	t35*t33/8+t36/8	-t35*t39/8-t41/8	-t30*t43/8-t45/8	t109/4	t110/4	-t110/4	-t109/4	t111/4	-t112*t1/2	-t111/4	-t114*t1/2	t116/4	-t112*t26/2	-t116/4	-t114*t26/2

DESCRIPTION OF TERMS IN MATRIX [JJ2] [2 x 20] WHICH WHEN MULTIPLIED BY COORDINATE MATRIX [20 x 2] GIVES JACOBIAN MATRIX [J] FOR $\xi = 1$

$t1 = 1+\zeta$

$t2 = -1+\eta+\zeta$

$t4 = 1+\eta$

$t5 = t4*t1$

$t7 = 1-\zeta$

$t8 = -1+\eta-\zeta$

$t10 = t4*t7$

$t12 = -1-\eta+\zeta$

$t14 = 1-\eta$

$t15 = t14*t1$

$t17 = -1-\eta-\zeta$

$t19 = t14*t7$

$t23 = \zeta**2$

$t34 = \eta**2$

MATRIX [JJ2] [2 × 20] WHICH WHEN MULTIPLIED BY COORDINATE

MATRIX [20 × 2] GIVES JACOBIAN MATRIX [J] FOR $\xi = 1$

t1*t2/4+t5/4	0	0	t7*t8/4+t10/4	-t1*t12/4-t15/4	0	0	-t7*t17/4-t19/4	0	0	0	1.E0/2.E0-t23/2	0	0	0	-1.E0/2.E0+t23/2	-eta*t1	0	0	-eta*t7
t4*t2/4+t5/4	0	0	-t4*t8/4-t10/4	t14*t12/4+t15/4	0	0	-t14*t17/4-t19/4	0	0	0	-zeta*t4	0	0	0	-zeta*t14	1.E0/2.E0-t34/2	0	0	-1.E0/2.E0+t34/2

DESCRIPTION OF TERMS IN MATRIX [JJ3] [2 × 20] WHICH WHEN MULTIPLIED BY COORDINATE MATRIX [20 × 2] GIVES JACOBIAN MATRIX [J] FOR $\xi = -1$

$t1 = 1+\zeta$

$t2 = -1+\eta+\zeta$

$t4 = 1+\eta$

$t5 = t4*t1$

$t7 = 1-\zeta$

$t8 = -1+\eta-\zeta$

$t10 = t4*t7$

$t12 = -1-\eta+\zeta$

$t14 = 1-\eta$

$t15 = t14*t1$

$t17 = -1-\eta-\zeta$

$t19 = t14*t7$

$t23 = \zeta**2$

$t34 = \eta**2$

MATRIX [JJ3] [2 × 20] WHICH WHEN MULTIPLIED BY COORDINATE

MATRIX [20 × 2] GIVES JACOBIAN MATRIX [J] FOR $\xi = -1$

0	t1*t2/4+t5/4	t7*t8/4+t10/4	0	0	-t1*t12/4-t15/4	-t7*t17/4-t19/4	0	0	1.E0/2.E0-t23/2	0	0	0	-1.E0/2.E0+t23/2	0	0	0	-eta*t1	-eta*t7	0
0	t4*t2/4+t5/4	-t4*t8/4-t10/4	0	0	t14*t12/4+t15/4	-t14*t17/4-t19/4	0	0	-zeta*t4	0	0	0	-zeta*t14	0	0	0	1.E0/2.E0-t34/2	-1.E0/2.E0+t34/2	0

DESCRIPTION OF TERMS IN MATRIX [JJ4] [2 × 20] WHICH WHEN MULTIPLIED BY COORDINATE MATRIX [20 × 2] GIVES JACOBIAN MATRIX [J] FOR $\eta = 1$

$t1 = 1+\zeta$

$t2 = \xi-1+\zeta$

$t4 = 1+\xi$

$t5 = t4*t1$

$t7 = -\xi-1+\zeta$

$t9 = 1-\xi$

$t10 = t9*t1$

$t12 = 1-\zeta$

$t13 = -\xi-1-\zeta$

$t15 = t9*t12$

$t17 = \xi-1-\zeta$

$t19 = t4*t12$

$t22 = \zeta**2$

$t34 = \xi**2$

MATRIX [JJ4] [2 × 20] WHICH WHEN MULTIPLIED BY COORDINATE

MATRIX [20 × 2] GIVES JACOBIAN MATRIX [J] FOR $\eta = 1$

t1*t2/4+t5/4	-t1*t7/4-t10/4	-t12*t13/4-t15/4	t12*t17/4+t19/4	0	0	0	0	-xi*t1	-1.E0/2.E0+t22/2	-xi*t12	1.E0/2.E0-t22/2	0	0	0	0	0	0	0	0
t4*t2/4+t5/4	t9*t7/4+t10/4	-t9*t13/4-t15/4	-t4*t17/4-t19/4	0	0	0	0	1.E0/2.E0-t34/2	-zeta*t9	-1.E0/2.E0+t34/2	-zeta*t4	0	0	0	0	0	0	0	0

DESCRIPTION OF TERMS IN MATRIX [JJ5] [2 × 20] WHICH WHEN MULTIPLIED BY COORDINATE MATRIX [20 × 2] GIVES JACOBIAN MATRIX [J] FOR $\eta = -1$

$t1 = 1+\zeta$

$t2 = \xi-1+\zeta$

$t4 = 1+\xi$

$t5 = t4*t1$

$t7 = -\xi-1+\zeta$

$t9 = 1-\xi$

$t10 = t9*t1$

$t12 = 1-\zeta$

$t13 = -\xi-1-\zeta$

$t15 = t9*t12$

$t17 = \xi-1-\zeta$

$t19 = t4*t12$

$t22 = \zeta**2$

$t34 = \xi**2$

MATRIX [JJ5] [2 × 20] WHICH WHEN MULTIPLIED BY COORDINATE

MATRIX [20 × 2] GIVES JACOBIAN MATRIX [J] FOR $\eta = -1$

0	0	0	0	t1*t2/4+t5/4	-t1*t7/4-t10/4	-t12*t13/4-t15/4	t12*t17/4+t19/4	0	0	0	0	-xi*t1	-1.E0/2.E0+t22/2	-xi*t12	1.E0/2.E0-t22/2	0	0	0	0
0	0	0	0	t4*t2/4+t5/4	t9*t7/4+t10/4	-t9*t13/4-t15/4	-t4*t17/4-t19/4	0	0	0	0	1.E0/2.E0-t34/2	-zeta*t9	-1.E0/2.E0+t34/2	-zeta*t4	0	0	0	0

DESCRIPTION OF TERMS IN MATRIX [JJ6] [2 × 20] WHICH WHEN MULTIPLIED BY COORDINATE MATRIX [20 × 2] GIVES JACOBIAN MATRIX [J] FOR $\zeta = 1$

t1 = 1+η

t2 = ξ+η-1

t4 = 1+ξ

t5 = t4*t1

t7 = -ξ+η-1

t9 = 1-ξ

t10 = t9*t1

t12 = 1-η

t13 = ξ-η-1

t15 = t4*t12

t17 = -ξ-η-1

t19 = t9*t12

t21 = η**2

t36 = ξ**2

MATRIX [JJ6] [2 × 20] WHICH WHEN MULTIPLIED BY COORDINATE

MATRIX [20 × 2] GIVES JACOBIAN MATRIX [J] FOR $\zeta = 1$

t1*t2/4+t5/4	-t1*t7/4-t10/4	0	0	t12*t13/4+t15/4	-t12*t17/4-t19/4	0	0	-xi*t1	0	0	0	-xi*t12	0	0	0	1.E0/2.E0-t21/2	-1.E0/2.E0+t21/2	0	0
t4*t2/4+t5/4	t9*t7/4+t10/4	0	0	-t4*t13/4-t15/4	-t9*t17/4-t19/4	0	0	1.E0/2.E0-t36/2	0	0	0	-1.E0/2.E0+t36/2	0	0	0	-eta*t4	-eta*t9	0	0

DESCRIPTION OF TERMS IN MATRIX [JJ7] [2 × 20] WHICH WHEN MULTIPLIED BY COORDINATE MATRIX [20 × 2] GIVES JACOBIAN MATRIX [J] FOR $\zeta = -1$

$t1 = 1+\eta$

$t2 = -\xi+\eta-1$

$t4 = 1-\xi$

$t5 = t4*t1$

$t7 = \xi+\eta-1$

$t9 = 1+\xi$

$t10 = t9*t1$

$t12 = 1-\eta$

$t13 = -\xi-\eta-1$

$t15 = t4*t12$

$t17 = \xi-\eta-1$

$t19 = t9*t12$

$t21 = \eta**2$

$t36 = \xi**2$

MATRIX [JJ7] [2 × 20] WHICH WHEN MULTIPLIED BY COORDINATE

MATRIX [20 × 2] GIVES JACOBIAN MATRIX [J] FOR $\zeta = -1$

0	0	-t1*t2/4-t5/4	t1*t7/4+t10/4	0	0	-t12*t13/4-t16/4	t12*t17/4+t19/4	0	0	-xi*t1	0	0	0	-xi*t12	0	0	0	-1.E0/2.E0+t21/2	1.E0/2.E0-t2 i/2
0	0	t4*t2/4+t5/4	t9*t7/4+t10/4	0	0	-t4*t13/4-t15/4	-t9*t17/4-t19/4	0	0	1.E0/2.E0-t36/2	0	0	0	-1.E0/2.E0+t36/2	0	0	0	-eta*t4	-eta*t9

APPENDIX D

VARIATION OF MATERIAL PROPERTIES OF THE TURBINE BLADE WITH TEMPERATURE

TEMP (C°)	E(GPa)	σ_{yield} (MPa)	α (μm/m°k)	c (J/kg)	K (W/m°k)
21	220	840	11.9	400	12.7
93	215	842	12.07	400	13.0
205	215	844	12.07	395	13.5
315	195	846.3	12.4	420	13.8
425	190	848.4	12.8	440	15.1
540	185	850	13.1	420	15.2
650	175	855	13.5	460	17.3
760	170	840	14.0	480	14.0
870	160	760	14.8	500	21.6
980	145	470	15.8	525	24.9

APPENDIX E

PHYSICAL INTERPRETATION OF STRESS STIFFNESS MATRIX $[K_\sigma]$:

If we consider a bar as shown in Fig (a) and assume that it can deform axially but is infinitely stiff in bending, so that it is straight in any displaced configuration, then the axial strain for small displacements is given by

$$\varepsilon_x = \varepsilon_u + \varepsilon_v \tag{E1}$$

where

$$\varepsilon_u = \frac{u_2 - u_1}{L} \tag{E2}$$

and

$$\varepsilon_v = \frac{1}{2}\left(\frac{v_2 - v_1}{L}\right)^2 \tag{E3}$$

$$\text{Strain } \varepsilon_v = \frac{\Delta L}{L} \tag{E4}$$

where ΔL is the lengthening associated with rotation of the bar through a small angle θ without any motion in x-direction and is given by

$$\Delta L = \frac{L}{\cos\theta} - L = L(\sec\theta - 1) = L\frac{\theta^2}{2} = \frac{L}{2}\left(\frac{v_2 - v_1}{L}\right)^2 \tag{E5}$$

Therefore strain energy in the bar is given by:

$$U = A\ E\ L\left(\frac{\varepsilon_u^2}{2} + \varepsilon_u\varepsilon_v + \frac{\varepsilon_v^2}{2}\right) = \frac{AEL}{2}\left(\varepsilon_u^2 + \varepsilon_v^2\right) + PL\varepsilon_v \tag{E6}$$

where $AE\varepsilon_u$ is the axial force F, positive in tension and

$$\varepsilon_u = \frac{1}{L}\begin{bmatrix}-1 & 1\end{bmatrix}\begin{Bmatrix}u_1 & u_2\end{Bmatrix} \tag{E7}$$

and

$$\varepsilon_v = \frac{1}{2L^2}\begin{Bmatrix}v_1\\ v_2\end{Bmatrix}^T \begin{bmatrix}-1 & 1\end{bmatrix}^T \begin{bmatrix}-1 & 1\end{bmatrix}\begin{Bmatrix}v_1\\ v_2\end{Bmatrix} \tag{E8}$$

The terms ε_u^2 and ε_v are quadratic in nature in nodal d.o.f. but ε_v^2 is quartic, so is negligible as compared to ε_u^2. Thus with $\{d\} = \{u_1, v_1, u_2, v_2\}$,

$$U = \frac{1}{2}\{d\}^T\left(\frac{AE}{L}\begin{bmatrix}1 & 0 & -1 & 0\\ 0 & 0 & 0 & 0\\ -1 & 0 & 1 & 0\\ 0 & 0 & 0 & 0\end{bmatrix} + \frac{F}{L}\begin{bmatrix}0 & 0 & 0 & 0\\ 0 & 1 & 0 & -1\\ 0 & 0 & 0 & 0\\ 0 & -1 & 0 & 1\end{bmatrix}\right)\{d\} \tag{E9}$$

It is clear from the equation above that the first 4 × 4 matrix with coefficient AE/L is the conventional stiffness matrix [K] and the second 4 × 4 matrix with the coefficient F/L (in which F is the axial force) and non-linear strain ε_v is the stress stiffness matrix $[K_\sigma]$. The element stress stiffness matrix $[K_\sigma^e]$ is a symmetric matrix and [G] must be arranged to yield displacement derivatives in the same order as shown below:

$$\{\delta\} = [G]\,\{d\} \tag{E10}$$

where

$$\{\delta\} = \{\, u_{,x},\ u_{,y},\ u_{,z},\ v_{,x},\ v_{,y},\ v_{,z},\ w_{,x},\ w_{,y},\ w_{,z} \,\} \tag{E11}$$

{d} is obtained by the relation:

$$\{F\} = \left[K_\sigma^e\right]\{d\} \tag{E12}$$

where

$[K_\sigma^e]$ is the stress stiffness of the rnatrix

{F} is the force vector for the system obtained after assembling {f}

{f} is the force vector for an element given by $\int_v N^T f'\, dv$

f' is the centrifugal force acting on the element

The matrix $[K_\sigma]$ is given as:

$$\left[K_\sigma^e\right] = \int_v [G]^T \begin{bmatrix} s & 0 & 0 \\ 0 & s & 0 \\ 0 & 0 & s \end{bmatrix} [G]\, dv \tag{E13}$$

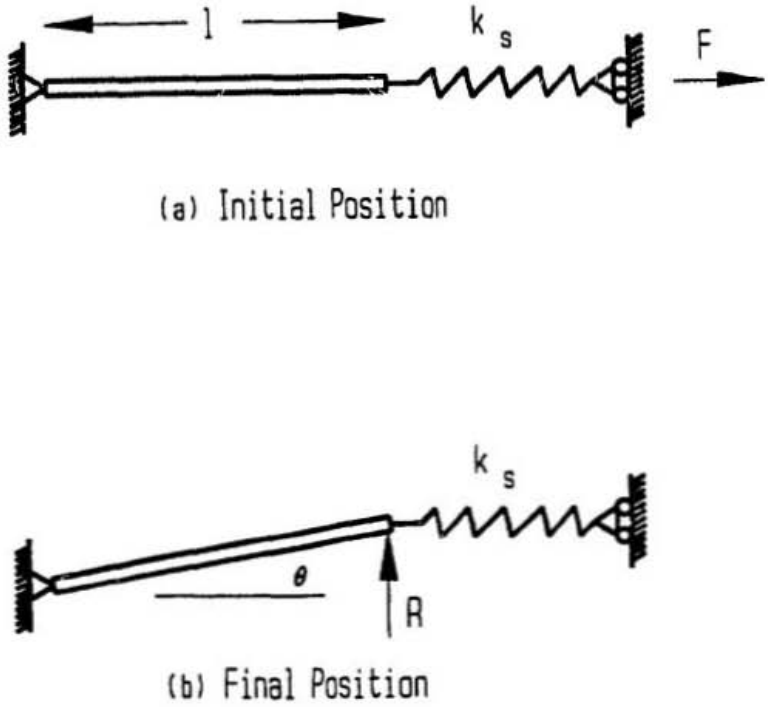

Fig. (a) TRANSVERSE FORCE ON AN AXIALLY LOADED TRUSS MEMBER (Warikoo, 1989)